A STUDY OF THE ORDER-DISORDER TRANSFORMATION IN A NICKEL-MANGANESE ALLOY.

by

R. Isaac Jaffee

Thesis submitted to the Faculty of the
Graduate School of the University
of Maryland in partial fulfillment
of the requirements for the
degree of Doctor of Philosophy
June 1943

ProQuest LLC.
789 East Eisenhower Parkway
P.O. Box 1346
Ann Arbor, MI 48106 - 1346

ACKNOWLEDGMENT

The writer desires to acknowledge his indebtedness to Dr. V. H. Gottschalk, who supervised the research incorporated in this thesis, and to Dr. W. J. Huff, who directed the Bureau of Mines Research Fellowship under which this work was done. Their counsel and aid were sincerely appreciated.

CONTENTS

LIST OF TABLES

LIST OF FIGURES

I. INTRODUCTION

The research incorporated in this thesis was begun as an investigation of a method for determining magnetic properties of metals, particularly the Curie Point from high frequency inductance measurements. The method had good promise for success with strongly ferromagnetic metals, because of the large effect that a core of a ferromagnetic material has on the inductance of a solenoid excited by a small magnetizing current of high frequency. It was believed that the method would be suitable for following structural changes in ferromagnetic alloys at different temperatures and in different physical conditions. For a suitable alloy it was suggested by Dr. H. S. Lean, then Chief Engineer of the Metallurgical Division of the Bureau of Mines, that the nickel-manganese alloy, Ni_3Mn, was strongly ferromagnetic when its lattice was in an ordered condition and that some interesting information about the formation and destruction of its superlattice might be obtained by studying it by this inductance method. This suggestion was adopted, and three rods of approximately the composition Ni_3Mn (23.78% by weight manganese) were cast and swaged at the Salt Lake City station of the Bureau of Mines. Mr. C. T. Anderson was kind enough to have prepared these specimens as well as several other specimens at a later date. The three rods were 21.5%, 23.2% and 24.4%

by weight manganese, two being on the high-nickel side and one on the high-manganese side of the theoretical superlattice composition.

The alternating magnetic fields generated by the solenoid as part of a bridge circuit being fed by an electric oscillator of high frequency were necessarily quite low, less than 1 oersted. Therefore, any unusually high inductance values recorded must be due to magnetic softness of the core material in the solenoid. When, in the course of the investigation, high values of inductance were consistently being found for the two alloys on the high-nickel side of the superlattice, it was decided to find out just how magnetically soft these alloys were. Comparison tests made in the same apparatus with alloys known to have great magnetic softness, permalloy and hipernik, gave inductance values of the same order of magnitude as those found for the ordered nickel-manganese alloys.

At this point in the research it was decided to veer somewhat from the original plan and include direct current magnetic measurements on these alloys because of the importance of the results obtained if they should prove to be as soft magnetically as the high frequency measurements had indicated. Normal magnetization and hysteresis curves measured by a ballistic galvanometer are accepted as standard measurements provided the demagnetizing effects of the induced poles in the test piece are properly taken into account. A test

piece in the form of a continuous ring has a demagnetizing factor of zero, and is particularly well suited for measuring magnetic properties at low fields. Accordingly, ring specimens of nickel-manganese alloy were prepared at the Salt Lake City station, and these measurements were carried out.

It would be well to include in this introduction some idea of the nature of ordered metallic lattices in alloys. Metallic solid solutions, which include most phases in alloy systems, are composed of homogeneous mixtures of the two kinds of atoms in binary systems and more than two kinds of atoms in the higher than binary alloy systems, each atom occupying a definite lattice site in a lattice system characteristic of the solid solution. Typical lattice arrangements for metallic phases are face centered cubic, body centered cubic, close packed hexagonal, etc. The solid solutions considered here are substitutional, wherein each atom occupies one of the lattice sites, as distinguished from interstitial solid solutions where certain small kinds of atoms like oxygen and carbon can exist between the lattice sites of the parent lattice.

Usually there will be found a completely random distribution of the two kinds of atoms in the lattices. In statistical terms the probability of finding one kind of atom in a given lattice site is just as good as that for finding the other.

In certain elevated temperature ranges the two kinds of atoms will tend to arrange themselves in an orderly manner, that is, atoms of each element will tend to take up a regular position relative to the others of its kind and the atoms of the other element. If the time at temperature is long enough, the more orderly arrangement will be formed, the degree of order being greater for longer times at temperature. A familiar example of an ordered arrangement of two kinds of atoms on a lattice is that of salt, NaCl, where the Na atoms form one face-centered cubic lattice and the Cl atoms another face-centered cubic lattice, each Na being surrounded by Cl atoms, and, conversely, each Cl being surrounded by Na atoms. The parent lattice is face center cubic in structure and is composed of the two intertwined face-centered lattices, Na and Cl. If it were possible to mix thoroughly the Na and Cl atoms on the lattice sites, the resultant structure would be a random distribution of Na and Cl atoms on the face-centered cubic parent lattice - this random distribution is customary in metallic solid solution, unless a "disorder-to-order" transformation has taken place.

The alloy compositions most susceptible to order-disorder transformations are those in which the atomic percentages of the two alloys bear simple numerical relationships to one another. For example, in an alloy system A-B, there might be superlattices (i.e., an ordered structure) formed from random solid solutions at or about the compositions

A_3B, AB, and AB_3. If the composition of the solid solution is exactly at one of these compositions the resulting ordered structure can approach perfection. With compositions on either side of these simple atomic ratios some of the lattice sites belonging to one kind of atom will necessarily have to be filled by the other.

If the alloy phase does have a tendency to form an ordered structure, an increase in temperature will increase the ease of atomic motion, and thus enable the atoms to move into the positions demanded by the superlattice type. However, this very freedom of atomic motion which made possible the ordered structure also increases the tendency for the atoms to move out of order, thus reducing the degree of perfection of the ordered structure. If sufficient time is allowed, there can be established at any temperature an equilibrium wherein the rate at which atoms are moving into right positions equals the rate at which those already in right positions are moving into wrong positions. Thus, there is an equilibrium degree of perfection of the superlattice which decreases as the temperature increases. When the temperature rises to the point where the atomic motion is such that the tendency for destruction of the superlattice is greater than that for its formation, the so-called critical ordering temperature is reached. The approach to this critical ordering temperature is what is technically called catastrophic, that is the degree of order decreases at an ever accelerating rate, until, at the critical temperature, it is zero. This type of behavior is

characteristic of alloy phases having "long-distance order", wherein large groups of atoms form ordered masses large enough to diffract x-rays from the new lattice planes set up by the ordered structure, and thus giving rise to "superlattice lines" in the x-ray pattern. The above-mentioned critical temperature is sometimes called "the critical temperature of long-distance order".

Short-distance order or "local order" results from the remaining tendency of the atoms to arrange themselves in an orderly manner, even after the temperature is too high for long-distance order to exist, and only small ordered clusters of atoms can be formed. These too disappear when the temperature is increased still further. Occasionally very little long-distance order is developed, and consequently, the catastrophic effects at the critical temperature are minimized.

The physical properties of the ordered structure are quite different from those of the random solid solution. The electrical resistivity is usually quite lower, the ordered structure may be magnetic and the disordered non-magnetic, different thermal emf's. are developed, the heat capacity during destruction of the superlattice is anomalous, etc. Indeed, it is by observing these different properties that we study superlattices. The only direct evidence that we have of these ordered structures is observed when we can detect the extra superlattice lines in the x-ray pattern, because from these the actual type of ordered structure may be derived.

II. LITERATURE

A. The Order-Disorder Transformation in Ni_3Mn.

The first investigators to observe the order-disorder transformation in Ni_3Mn were S. Kaya and A. Kussmann in 1931 (1). They found the alloys around this composition to be practically nonferromagnetic, when quenched from 900° C. After cooling the alloys, from 900° C at 50° C per hour or after annealing for three days at 430° C, they found the alloys to be strongly ferromagnetic, the condition after the three day anneal being more ferromagnetic than that after slow cooling (Fig. 1a). The electrical resistivities of the alloys around Ni_3Mn annealed two days at 450° C were found to be lower than those of the alloys quenched from 900° C (Fig. 1b). On reheating alloys that had previously been annealed they found that the saturation magnetization became zero at about 460° C (Fig. 1c), and that the resistivity changed slope, leveling off, at about the same temperature (Fig. 1d). Kaya and Kussmann called this temperature the Curie temperature. They made no distinction between a Curie temperature and a critical ordering temperature, although they offered saturation magnetization data on these alloys after prolonged annealing and quenching from temperature, which showed the sharp fall in the property at about 500° C.

Figure 1. Data Taken from Kaya and Kussmann's Paper (1)

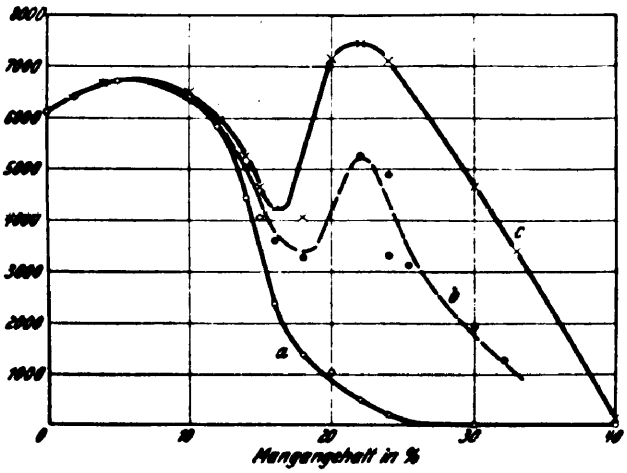

(a). "Saturation magnetization, $4\pi I_\infty$ of Ni-Mn alloys (a) after rapid cooling, (b) after slow cooling, (c) after three days annealing."

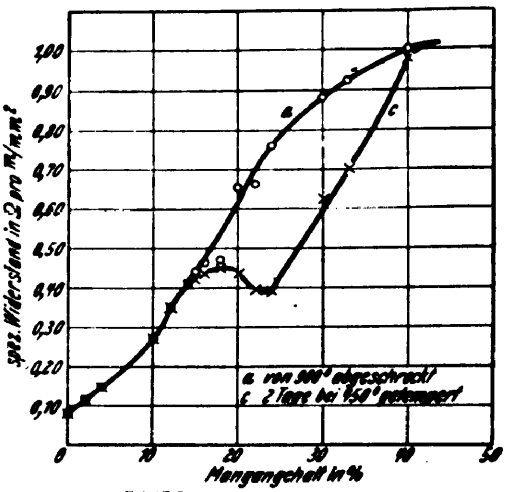

(b). "Specific electrical resistance of Ni-Mn alloys, (a) quenched from 900°C, (b) annealed two days at 450°C."

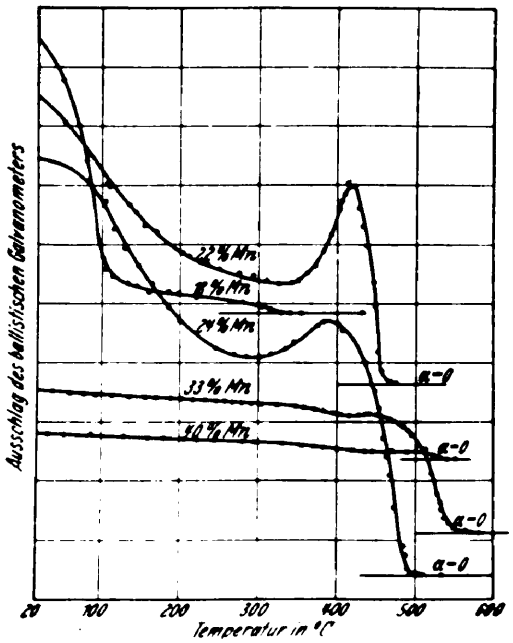

(c). "Magnetization-temperature curve (annealed specimens)."

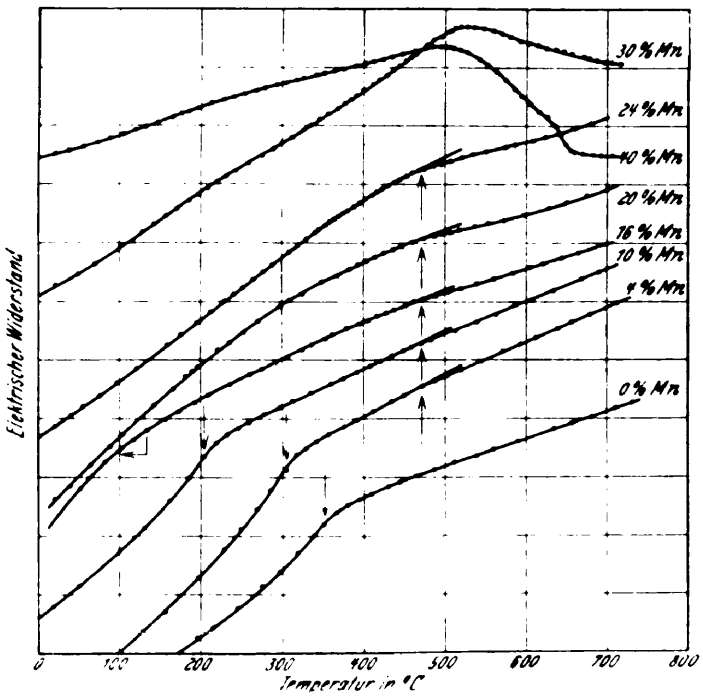

(d). Resistance-temperature curve of Ni-Mn alloys."

This matter of two critical temperatures which Kaya and Kussmann's data indicated was clearly brought out by N. Thompson in 1940. (2) Thompson repeated Kaya and Kussmann's magnetization and resistivity work, and interpreted the falling off of these properties at 460° C as evidence of the magnetic Curie temperature (Fig. 2a), and the persistence of magnetization in the alloys quenched after annealing up to about 510° C as evidence that the critical ordering temperature is at about 510° C (Fig. 2b). Thompson also presented specific heat data on Ni_3Mn when in an ordered condition while it was being slowly heated to 600° C. The specific heat vs. temperature curves showed two anomalies in the form of maxima, one taking place at 490° C, presumably evidence of the magnetic Curie temperature, and the other at about 540° C, taken as evidence of the critical ordering temperature. It is generally accepted that specific heat anomalies occur both at critical ordering temperatures and magnetic Curie temperature, although usually they are much more pronounced and sharper than those Thompson found for Ni_3Mn. The magnetic transformation temperatures and critical ordering temperatures which Thompson found or adapted from Kaya and Kussmann's data are given in Figure 2c.

Further light was thrown on the transformations of Ni_3Mn in a recent publication by S. Kaya and M. Nakayama. (3) They also found that the leveling off of the resistivity vs. temperature coincided with the magnetic Curie temperature as measured by the rapid drop to zero of the saturation magnetization vs. temperature curve and that the leveled-off resistivity

Figure 2. Data taken from K. Thompson's paper (2).

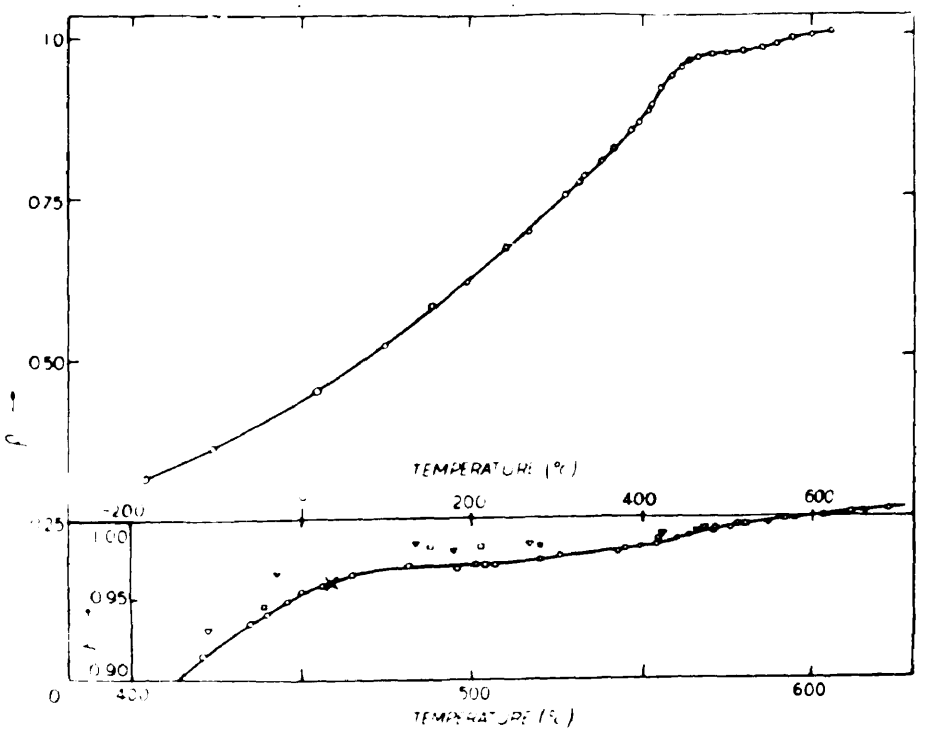

(a). "The equilibrium resistance of Ni_3Mn from -200°C to 600°C. Inset, the upper end of the curve on a larger scale."

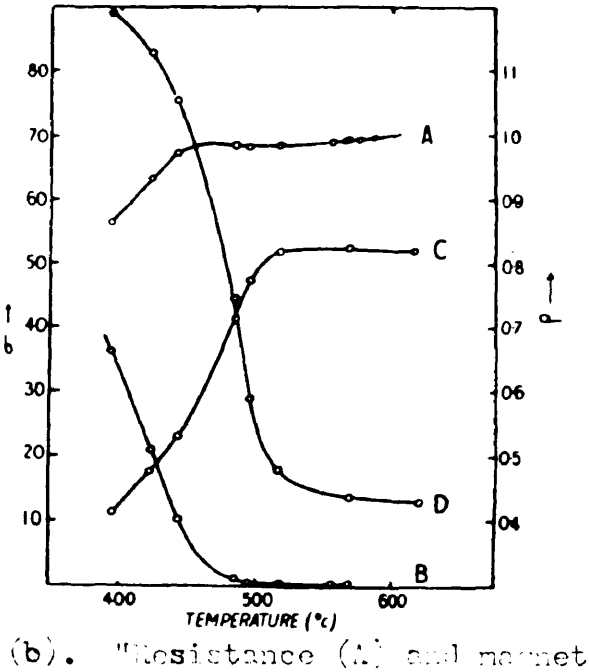

(b). "Resistance (A) and magnetization (B) at temperature T. Resistance (C) and magnetization (D) after annealing at temperature T."

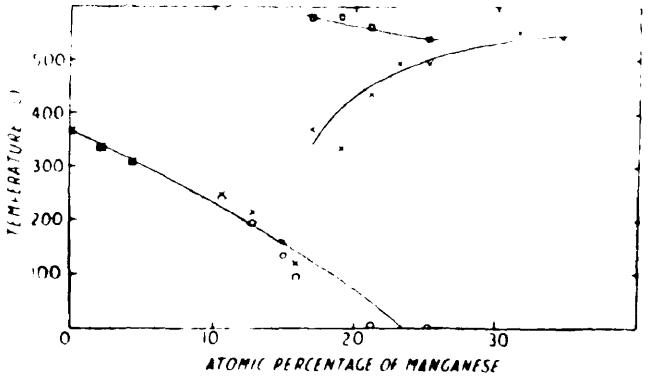

(c). "The magnetic transformations of the nickel-manganese system. , Curie point of quenched alloy; , critical temperature for order - disorder change. Adapted from Kaya and Hussmann (3)."

curve remained constant for a small temperature interval after the initial bend at the Curie temperature, and then started increasing somewhat linearly but with less slope than it showed while it was still ferromagnetic. They brought out the idea that the high temperature coefficient of resistivity shown by the alloy while still ferromagnetic is a common characteristic of ferromagnetics, that the high resistivity coefficient becomes zero just after the magnetic Curie temperature, and that the ordering of the alloy has little effect on the resistivity, particularly in the matter of the initial bend. Reasoning from Kaya and Nakayama's analysis leads one to believe that if the ordered alloy did not undergo a magnetic transformation, the temperature coefficient of resistance would be low all the way down to room temperature. The eventual picking-up of the resistivity after about 600° C indicates that all of the effect of order must have disappeared, and the resistivity vs. temperature curve is now following a course characteristic of the disordered alloy. Their measurement of specific heat during heating at a rate of 2° C per minute showed a pronounced maximum at the Curie temperature (as simultaneously indicated by other properties), and a somewhat gradual decrease up to about 640° C, which may be taken as meaning that energy was being supplied to break down the superlattice, but doing it rather gradually, thus showing no pronounced critical points (Fig. 3a). In their abstract, Kaya and Nakayama wrote, "Variations with temperature do not follow the courses shown by the CuzAu alloys and NizFe alloys, the main difference being that in the cases

Figure 3. Data Taken from Kaya and Nakayama's Paper (3).

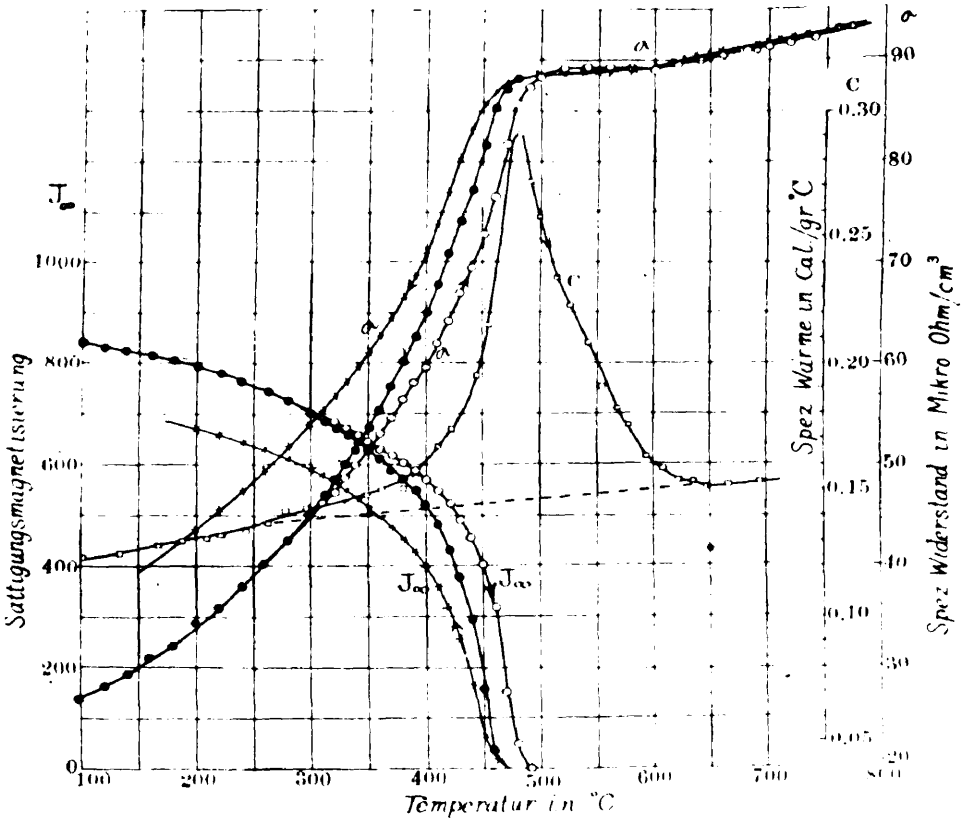

(a). "Resistance, saturation magnetization, and specific heat of Ni_2Mn. , equilibrium curve; , heating curve (2°C/min.); , cooling curve (2°C/min.)."

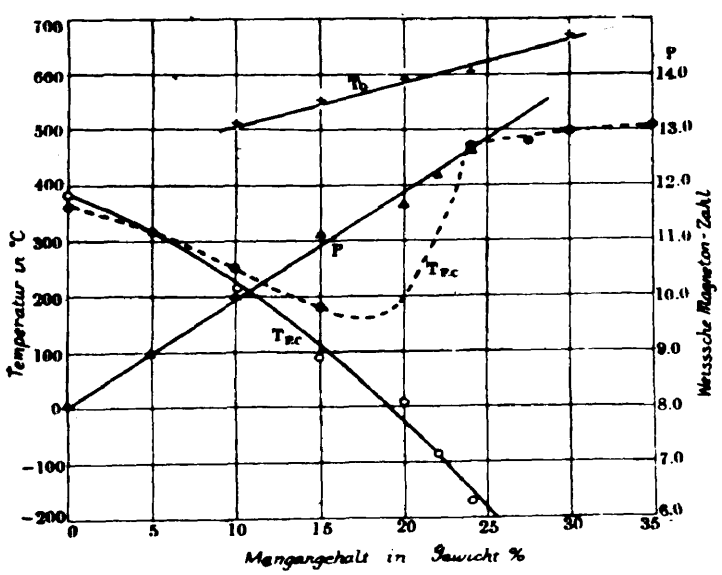

(b). "Dependence of the upper limit of vicinal order on the composition. T_o, upper limit of vicinal order; $T_{F\leftrightarrow C}$, ferromagnetic Curie point; $T_{P\leftrightarrow C}$, paramagnetic Curie Point; P, Weiss magneton number."

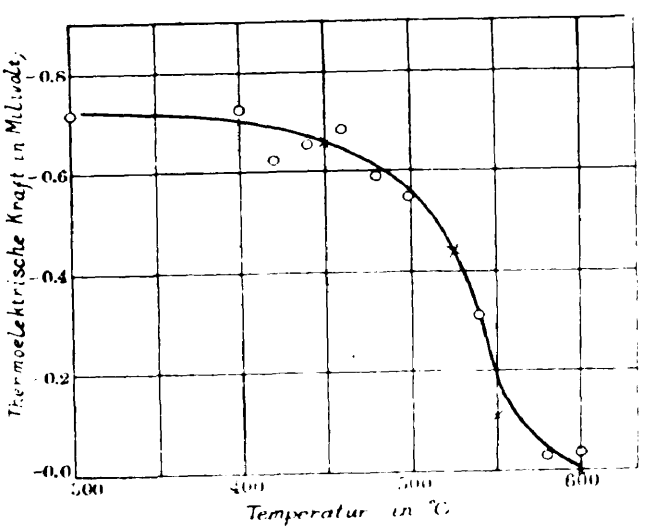

(c). "Thermoelectricity of Ni_2Mn quenched from different temperatures against the alloy quenched from 750°C between 0° and 100°C. , heating; , cooling."

now considered, a relatively large temperature band (600 - 300°) exists within which no critical points appear to occur." If by this Kaya and Nakayama meant a critical point in respect to the ordering phenomena, and not magnetic phenomena, and by critical point, a temperature at which a catastrophic change (i.e., rate of change accelerating rapidly as the point is approached) takes place, then their data would seem to be in accord with this conclusion.

Kaya and Nakayama have called the type of order found in Ni_3Mn "Nachbarschaftsordnung", meaning vicinal or neighborhood order. It can exist up to around 600° C, as may be seen in Figure 3b. They do not call the "upper limit of vicinal order" a critical ordering temperature as did Thompson, (2) because the ordered alloy does not exhibit normal behavior when going through the order to disorder transformation. It may be seen in Figure 3b that the magnetic Curie points on the nickel-rich side of Ni_3Mn are lower than those Kaya and Kussmann found (Fig. 2c).

Most of the investigators of the ordered alloy Ni_3Mn have used saturation magnetization in their researches. S. Valentiner and G. Becker (4) have measured the normal magnetization and hysteresis curves of Ni_3Mn and other manganese-nickel alloys in ordered and disordered conditions. They found the ordered alloys at and around Ni_3Mn to be fairly magnetically hard, and showing no unusual magnetic softness at all for any of the alloys investigated. The quenched, and therefore disordered, alloys were found to be ferromagnetic. Using the intensity of magnetization, J, at 340 oersteds, they found

the magnetic Curie temperature of the 25% Mn alloy in an ordered state to be about 450° C.

Kaya and Kussmann (1) used permeability at low fields vs. temperature curves in order to determine the Curie temperatures of the high nickel alloys (greater than 80% Ni) which have Curie temperatures higher than room temperature in the as-quenched condition. Initial permeability has been used to measure Curie temperatures of ferromagnetics because of the sharp rise to a maximum just before the Curie temperature (5). However, Kaya and Kussmann did not use this method for the ordered alloys around Ni_3Mn.

X-ray attempts to find the superlattice in Ni_3Mn have been unsuccessful (2). This has been variously attributed to the fact that the x-ray scattering power of manganese and nickel atoms are almost the same, and to the lack of sufficient long-distance order in the ordered alloy. Special x-ray techniques have been devised by investigators of other systems wherein the scattering power of the constituent atoms of the suspected superlattice have been nearly the same, and the superlattice was successfully found. The superlattice CuZn is a notable example. These techniques have been repeatedly tried in the case of Ni_3Mn without success. The peculiar nature of the superlattice in Ni_3Mn as is shown by the small effects of the superlattice itself, i.e., absence of pronounced anomalies at the critical temperature, etc., would seem to indicate that the failure of x-rays to isolate the superlattice was due more to the intrinsic nature of the

superlattice rather than to the closeness of the scattering power of the constituent atoms.

The only thermoelectric evidence of the ordering in Ni_3Mn is found in Kaya and Nakayama's paper. (5) They put the alloy into an ordered condition at various temperatures, quenched, and measured the thermoelectric force exerted by a couple of the ordered alloy and a specimen of disordered alloy between 0° C and 100° C. When ordering had not taken place, the thermoelectric force generated was zero; when it had, an emf. of up to 0.7 mv. was generated, depending on how well ordering had taken place. They found measurable emf's. starting at about 600° C, the emf's. rising sharply between 600° C and 500° C, and leveling off below 500° C (Fig. 3c). The data showed considerable scatter, and no particular critical points could be detected below 600° C. This indicated that they found no thermoelectric effect at the magnetic Curie temperature. Tait (6) has found discontinuities in the curve of thermoelectric power vs. temperature at the magnetic Curie temperature for normally ferromagnetic materials.

In summary of the published data on ordering transformation in Ni_3Mn the following points are given:

1. Manganese-nickel alloys in the vicinity of Ni_3Mn (23.78% Mn) undergo an order-disorder transformation when heated between 350° C and 500° C.

2. The ordered alloy is ferromagnetic, and the disordered alloy is paramagnetic.

3. The Curie temperature of the ferromagnetism of ordered Ni_3Mn is about 450° C, and is lower for ordered alloys on the nickel-rich side of Ni_3Mn.

4. The order-disorder transformation is not of the usual type wherein the degree of order decreases catastrophically at the critical temperature, but the degree of order seems to decrease in a gradual manner as the "critical temperature" of about 500° C is approached, showing no anomalies in the transition from order to disorder.

B. High Frequency Inductance Measurements for Magnetic Properties.

Inductance measurements on coils with test cores inside of them have frequently been used for measuring magnetic properties of the material of the test core. L. W. McKeehan (7) writes:

> "The inductance of a coil of wire depends upon the magnetic quantity of everything within its magnetic field. An inductance bridge is therefore an extremely sensitive detector for changes in the magnetic environment of one of a pair of coils for which the bridge has been balanced."

According to McKeehan, Hughes (8) first applied this method, modern applications being described by A. Campbell and W. Steinhaus. These investigators have used low frequencies, and have attempted to eliminate or evaluate the relatively small eddy current effects obtained. V. H. Gottschalk has used the inductance of a solenoid with test core inserted at

frequencies of about 40,000 cycles for investigating the production of ferromagnetism in the ternary alloys of iron, manganese, and chromium (9).

V. E. Legg (10) has published methods for measuring magnetic properties of laminated annular cores of circular and square cross-section using alternating current. Legg gives mathematical methods and experimental procedures for the determination of the fundamental qualities: Permeability, effective resistance, induction, and magnetic field. Unavoidable effects of eddy currents and hysteresis are evaluated. In his experimental procedures Legg attempts to minimize eddy currents by laminating the core.

Several investigators have, however, used the eddy current effect in their methods. For example, J. M. Bryant and J. B. Welch (11) have used tables of the increase in effective resistance due to eddy current shielding in wires having high frequency currents passed through them. Their specimen was in wire form; and consisted of a few turns of wire around a thin asbestos form. Bryant and Welch have used the so-called "skin effect" in a ferromagnetic conductor as a basis of their application of eddy current shielding to magnetic measurements; many other investigators have done the same, notably Van Lanchner, (12) G. Potapenko and R. Sanger, (13) R. Becker, (14) and K. Kreielsheimer (15) to mention four of the many papers.

Many other investigators have used the skin effect or eddy current shielding induced in a coil transversed by very high frequency. Usually the coil is an oscillatory coil of a high frequency transmitter. The change of inductance changes the frequency of oscillation, which may be evaluated by heterodyning the altered high frequency wave with another high frequency wave of the original frequency. A resonance method is also used to obtain the change in frequency. From this change in frequency the change in inductance of the coil is calculated, and from a suitable mathematical analysis the permeability of the core material may be calculated. A good example of the use of this method is given by G. R. Wait (16).

A method for determining electrical resistivity by eddy current shielding was proposed by W. B. Kouwenhoven (17). Kouwenhoven used moderately high frequencies corresponding to a depth of penetration of the magnetic flux of a solenoid into a test core of 0.117 cm. or less. His method used the distribution of flux in the surface layer occupied by the flux and in the surrounding air space to calculate the inductance of the solenoid. The equation derived contained resistivity and permeability in addition to inductance and frequency. Kouwenhoven applied his equations to non-magnetic materials, where the permeability was 1. Since Kouwenhoven's analysis was used in interpreting some of the data to be presented, and will be given extensively later, no further discussion of it will be made.

III. THEORY AND INTERPRETATION OF QUANTITIES MEASURED

A. High Frequency Measurements.

The inductance and effective resistance of a solenoid when a rod of the magnetic material is inserted was used to indicate magnetic properties. In order to understand what these quantities mean in terms of the customary magnetic quantities and concepts, a short review of the analysis given by W. B. Kouwenhoven (17) will be presented. As a basis he used the Bessel function solution of the differential equations governing the distribution of magnetic flux Φ in a round bar. This solution is rather complicated and was considerably simplified by considering the flux to be uniformly distributed in a narrow ring on the outside of the bar. This requirement is approached when high frequency fields are used due to the well-known skin effect. The approximate equation was

$$\Phi = 2\pi r \frac{\delta}{2} B_s - j\left(2\pi r \frac{\delta}{2} B_s\right)$$

where the factor $2\pi r \frac{\delta}{2}$ is the area of the ring of flux, B_s is the flux density at the surface, δ is Maxwell's equivalent penetration of flux and is based on the artifice of considering the flux as uniformly distributed over δ, j is $\sqrt{-1}$. The meaning of the equation is that the flux is composed of a real and an imaginary part, the real being in phase with the exciting current, and the imaginary lagging by a phase angle of $\frac{\pi}{2}$.

The equivalent penetration of the flux into the core is given by Maxwell's formula

$$\delta = \frac{1}{2\pi}\left(\frac{\rho}{\mu f}\right)^{\frac{1}{2}} \qquad \text{where } \rho \text{ is in abohms per cu. cm.}$$

$$= 5033\left(\frac{\rho}{\mu f}\right)^{\frac{1}{2}} \qquad \text{where } \rho \text{ is in ohms per cu. cm.}$$

Calculations from Kouwenhoven's frequency vs. resistivity requirements indicate that δ = 0.177 cm. for an approximate solution to the Bessel solution to be correct to ±0.1%.

When the solenoid has no metallic core the inductance is given by

$$L_a = \left(\frac{\Phi_s}{I}\right) N \times 10^{-8} \qquad \text{henrys}$$

$$= \left(\frac{B_s A_a}{I}\right) N \times 10^{-8} \qquad \text{henrys}$$

where B_s is the flux density in air, A_a = area of cross-section of the solenoid. With a round core inside the flux will be given by $\Phi_r + \Phi_c$, where Φ_r is the flux in the core and Φ_c outside of the core. The inductance will now be given by

$$L_m = \left(\frac{\Phi_r + \Phi_c}{I}\right) N \times 10^{-8} \qquad \text{henrys}$$

$$= \left(\frac{\Phi_r}{I} N + \frac{\Phi_c}{I} N\right) \times 10^{-8} \qquad \text{henrys}$$

but $\Phi_r = (2\pi r \frac{\delta}{2}) \mu B_s = \pi r \delta \mu B_s$, $\Phi_c = (A_a - A_b) B_s$

where A_b cross-sectional area of the rod

then $$L_m = \left[\frac{\pi r \delta \mu B_s N}{I} + \frac{(A_a - A_b) B_s N}{I}\right] \times 10^{-8} \text{ henrys}$$

Knowing that $L_a = \frac{B_s A_a N}{I} \times 10^{-8}$

it follows that $\frac{L_m}{L_a} = \frac{\pi r \delta \mu}{A_a} + \frac{A_a - A_b}{A_a}$

and since $\pi r^2 =$ area of bar, A_b,

substituting $\frac{L_m}{L_a} = \frac{\pi \delta A_b}{r A_a} + \frac{A_a - A_b}{A_a}$

$$\delta = 5033 \sqrt{\frac{\rho}{\mu f}}$$

$$\frac{L_m}{L_a} = \frac{5033 A_b}{r A_a} \sqrt{\frac{\rho \mu}{f}} + \frac{A_a - A_b}{A_a}$$

or $$L_m = \frac{5033 A_b L_a}{r A_a} \sqrt{\frac{\rho \mu}{f}} + \frac{A_a - A_b}{A_a} L_a$$

$$= \frac{5033 \pi r L_a}{A_a} \sqrt{\frac{\rho \mu}{f}} + L_c$$

The above equation relates the resistivity and permeability of the rod to the measured inductance of the solenoid with rod inserted at frequency f and the physical constants of the solenoid and rod. The equation as given in Kouwenhoven's paper was erroneous in that the permeability was given in the denominator of the fraction under the square root sign instead of in the numerator. This mistake resulted from Kouwenhoven's not multiplying the surface flux density (really the air core flux density) by μ. Since Kouwenhoven was interested in determining resistivity of non-magnetic materials by this eddy current shielding method, where μ is always unity, this error did not affect his results.

The solenoid which was used in measuring the magnetic properties as a function of temperature was necessarily

relatively short. Hence, these equations cannot be applied with accuracy, and in order to calculate permeabilities, a calibration of the solenoid against non-magnetic materials whose resistivity is known can be made. A procedure which could be followed in this case would be to convert the above equation to the form

$$K = \left(\frac{L_m - L_c}{\pi r}\right)^2 \frac{1}{\rho}$$

where $L_c = \frac{A_a - A_b}{A_a} L_a$

The constant K contains all quantities in the equation which are held constant including the frequency. A difficulty appears in the use of this equation because L_m and L_c are of the same order of magnitude for non-magnetic materials and consequently the inductance measurement must be made to an additional degree of precision over that used for ferromagnetic material where $L_m - L_c$ is comparatively large. Since the inductance of small air core solenoids is of the order of a few hundred microhenrys, the method of measuring inductance must be capable of an accuracy of 0.1 microhenry if 1% precision is to be realized in the calibration. This degree of precision was not available with the inductance measuring equipment used. A calibration to within about 5-10% relative accuracy can be made nevertheless, or the theoretical constant may be calculated and used. It must be stated, however, that when the permeability of a magnetic material is calculated using this equation, the d.c. resistivity must

have been previously determined. Even if a calibration of a low order of absolute precision was used, there may be calculated relative values of approximate permeability whose relative precision is comparatively good.

It might be stated that Kouwenhoven's equation holds only for non-magnetic materials, because only the eddy current effect of high frequency fields was considered. R. Becker (18) has concluded that the behavior of ferromagnetic bodies in high frequency alternating fields is completely determined by the eddy current effect. It is true that the frequencies Becker had reference to were no doubt higher than those used in the present investigation, but it is believed that the eddy current effect is the principal factor affecting the inductance measurement. Apparently hysteresis and other magnetic effects are of secondary importance in reference to inductance; this certainly is not the case with other magnetic quantities like effective resistance.

The other high frequency quantity measured in this work was the effective resistance of the solenoid. Hysteresis and eddy current effects in the core of the solenoid, which make up the principal magnetic losses, very markedly influence the effective resistance of the solenoid. The increase in effective resistance of the solenoid when a magnetic core was inserted over that of an air core may be taken as a measure of the magnitude of the magnetic losses in the core. No attempt was made to separate hysteresis and eddy current losses the sum of which is contained in the increase of effective resistance.

B. Magnetization and Hysteresis Measurements.

Two important measurements of the magnetic properties of materials are the determination of the normal magnetization curve and of the hysteresis loop. The theory and significance of these curves are well known and will be summarized only briefly. Figure 4a shows the typical form of a normal magnetization curve and hysteresis loop, and a typical permeability vs. magnetic force curve for ferromagnetic materials. The quantities usually determined are shown on the diagram.

Magnetic field is usually expressed in oersteds, and magnetic induction in gausses, both quantities having the units maxwells per square centimeter. Referring to Figure 4b, $H_{max.}$ is the value of the maximum field attained, $B_{max.}$ is the induction corresponding to the maximum field, B_r is the magnetic remanence left after the magnetic field $H_{max.}$ is removed, and H_c, the coercive force, is the negative field required to reduce the residual magnetism to zero. Referring to Figure 4b,

μ is the permeability of the material and is defined as the ratio of normal induction to field, $\mu = \frac{B}{H}$, μ_o is the initial permeability, which is the limiting slope of the B-H curve as H approaches zero field, $\mu_{max.}$ is the maximum value of the $\frac{B}{H}$ ratio.

For magnetic softness it is desirable to have high inductions at low fields, or, what is the same thing, high permeabilities at low fields, and to have low values of the coercive force. The area enclosed by the hysteresis loop is a measure of the energy which has been dissipated in the form

FIGURE 4.

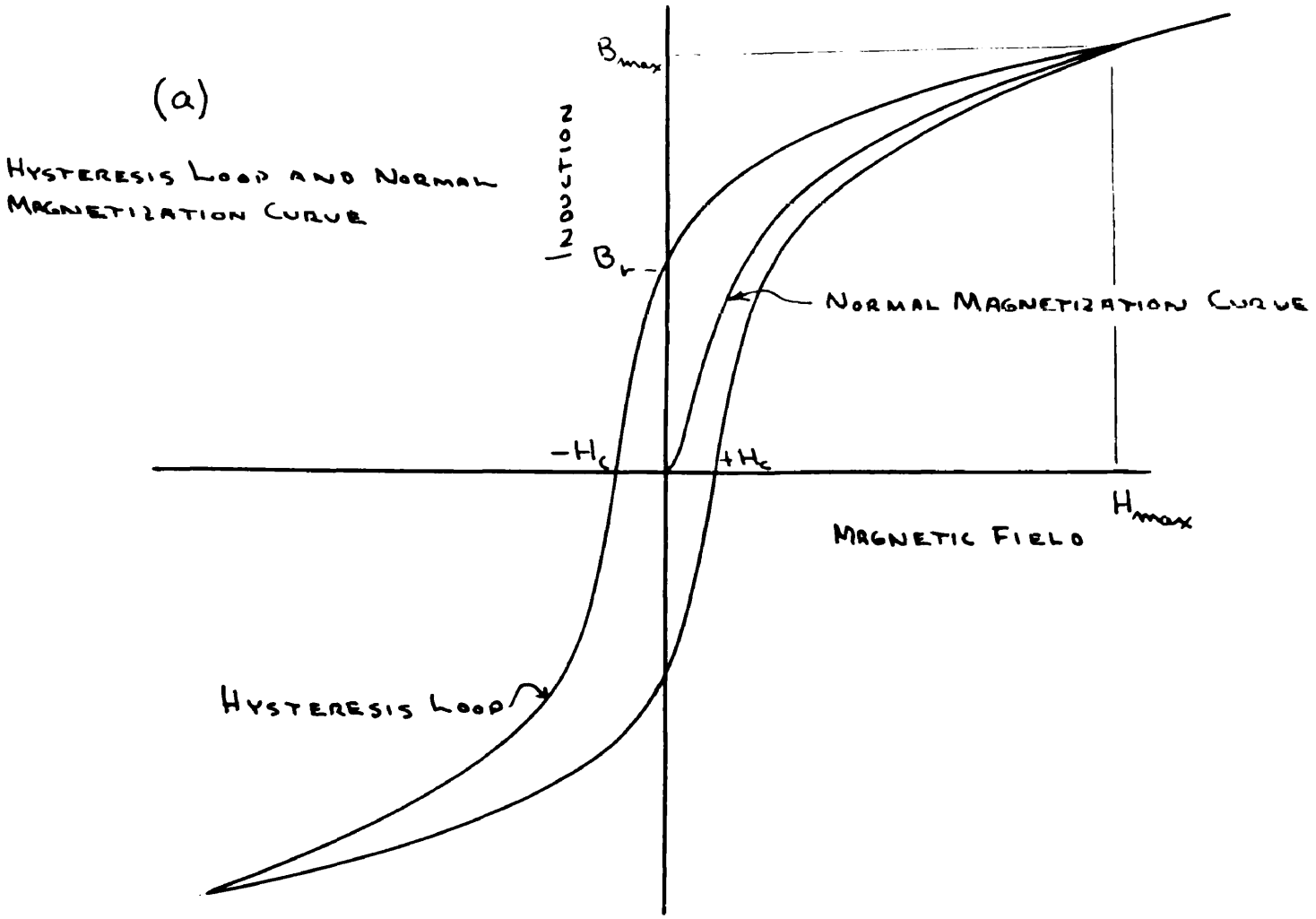
(a)
HYSTERESIS LOOP AND NORMAL MAGNETIZATION CURVE
B_{max}
INDUCTION
B_r
$-H_c$
$+H_c$
H_{max}
MAGNETIC FIELD
NORMAL MAGNETIZATION CURVE
HYSTERESIS LOOP

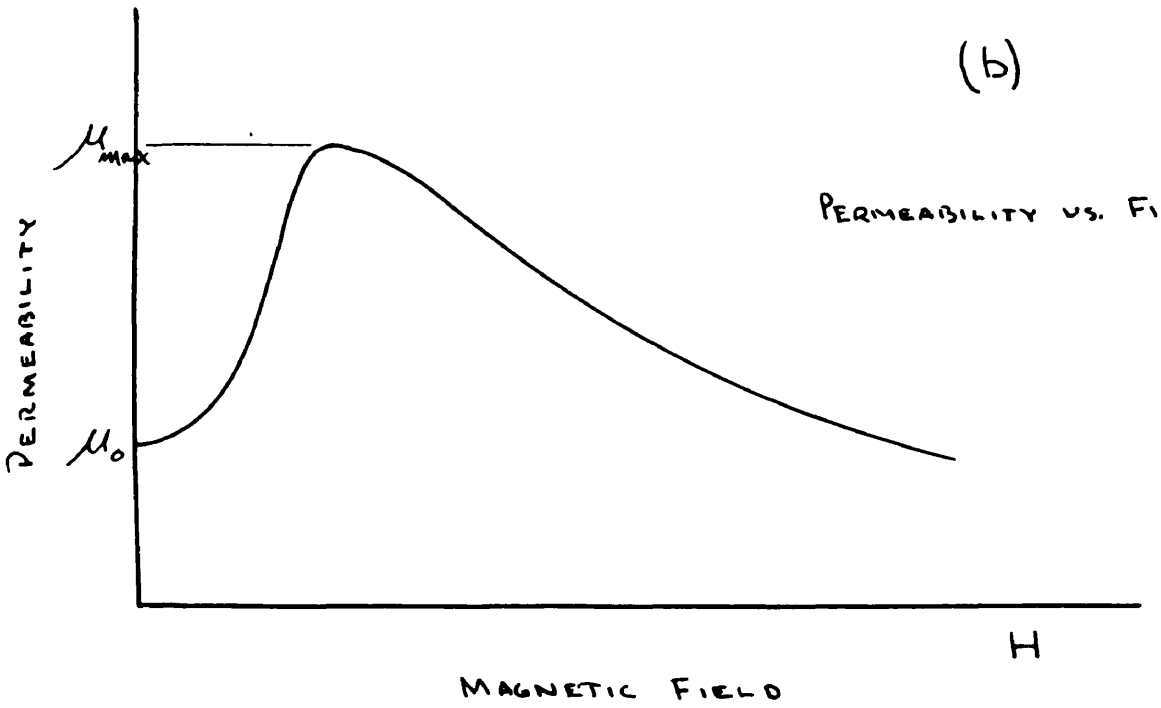
(b)
PERMEABILITY VS. FIELD CURVE
μ_{max}
μ_0
PERMEABILITY
H
MAGNETIC FIELD

of heat when the magnetization has been carried through one complete cycle, and is given by the equation

$$Q = \frac{1}{4\pi} \oint H \partial B$$

where Q is energy loss in ergs per cubic centimeter of the material. It is desirable to have low hysteresis losses in soft magnetic materials.

Magnetically hard materials are characterized by high coercive forces. The maximum value of the product of B and H on the demagnetization curve between B_r and H_c is often taken as a measure of magnetic hardness.

In measuring the normal magnetization curve and hysteresis loop by means of a ballistic galvanometer, use is made of the ability of this instrument to deflect through angles proportional to the quantity of electricity discharged through its coil. The instrument is usually used in the critically damped (electrical) condition, or in a slightly underdamped condition. With the resistance in the galvanometer circuit of such a magnitude as to produce the desired damping, a calibration of the galvanometer is made by discharging known quantities of electricity through the galvanometer coil and measuring the deflection.

C. Electrical Resistivity Measurements.

The electrical resistivity of a rod of material of uniform cross-section may be calculated from the equation

$$\rho = \frac{RA}{L}$$

where ρ is the resistivity of the material in ohms per cubic centimeter, R is the resistance in ohms of the rod between two points on it, A is the cross-sectional area of the rod in square centimeters, and L is the length in centimeters between the two points on the rod. Resistivity is a specific property of a material, and is a characteristic of the material in any shape.

Methods of determining resistivity by use of the above formula vary in the way the resistance between the two points along the rod is measured. The resistance is usually quite low, in the order of a few thousandths of an ohm, and methods of accurately measuring very low resistances must be used. Two suitable methods of measuring low resistances are the Kelvin bridge and the potentiometer method. The potentiometer method, which was used in this work, consisted of passing a current through the specimen and through a standard resistance, and measuring the voltage drop across each with the potentiometer. The specimen has attached to it, or is resting on, two potential leads a known distance apart. The potential drop across the standard resistance, measured by the potentiometer, makes known the current flowing through the specimen, $I = \frac{V}{R_s}$. The resistance of the specimen between the potential leads may be computed from the voltage drop across them, as measured by the potentiometer, $R = \frac{V}{I}$. Variations in this method may be made by substituting a calibrated ammeter for the standard resistance-potentiometer combination in order to measure the current and by substituting a calibrated millivoltmeter for the potentiometer in order to measure the voltage drop across the specimen.

D. Thermoelectric Force Measurements.

The theory of thermoelectric forces and their measurement are well known and will not be gone into here. It is pertinent to say that the thermoelectric force is a structure sensitive property, which will probably change if one of the component metals of the couple undergoes a structure transformation, a Curie transformation (ferromagnetic to paramagnetic condition), or an order-disorder transformation.

IV. EXPERIMENTAL PROCEDURE

A. High Frequency Measurement of Inductance and Effective Resistance.

The Owen's bridge was used for these measurements. It measures inductance in terms of resistance and capacity. The diagram shown below illustrates the components of the bridge.

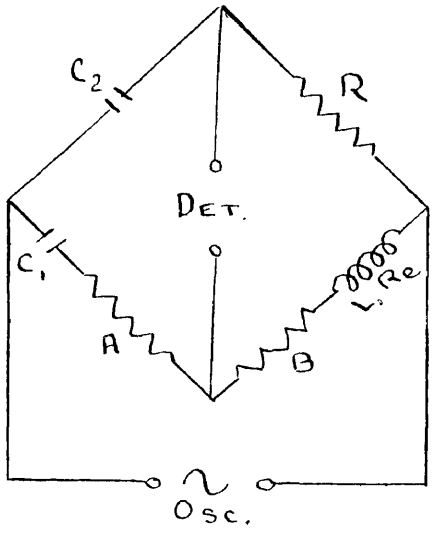

The balance equations are

$$L = C_2R(A - A_0)$$

$$C_1(R_e + B) = C_2R$$

In order to get values of $A - A_0$ with at least three significant figures for the inductance range of 100 - 1000 microhenrys, which was that found for the solenoid with magnetic rods inserted, it was necessary to use a C_2 of at most 0.001 microfarads. In order to obtain the sensitivity found with a balanced bridge, an R of 1000 ohms was necessary. Using a

standard condenser for C_2 and a standard resistance for R, and determining A_o by shorting the inductance to be measured, no calibration would apparently be needed. The 0.001 microfarad condenser used was of good quality, made of mica, but was not a calibrated standard. A calibration scheme was therefore necessary. For this a standard variable inductance was used. The equation for inductance therefore became $L = K(A - A_o)$. Several values of inductance on the variable inductor were used, A-values being taken for each. Using an A_o found by shorting the inductor did not give constant K's. Concordant values of K and A_o were calculated by solving the equations

$$K = \frac{L_1}{A_1 - A_o} = \frac{L_2}{A_2 - A_o} = \frac{L_3}{A_3 - A_o} = \cdots$$

In illustration of this the following table and calculations are shown

L - appl. microhenrys	A ohms	
500	545.2	(last significant figure estimated)
400	451.8	
300	357.5	

$$\frac{500}{545.2 - A_o} = \frac{400}{451.8 - A_o} = \frac{300}{357.5 - A_o}$$

$(A_o)_1 = 78.2$ $\quad K_1 = 1.069$ $\quad A_o = 76 \pm 1$ ohms

$(A_o)_2 = 76.0$ $\quad K_2 = 1.066$ $\quad K = 1.067 \pm 0.001$

$(A_o)_3 = \frac{74.9}{76.4 \text{ av.}}$ $\quad K_3 = \frac{1.067}{1.067 \text{ av.}}$

Thus, in estimating the error in a given calculation of inductance we may take a typical value of A as 500 ohms. The fractional error in inductance would then be

$$\frac{\Delta L}{L} = \sqrt{\left(\frac{1}{500-16}\right)^2 + \left(\frac{0.001}{1.067}\right)^2} = 0.0025 \text{ or } 0.25\%$$

The maximum error will occur at the small values of $A - A_o$. A typical low value of A such as would be found for a metal after it has passed through its Curie point is about 220 ohms. The fractional error in inductance will be equal to the fractional error in $A - A_o$ in this case, or

$$\sqrt{\left(\frac{1}{220-16}\right)^2} = 0.007 \text{ or } 0.7\%$$

This is a small enough error to be negligible in the process of finding Curie temperatures by plotting inductance vs. temperature. In the calculation of permeability the fractional error in inductance, although this term is squared, has less effect on the fractional error in permeability than the uncertainty in the calibration constants as may be seen from the following calculation:

$$\mu = \left(\frac{L_m - L_c}{\pi r}\right)^2 \frac{1}{K\rho}$$

$$\frac{\Delta \mu}{\mu} = \sqrt{\left[\frac{2 \times \Delta\left(\frac{L_m - L_c}{\pi r}\right)}{\frac{L_m - L_c}{\pi r}}\right]^2 + \left[\frac{-1 \times \Delta K\rho}{K\rho}\right]^2} = \sqrt{(2 \times 0.007)^2 + (0.05)^2}$$

$$= 0.052 \text{ or } 5\%$$

The second of the balance equations for the Owens bridge enables the calculation of the effective resistance of the solenoid to be made. Solving the equation through for $R_e + r = \frac{C_2 R}{C_1}$ it will be seen that the sum of the effective

resistance and the reading of the B resistance decades will be constant. When the inductance is shunted it may safely be assumed that the effective resistance is zero, hence the reading of B in that case will be the value of the constant. Experimentally, a vacuum thermocouple is in that branch of the bridge, but since its resistance may be considered constant the sum of R_e + B will still remain constant. When R is 1000 ohms and C_1 and C_2 are 0.001 μf condensers, R_e + B will be about 1000 ohms. The maximum error in the assumption that the effective resistance of the shunt is zero is about 1 ohm. Hence the relative error in effective resistance is about 0.1%.

Since inductances of from 100 to 1000 microhenrys are relatively small, the frequency of applied oscillation must be high enough to make the inductive impedance of the solenoid an appreciable factor in the sum total of the impedances in the bridge. Thus, at 50,000 cycles an inductance of 1000 microhenrys has about 300 ohms inductive reactance. Another consideration in the frequency to be used comes from the minimum penetration of magnetic flux into the core, upon which the approximate solution to the Bessel function, mentioned in the theoretical section, is based. This minimum penetration was 0.177 cm. Thus, with a resistivity of about 50 micro-ohms per cubic cm. and a permeability of about 1000 the required minimum frequency according to Maxwell's equation would be $f = \left(\frac{5033}{\delta}\right)^2 \frac{\rho}{\mu} = \left(\frac{5033}{0.177}\right)^2 \times \frac{50\times10^{-6}}{1000} =$ 40 cycles.

With the same resistivity but a permeability of 1 the requisite frequency would be 40,000 cycles. Thus, we see that to take all possible conditions into consideration a frequency of at least 40,000 to 50,000 cycles is needed. These frequencies were used throughout.

The bridge which was used was shielded from stray radiation according to a scheme proposed by J. H. Ferguson (19). This scheme together with a listing of the actual equipment used in the bridge, oscillator, and detector is shown in Figure 9.

In order to determine the actual field inside of the solenoid a vacuum thermocouple was inserted into the branch of the bridge containing the solenoid. This thermocouple was calibrated against d.c. current. Since such a device operates on the heating of a very thin resistance wire to which is welded a minute thermocouple junction, any given thermoelectric emf. generated by the couple corresponds to a given heating current. In alternating current the heating current is proportional to the root mean square current. Hence, the d.c. calibrating current is equivalent to a root mean square high frequency current, and if a sinusoidal high frequency current is assumed the maximum magnetizing current passed through the solenoid may be calculated by multiplying the root mean square current by $\sqrt{2}$. The maximum field generated by the solenoid may be calculated from the equation $H = 2\pi n I_{max.}(\cos\phi_1 - \cos\phi_2)$. This equation enables one to calculate the field at any point inside or outside of the solenoid along its axis. ϕ_1 and ϕ_2

are the angles made by the point in question with the two end peripheries of the solenoid, $I_{max.}$ is the maximum value of the magnetizing current in abamperes (amperes/10), and n is the number of turns of winding per cm. of length of solenoid. The actual distribution of flux in the solenoid as calculated by this formula and the variation of it with current are shown in Figure 12.

The permeabilities of soft magnetic materials rise sharply with magnetic field at low fields, and according to the equations developed in the theoretical section on high frequency measurements, this should be followed by the inductance, and probably the effective resistance, of the solenoid. Because of this it was attempted to keep the maximum value of the alternating field constant at about 0.75 oersteds, which corresponded to a R.M.S. current through the solenoid of 12 milliamperes.

In determining the Curie point from permeability (or inductance, in this case) vs. temperature measurements, the question of choosing the exact point on the curve is open to a certain extent - as, for example, whether to take Θ_c as the temperature corresponding to the greatest negative slope of the μ vs. T curve or to take it as the temperature corresponding to complete disappearance of ferromagnetism. The former alternative is more commonly used at present, but in this paper the latter, older method will be followed.

B. Magnetic Measurements with Ballistic Galvanometer.

A versatile circuit for these measurements was designed which permitted, by suitable switching arrangements, the demagnetization of a ring specimen from about 40 oersteds to about 0.01 oersteds, determination of the normal magnetization curve at any field up to about 40 oersteds, determination of the normal magnetization at ten predetermined fields, or the determination of the hysteresis curve at ten predetermined fields up to about 40 oersteds. This circuit is shown in Figure 5.

The specimens were toroidal in form. A toroid is the solid generated by revolving a circular or square area around an axis outside of the area. The specimens used were square in cross-section, because of the ease with which they may be made by casting and rolling out a plate of the material whose magnetic properties are to be determined, and machining a ring from the plate on a lathe.

The procedure followed in putting the windings on the specimen was improved as more specimens were prepared. The most satisfactory method was to first insulate the specimen by a layer of scotch masking tape, a secondary winding of No. 30 cotton covered, enameled magnet wire was wound around the ring, a second layer of scotch masking tape was wound over this, and then the primary winding of No. 25 cotton covered enameled magnet wire was wound around the ring. After the secondary was put on the specimen, it was coated with a thin

FIGURE 5

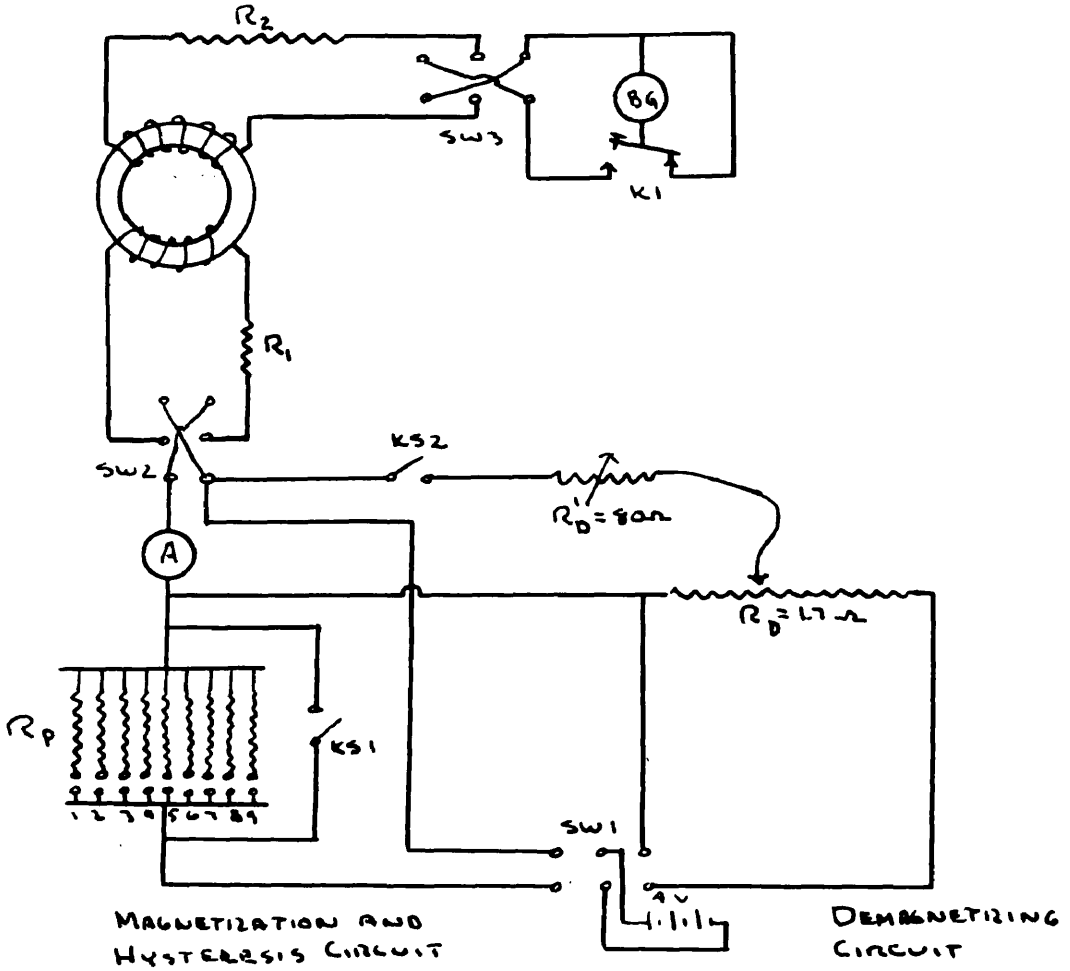

CIRCUIT USED IN BALLISTIC MAGNETIC MEASUREMENTS

layer of clear glyptal cement; glyptal cement was also coated over the primary winding. The reason for putting the primary winding on the outside was to avoid the excessive heating of the specimen which occurred when the primary winding was inside both the secondary winding and a layer of scotch masking tape.

The theory of ballistic magnetic measurements using a ballistic galvanometer and a ring specimen is relatively simple. The principles set forth by T. F. Wall (20) have for the most part been followed. His circuits have been changed somewhat, but are fundamentally the same. If the ring specimen has an evenly wound primary winding, the magnetizing field may be calculated from the equation

$$H = \frac{1.257\, I_1 w_1}{l_m}$$

where H is the magnetizing field in oersteds, I_1 is the primary current in amperes, w_1 is the number of primary turns, and l_m is the average circumference of the ring. According to R. L. Sanford (21) the flux density will be uniform throughout a cross-section of the rings to within 0.5% if the ratio of radial thickness of specimen to average diameter of specimen is 1:10. This ratio was used in the designing of the ring specimens. The induction on magnetizing may be calculated from a reversal of the field by the equation

$$B = \frac{R_2\, b\, d}{2\, A\, w_2} \times 10^8$$

where B is the induction in gauses, R_2 is the total resistance in ohms in the secondary circuit including that of the galvanometer, b is the ballistic constant of the ballistic galvanometer in coulombs per mm. deflection, d is the deflection of the galvanometer in mm., A is the cross-sectional area of the specimen, and w_2 is the number of secondary turns wound around the specimen.

In determining hysteresis loops the switching arrangement was such that the field could be changed rapidly from a maximum of 30 oersteds to any one of nine predetermined positive fields, zero, or any of the ten corresponding negative fields including -30 oersteds. The change of induction resulting from one of these changes of field may be calculated by

$$\Delta B = \frac{R_2 \, b \, d}{A w_2} \times 10^8$$

where the quantities have the same significance as is given above.

The slide wire and parallel resistor switching arrangement were constructed. The slide wire was 1 meter long and made of No. 24 ga. constantan wire, its resistance being about 1 ohm. The slider was made of a small bakelite form containing a pool of mercury to insure good electrical contact between the movable contact and the wire. A meter stick was mounted below the wire so that the voltage drop could be varied uniformly. The resistors in the parallel resistance arrangement were so set that the sum of the number whose

switches were closed gave a primary current equivalent to a desired field. Thus with the first closed, the field was 0.1 oersteds, with first two closed, 0.25 oersteds, with first three closed, 0.5 oersteds, and so on. The resistance R_1 was set so that when the switch which shorted the parallel resistors was closed, the desired maximum field would be obtained.

The procedure followed for the various kinds of operations was:

1. Demagnetization. Switch sw 1 is thrown to the right, R'_D is at zero resistance, and R_D is set at a position to give a current through the primary slightly greater than that equivalent to the highest field to be used, and KS 2 is closed. Sw 2 is reversed at a rate of about 1 cycle per second while R_D is slowly decreased (to the left). After R_D is as far to the left as possible, R'_D is slowly increased to its limit. The specimen is then taken as completely demagnetized.

2. Magnetization Curve Using Slide Wire. The switches are kept in the same position they were in during demagnetization. The current through the primary is increased to a value equivalent to the first desired field, and the reversing switch sw 2 is reversed about ten times to get the specimen in a cyclic state at the desired field. K 1 is closed. Sw 2 is reversed sharply, and the throw of the galvanometer read. Sw 3 is reversed, K 1 closed, and sw 2 is

reversed sharply in the opposite direction, and the throw of the galvanometer read. (Both of the galvanometer throws will be in the same direction, sw 3 being kept in a position to do this. The galvanometer zero was set over to the left of the scale, and all throws were made to the right. The galvanometer was calibrated for throws to the right). The current is then increased to that equivalent to the next desired field, and the procedure is repeated.

3. Magnetization Curve Using Parallel Resistor Arrangement. Ks 1 is open. All of the resistances in R_p are open. Sw 1 is thrown to the left. $(R_p)_1$, corresponding to the smallest desired field, is closed. Sw 2 is reversed about ten times to obtain a cyclic condition in the specimen. K 1 is closed, sw 2 is reversed sharply, and the throw of the galvanometer read. The throw corresponding to an opposite throw of sw 2 is then obtained. $(R_p)_2$, the next resistor, is put into parallel with the first by closing its switch, thus making the current equivalent to the next desired field. The procedure followed for the first field is repeated. All the other switches in R_p are closed in turn, thus enabling galvanometer throws to be obtained for each field.

4. Hysteresis. All of the parallel switches are opened. Ks 1 is closed, and the field is $H_{max.}$. Sw 2 is reversed several times. Ks 1 is closed, sw 2 is opened, and the throw of the galvanometer throw read. Sw 2 is then closed to the other side, and the galvanometer throw is read.

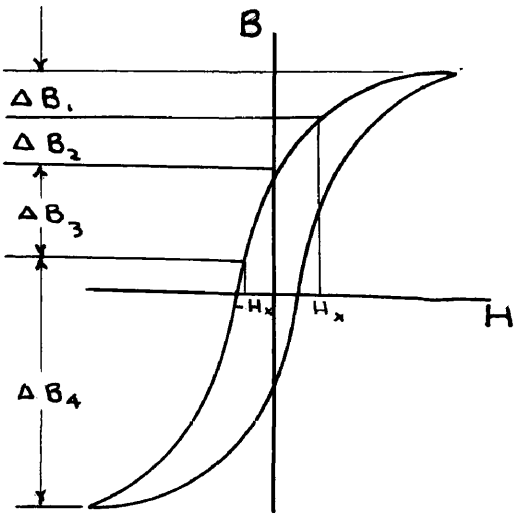

Thus, ΔB data is obtained for each field. Relations which permit the calculation of $B_{max.}$ and B_r are

$$2B_{MAX.} = \Delta B_1 + \Delta B_2 + \Delta B_3 + \Delta B_4$$

$$B_{MAX.} - B_r = \Delta B_1 + \Delta B_2$$

$$B_{MAX.} + B_r = \Delta B_3 + \Delta B_4$$

By averaging the data,

$$B_{MAX.} = \left[\frac{\Delta B_1 + \Delta B_2 + \Delta B_3 + \Delta B_4}{2} \right]_{AVE.}$$

$$B_r = \frac{[\Delta B_3 + \Delta B_4]_{AVE.} - [\Delta B_1 + \Delta B_2]_{AVE.}}{2}$$

Relations permitting the calculation of the B's corresponding to H_x and to $-H_x$ are

$$(B)_{H_x} = B_{MAX.} - \Delta B_1$$

$$= B_r + \Delta B_2$$

or

$$(B)_{H_x} = \frac{B_{MAX.} + B_r + \Delta B_2 - \Delta B_1}{2}$$

$$(B)_{-H_x} = \Delta B_4 - B_{MAX.}$$

$$= B_r - \Delta B_3$$

or

$$(B)_{-H_x} = \frac{B_r - B_{MAX.} + \Delta B_4 - \Delta B_3}{2}$$

The coercive force is found from a plot of the B-h data obtained. The rest of the hysteresis loop is drawn from symmetry.

In estimating the errors of these measurements it is easily seen that the greatest source of error is the ballistic galvanometer. The error in field is relatively small even at the low field strengths. According to T. F. Wall (5) the demagnetizing factor for a ring specimen is zero, and hence there are no free poles induced in the specimen to reduce the field to a lower value than that calculated. If the errors in the quantities of $H = 1.257 \frac{I_1 \omega_1}{l_m}$ are I_1 to $\pm 0.5\%$, w_1 to $\pm 0.2\%$, and l_m to $\pm 0.2\%$, all of which precisions are easily obtainable, the percentage error in H is

$$\frac{\Delta H}{H} \times 100 = \sqrt{0.5^2 + 0.2^2 + 0.2^2} = 0.54\%$$

The deflection of the ballistic galvanometer can be read with a precision of $\pm 0.2\%$ for a deflection of 200 mm. and a precision of $\pm 4\%$ for a deflection of 10 mm., assuming that 0.4 mm. may be easily detected. The calibration from day to day may shift somewhat, sometimes as much as $\pm 2\%$. Hence the computation of $\frac{\Delta B}{B}$ from $B = \frac{R_2 bd}{2Aw_2} \times 10^8$, where the errors in R_2, A, and w_2 are negligible will be

$$\frac{\Delta B}{B} \times 100 = \sqrt{2^2 + .2^2} = 2\% \text{ maximum for a 200 mm. deflection}$$

$$\frac{\Delta B}{B} \times 100 = \sqrt{2^2 + 4^2} = 4.5\% \text{ maximum for a 10 mm. deflection}$$

C. Measurement of Resistivity.

1. Room Temperature Measurement of Resistivity. The arrangement of potentiometer, standard resistance, specimen, resistors, etc., is shown in Figure 6. The specimen rests on

FIGURE 6

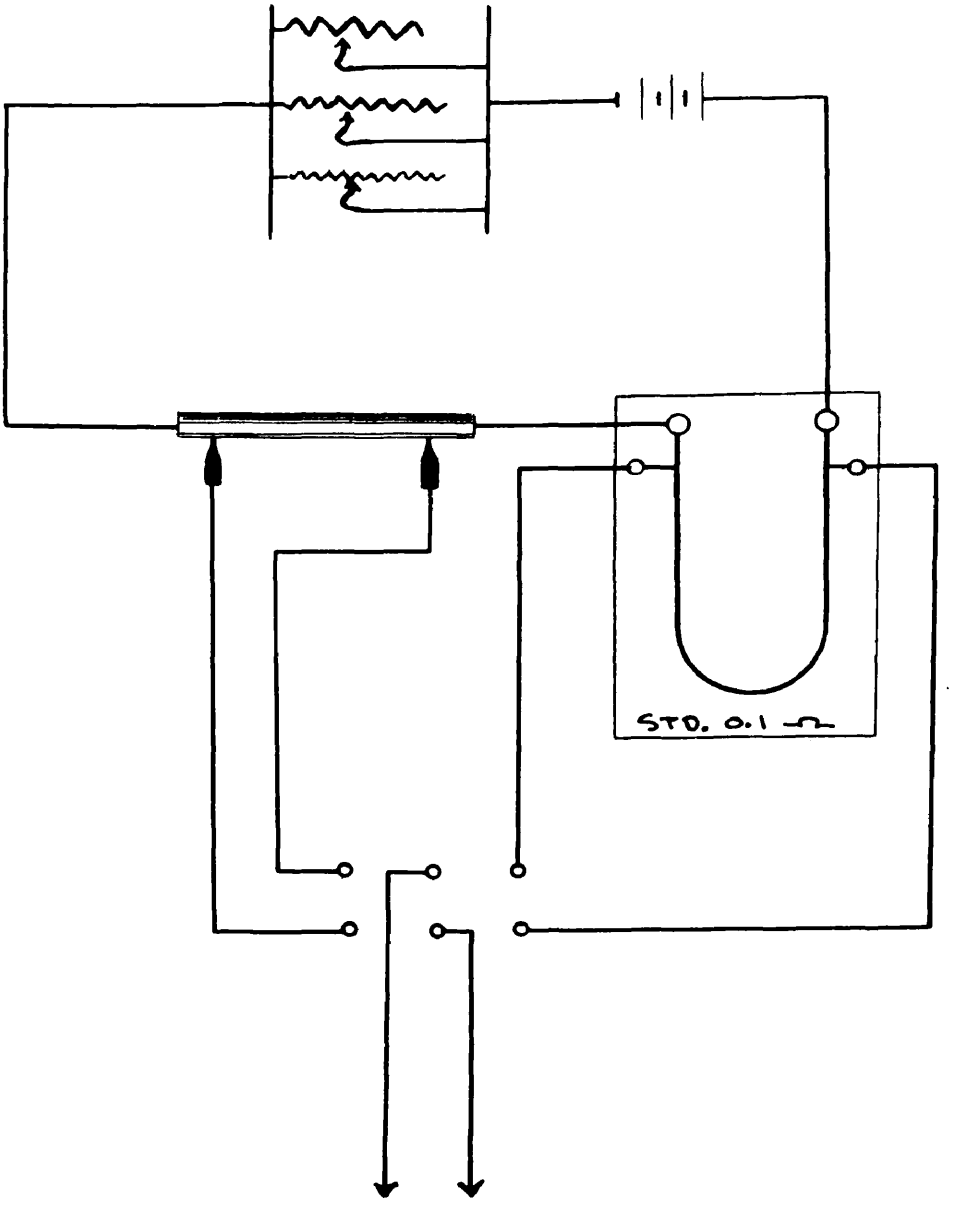

CIRCUIT USED FOR MEASURING RESISTIVITY AT ROOM TEMPERATURE

knife edges which are connected to the emf. terminals of a type K potentiometer. The distance apart of the knife edges was determined with a 22 cm. vernier caliper, Starrett No. 122 M, and an ohm-meter connected across the blades. When the calipers had just made contact with the inside of the blades, the ohm-meter would swing from an indication of infinite resistance to an indication of a very small resistance. This distance plus the thickness of one blade was taken as the distance between the knife edges. Current from a 6 volt battery was passed through a current controlling parallel set of rheostats a standard 0.1 ohm resistance, and the specimen. The double pull double throw switch was set to apply the standard resistance potential leads to the emf. terminals of the potentiometer, which was set for a balance at either 2-1/2, 3 or 4 amperes, and the rheostats were adjusted until a balance was reached. The potential leads of the specimen were then applied to the emf. terminals of the potentiometer by means of the switch and the voltage drop across the known distance between the knife edges when the known current was passing through the specimen was determined. The cross-sectional area of the rods was determined with a good micrometer caliper, 2-1/2 cm. Starrett No. 230 M. After obtaining good checks as to the resistance of the rod at several currents, the resistivity was calculated from $\rho = \frac{R A}{\ell}$ (see theoretical section, part C). Since A is good to $\pm 0.1\%$ and ℓ to $\pm 0.1\%$, ρ is good to $\sqrt{.1^2 - .1^2} = 0.14\%$.

2. <u>High Temperature Measurement of Resistivity</u>. The use of knife edges or similar devices whose length may be mea-

sured directly was not considered feasible at high temperatures. A satisfactory substitute for this type of potential leads was a pair of heavy contacts fastened firmly on to the specimen by set screws. The equivalent length between the contacts was calculated from the resistance between them, as measured by an ammeter-potentiometer method at room temperature, and the data obtained by a previous determination at room temperature by the potentiometer method above. Thus, if R_x was the resistance found between the heavy contacts and R_ℓ that between the knife edges of distance apart ℓ cm. by the direct method, the equivalent length between the heavy contacts is

$$\ell_x = \frac{R_x}{R_\ell} \ell_\ell \text{ cm.}$$

This length was assumed to remain constant at the higher temperature, which it will to 1% at least. Then, in order to make a measurement of resistivity at higher temperatures, a current I is passed through the specimen, and voltage V_T found between the potential. The resistivity is

$$\rho = \frac{V_T A}{I \ell_x} \quad \text{ohms per cm.}^3$$

The probable error in ρ, assuming V_T good to 0.5%, A to 0.1%, I to 0.5%, and ℓ_x to 1% is $\sqrt{.5^2 + .1^2 + .5^2 + 1^2} = 1.2\%$. However, the scatter of data will not be that high since the sources of error will probably lead to a slowly changing systematic error as the temperature rises.

A single value of current of 3.00 amperes was used in all temperature runs.

D. High Temperature Runs.

The arrangement of gas train, furnaces, and measuring apparatus used in making a temperature run of inductance, effective resistance, and resistivity in a nickel-manganese alloy put into a given state of order by prolonged annealing at high temperature is shown in Figure 7. A variac proved very convenient for controlling the rate of heating of the furnace containing the specimen. The procedure followed in making a temperature run was as follows:

1. The resistivity at room temperature was accurately determined by the potentiometer-knife edge method.

2. The specimen was inserted in the solenoid, the current and potential leads were firmly clamped, and the specimen holder put into the measuring furnace. The apparatus was made gas tight. The solenoid leads were inserted into the bridge, and the oscillator and detector started.

3. A measurement of resistance was made at room temperature in order to fix the equivalent length between the potential leads.

4. Hydrogen was swept through the gas train and apparatus, and the furnace with the tube of copper turnings started up.

5. The thermocouple potentiometer was set at a desired millivoltage at which the first set of readings was to be taken, and the current through the furnace set at a value to heat the specimen to that temperature at about 2° C per minute. When the galvanometer needle swung almost over to

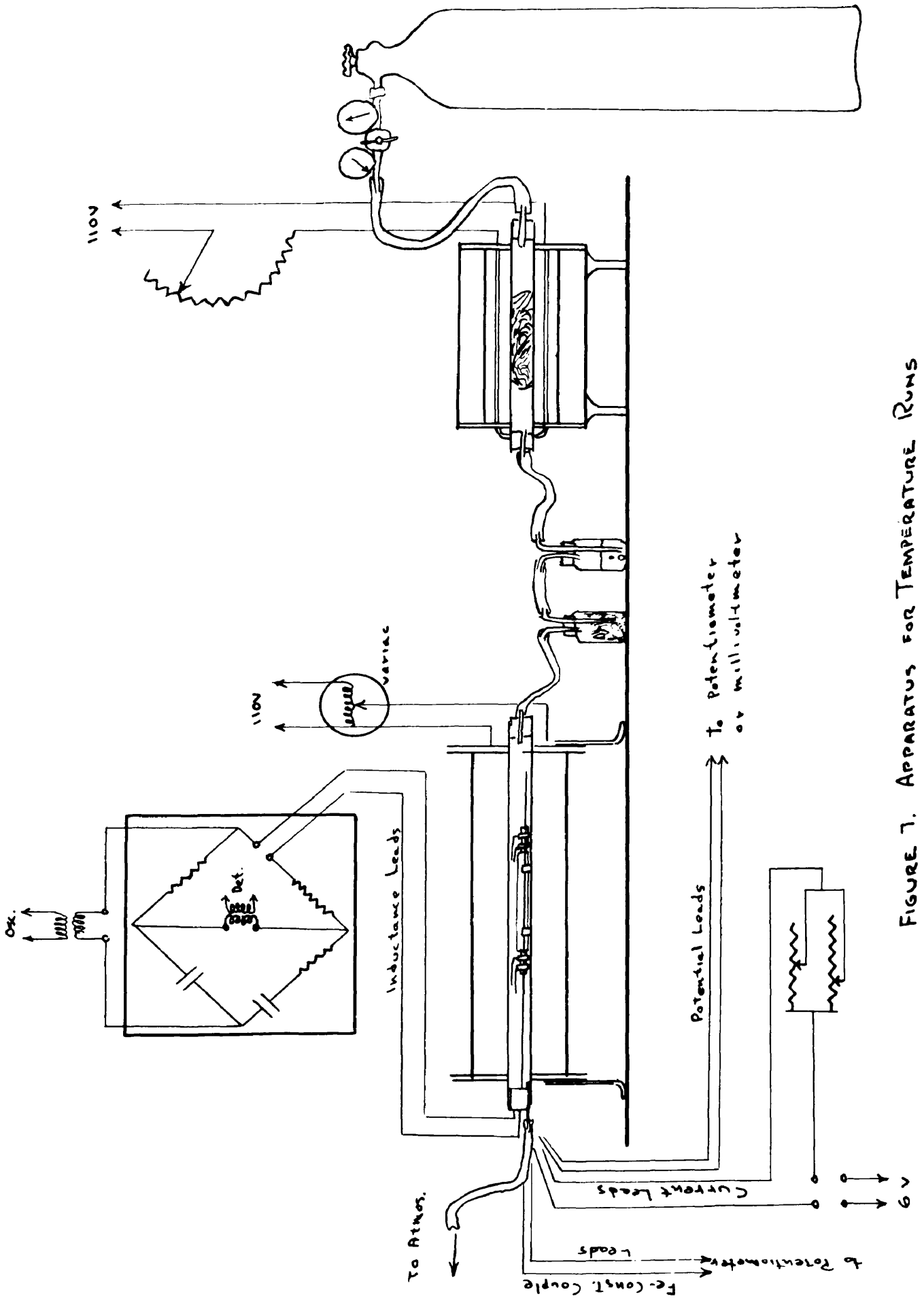

FIGURE 7. APPARATUS FOR TEMPERATURE RUNS

the balanced position, the rate of heating was cut down so that the furnace would slowly coast over the desired temperature, allowing the measurements to be made.

6. The bridge was balanced and while the specimen was at temperature, the millivoltage across the potential leads was determined when 5 amperes flowed through the specimen. These data were then recorded and the heating started up again.

7. Between readings the millivoltage across the potential leads with no current flowing was determined in order to evaluate any thermal or parasitic emf's. so that the millivoltage with current flowing might be evaluated.

E. Thermoelectric Measurements.

These measurements were made in an attempt to show thermoelectric evidence of the magnetic Curie temperature as well as the onset of order. Accordingly, a length of Q62 alloy in wire form, about 22 ga., in a disordered condition was brazed on the junction of a National Bureau of Standards standard chromel-alumel thermocouple, thus producing two thermocouples: The chromel-alumel for measuring temperature of the junction and the Q62-alumel for measuring the emf. of Q62 against a standard at the same temperature. A diagram of the arrangement of the couples and measuring apparatus is shown in Figure 8. The two couples were put into a furnace and heated up to 540° C at a rate of about 2° C per minute, the emf's. between 0° C and T being read simultaneously on two portable potentiometers.

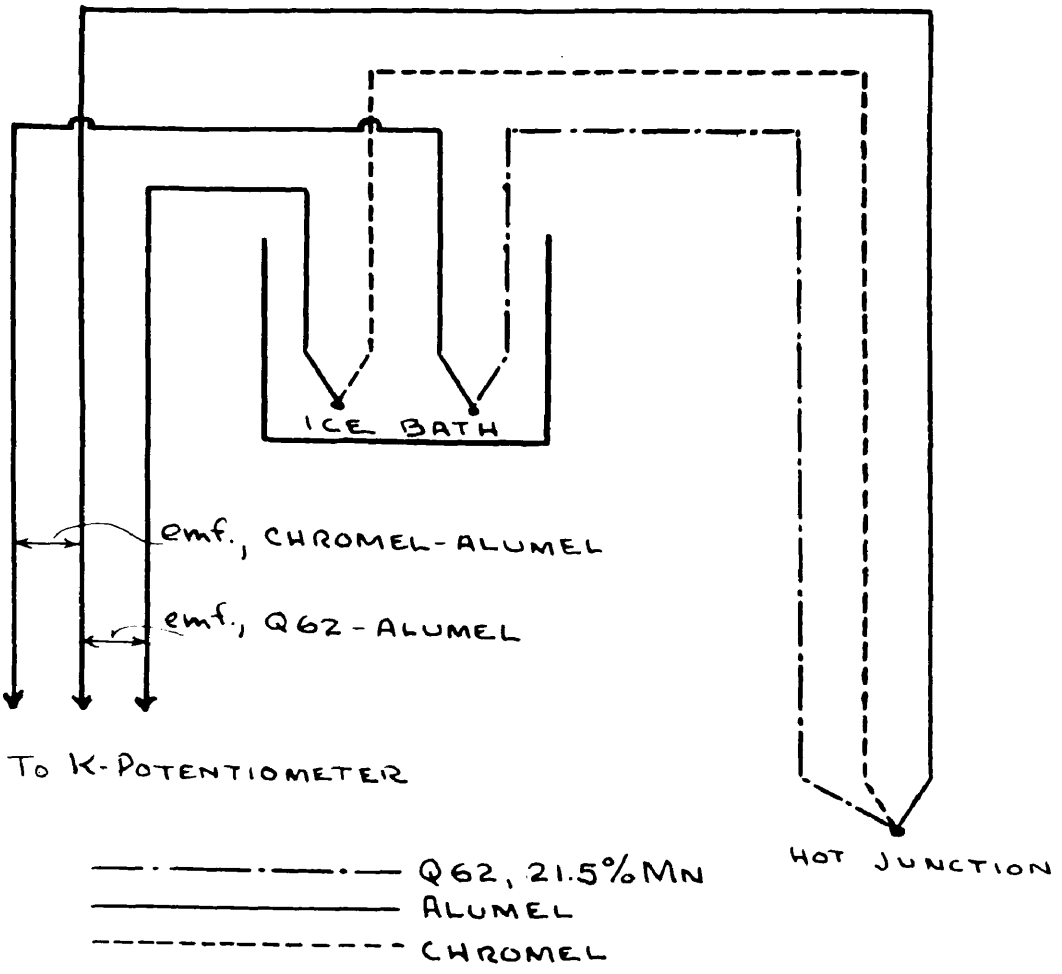

FIGURE 8. THERMOELECTRIC CIRCUIT

The couples were then cooled at the rate of about 1° C per hour, the emf's. between 0° C and T being measured on a K-potentiometer. This cooling rate was not a constant, the temperature being lowered about 5° C at a time, readings being taken at each interval for several hours until they became constant.

V. APPARATUS AND CALIBRATIONS

A. High Frequency.

The oscillator was a rather old, tuned-circuit Western Electric, W. E. 210. Its wave form was not very pure, but it proved satisfactory for the measurements made. It could be set at a desired frequency by using either a low or high frequency coil and a setting of three mica condenser decades and a variable air condenser. A frequency calibration made by Dr. E. V. Potter of the Bureau of Mines was available. This calibration was checked to within 1% by means of a General Radio, G. R. G13B, beat frequency oscillator and an oscillograph through the use of Lissajous figures. Two frequencies were used in the work, one at 46,500 cycles and the other at 50,000 cycles.

The detector was a visual cathode ray tube type using a 6E5 tube and is similar to that described by J. F. Koehler (22). Its sensitivity was sufficient to detect a bridge balance using the smallest of the resistance decades in the bridge.

The Owen bridge was set up on a G. R. Universal Bridge, Type 293A, which is a "fundamental bridge circuit which can be connected to produce a wide variety of direct and alternating current bridges" (23). The three variable resistors in it are accurate to 0.1% except the 1 ohm units which are accurate to 0.25%, and they are so wound that the bridge may be used up to

50,000 cycles (23). The 0.001μf condensers are of types G. R. 107f, and the shielded transformers of type G. R. 578C.

B. Resistivity.

The potentiometer used in the room temperature measurements was a Leeds and Northrup Type K, which is so well known as to need no further description. The standard resistance was a Leeds and Northrup 0.1 ohm, 15 ampere, standard. The ammeter used in determining resistivity at elevated temperatures was a 0-5 ampere Weston Model No. 45, and was calibrated with the K-potentiometer and 0.1 ohm resistance standard.

Table 1. Calibration of Weston No. 45 Ammeter No. 43957.

Weston (corr. for temp.) amperes	K-Potentiometer value amperes	Correction
0.502	0.489	-0.013
1.003	0.995	-0.008
1.505	1.495	-0.010
2.006	1.995	-0.011
2.508	2.504	-0.004
3.009	3.008	-0.001
3.510	3.508	-0.002
4.012	4.012	0.000
4.514	4.516	+0.002
5.015	5.019	+0.004

The millivoltage across the potential leads was measured by a Brown Model potentiometer or by the millivoltage ranges on a Sensitive Research Instrument Company Universal Polyranger, which was accurate to 0.25%.

C. Ballistic.

The ballistic galvanometer was a Leeds and Northrup Type HS No. 2285-d; it had a 27 second period, 640 ohm resistance, and a critical damping resistance of about 24,000 ohms. The galvanometer was used slightly underdamped with an external resistance circuit of 25,000 ohms. The calibration was made by charging a standard condenser with a standard cell and discharging the condenser through the galvanometer and 25,000 ohm shunt. With this arrangement it is easily shown that the ballistic constant is

$$b = \frac{R_x}{R_G + R_x} E_{s.c.} \frac{C}{d}$$

using $R_x = 25{,}000$, $R_G = 640$, and $E_{s.c.} = 1.0188_3$ volts

$$b = \frac{25000}{640 + 25000} \times 1.0188 \frac{C}{d} = 0.996 \frac{C}{d} \ \mu coul/mm.$$

where b is the ballistic constant in μcoul. per mm., C is the capacity of the condenser in μf, and d is the galvanometer throw in mm. One of the calibrations made is shown in Figure 10.

D. Solenoid and Mounting.

A photograph of the solenoid, mounting, and resistivity leads is shown in Figure 11. The solenoid consisted of a single layer winding of No. 38 ga. platinum wire, 92 turns per inch, 3-7/8 inches long, on a 6-inch length of fused silica tubing, 0.956 cm. in diameter. A plot of the field calculations made from the dimensions and constants of the solenoid is given in Figure 12. The winding was insulated by a coating of alundum cement. The leads from the solenoid to the bridge were of No. 22 ga. pure silver wire. A small iron-constantan

Figure 8. Shielded Owen Bridge for High Frequency Measurements

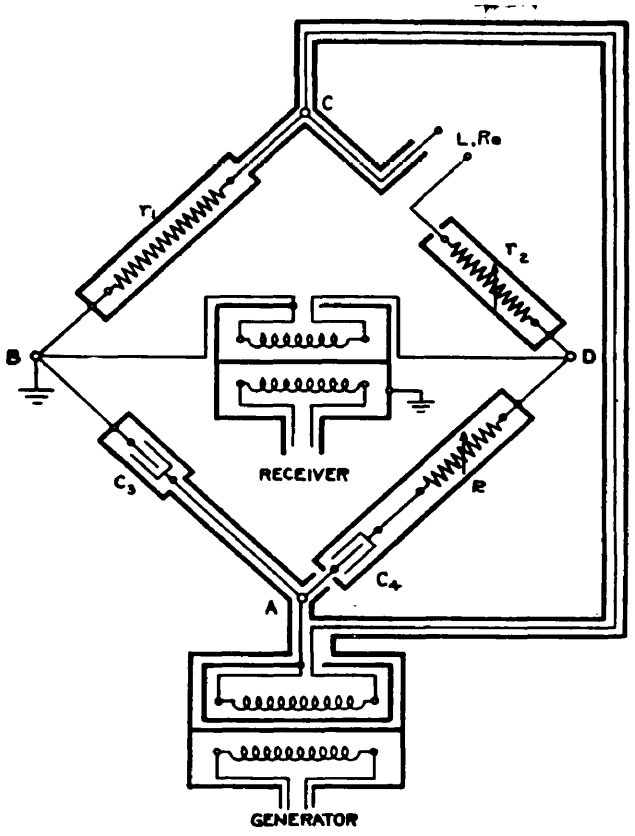

Generator: Western Electric W. E. 610 oscillator.

Receiver: 6E5 Electric Eye, two stage detector.

Shielded Transformers: General Radio Type 578C.

r_2 and R: 4-Decade shielded resistors, G. R. Type 602J.

r: Shielded resistor, (1000 ohm), G. R. Type 602

C_3 and C_4: 0.001 f Mica condensers, G. R. Type 107f.

FIGURE 10. CALIBRATION OF BALLISTIC GALVANOMETER

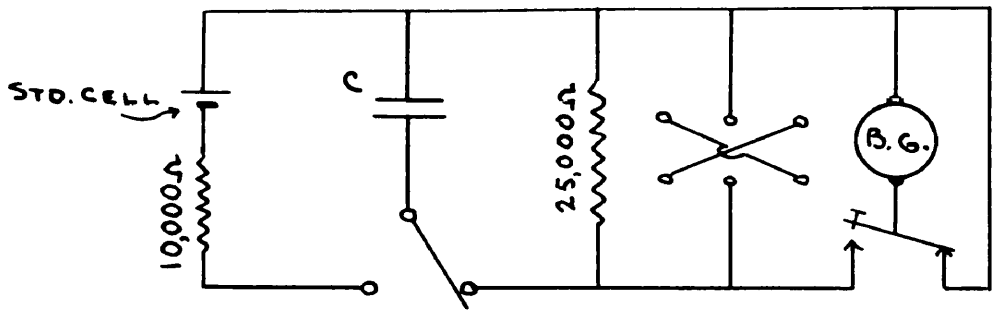

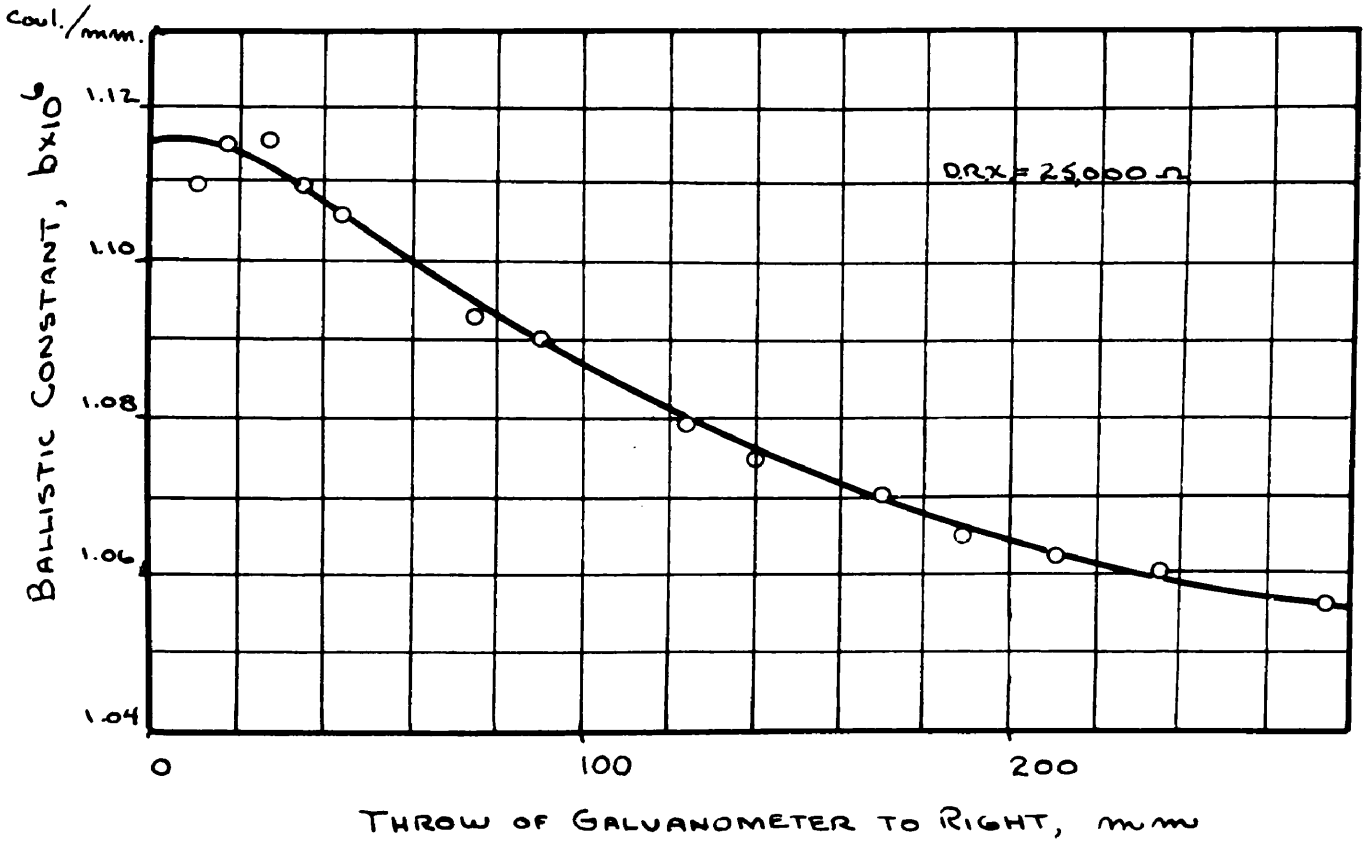

Figure 11. Solenoid, Resistivity Leads, and Supports.

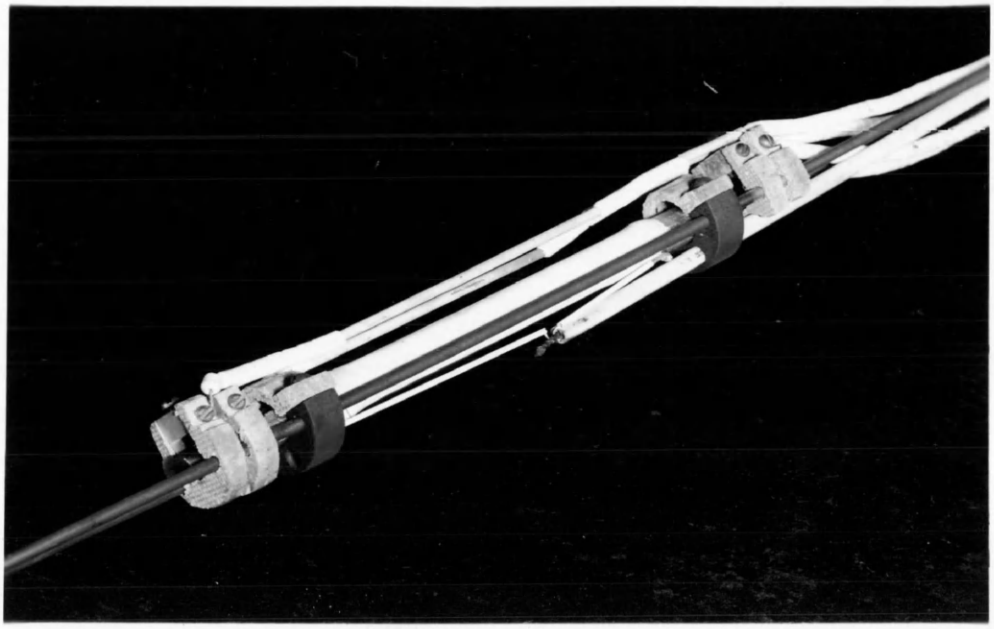

This view is from the side and slightly underneath. Visible are the solenoid, the central alundum insulated quartz tube; the specimen, seen projecting from the solenoid at the left; the thermocouple and solenoid leads, on the under side going into the 4-hole ceramic tube; and the resistivity current and potential leads fastened to the specimen.

FIGURE 12.

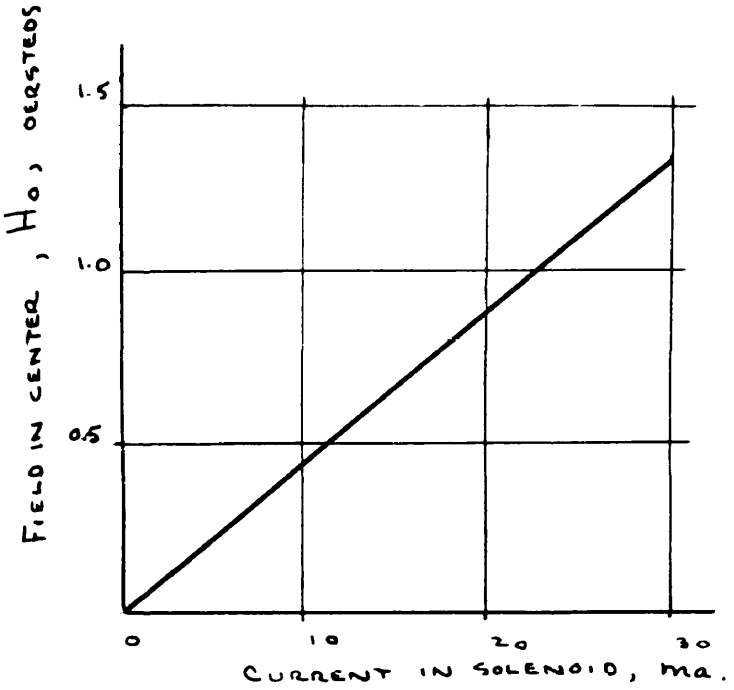

VARIATION OF FIELD AT CENTER OF SOLENOID WITH EXCITING CURRENT.

DISTRIBUTION OF FIELD IN SOLENOID

H= FIELD AT ANY POINT ON AXIS

H_0= FIELD IN CENTER, ON AXIS

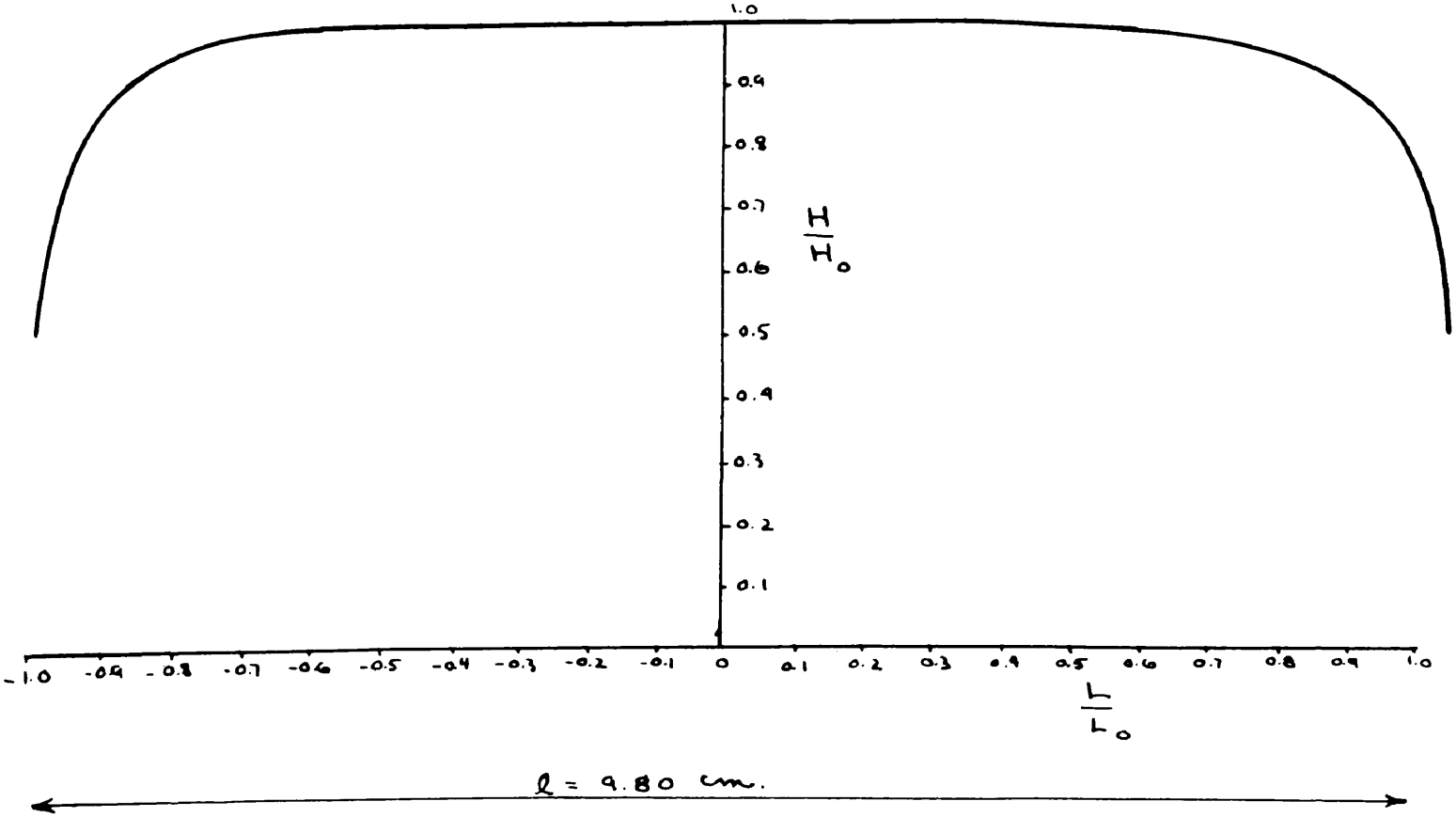

thermocouple was mounted under the solenoid. The calibration of the second iron-constantan couple used against a Bureau of Standards standard chromel-alumel thermocouple is given in a difference table, which was derived from the data obtained.

Table 2. Calibration of Iron-Constantan Thermocouple. Difference between Millivoltages of Couple and the Millivoltages in the Leeds and Northrup Tables.

Observed Millivoltage	Correction for L. & N. Tables	Observed Millivoltage	Correction for L. & N. Tables
2.00	-0.02	15.00	-0.28
3.00	-0.03	16.00	-0.30
4.00	-0.04	17.00	-0.33
5.00	-0.06	18.00	-0.36
6.00	-0.07	19.00	-0.39
7.00	-0.09	20.00	-0.43
8.00	-0.11	21.00	-0.46
9.00	-0.13	22.00	-0.50
10.00	-0.15	23.00	-0.55
11.00	-0.17	24.00	-0.57
12.00	-0.20	25.00	-0.58
13.00	-0.22	26.00	-0.58
14.00	-0.25	27.00	-0.58

a. Furnaces and Temperature Control.

Two horizontal tube furnaces were designed and constructed for the purpose of giving constant temperature zones at least 10 inches long. This end was achieved by the use of long, very uniform windings of No. 18 Chromel A resistance wire. The overall length of winding was about 22 inches, and the insulation was made quite uniform. Two heater windings of about 8.5 ohms each were used, one to support the main heating load, and the other for control purposes. Also, for the

temperature controller, there was imbedded in the alundum cement insulation around the heaters, a bifilarly wound coil of wire having a high temperature coefficient of resistance, No. 36 ga. platinum in one furnace and No. 25 ga. Hytemco alloy in the other. The temperature controller was a bridge controlled thyratron circuit, described by M. Benedict (24). This controller had excellent sensitivity, but also an unfortunate tendency to drift when used for long anneals.

VI. MATERIALS AND SPECIMENS

The rods of nickel-manganese alloys were made of electrolytic manganese, which is about 99.5% pure, (25) and of electrolytic nickel. They were made by casting the alloy and swaging into rod form. The data of analysis and the dimensions of these rods are given in Table 3.

Table 3. Nickel-Manganese Rod Specimens.

Number	Analysis		Atomic composition		Diameter	Length
	Mn wt. %	wt. %	Mn at. %	Ni at. %	cm.	in.
461	24.4	75.2	26.1	73.9	0.675	7.5
462	23.2	76.9	24.4	75.6	0.672	10
463	21.5	78.5	22.7	77.3	0.673	7.5

Precautions were taken against oxidation of these rod specimens by sealing them in vacuum in pyrex tubes during long annealing times at elevated temperatures, and by making the temperature runs in a hydrogen atmosphere.

The nickel-manganese wire used in the thermoelectric measurements were made from a 7 inch length of 4-62 rod, which, by alternate drawing and annealing, was reduced in diameter until about 50 inches of No. 22 ga. wire was obtained.

The rings used in the ballistic measurements were also made from electrolytic manganese and electrolytic nickel. They were made by casting and forging plates of the desired manganese content. From these, rings of uniform dimensions were machined on a lathe. The analyses and dimensions of the three rings on which measurements were made are shown in Table 4.

Table 4. Nickel-Manganese Ring Specimens.

	B12	B22	B31
Analysis			
Manganese, wt. %	20.1	25.3	21.4
Nickel, wt. %	79.5	74.4	78.6
Atomic Composition			
Manganese, at. %	21.3	26.7	22.6
Nickel, at. %	78.7	73.3	77.4
Inside Diameter, cm.	5.510	6.160	5.766
Outside Diameter, cm.	6.752	7.405	7.055
Radial Thickness, cm.	0.621	0.623	0.645
Width, cm.	0.850	1.104	1.018
Cross-sectional Area, cm^2	0.528	0.688	0.657
Average Diameter, cm.	6.131	6.783	6.411
Average Circumference, cm.	19.26	21.31	20.14

There were three other ring specimens, machined from the same plates as those above; they are not listed, because most of the data was obtained with the above specimens. The ring specimens were protected from oxidation during annealing

by keeping them in a heavy iron bomb kept evacuated by a Hy-vac pump.

In some of the preliminary work a rod of electrolytic nickel, 10 inches long and 1/4 inch in diameter, was used.

VII. DATA AND SAMPLE COMPUTATIONS

A. Temperature Run with Rod Specimens.

1. Specimen: Q61 (24.4% Mn, 75.2% Ni) heated at 600° C 2-1/2 hours to disorder it, annealed in vacuum 87 hours at 425-430° C, air quenched on heavy copper plate.

2. Room temperature resistivity:

Current	Voltage	Resistance
2.500	0.00560	0.00224
3.000	0.00672	0.00224
4.000	0.00895	0.00223_8
5.000	0.01120	0.00224_0

Best value of $R = 0.00224_0$

Distance between knife edges = 15.68_3 cm.

Cross-sectional area = $\frac{\pi}{4} (0.675_6)^2 = 0.358_2$ cm^2

Resistivity = $\frac{0.002240 \times 0.3582}{15.683} = 51.18 \times 10^{-6}$ $\frac{\text{ohms}}{\text{cm}^3}$

3. Equivalent length between potential leads in furnace:

Temperature = 28° C

Current = 3.00 amperes

Voltage = 6.90 millivolts

Resistance = $\frac{0.00690}{3.00} = 0.00230$ ohms

$L = \frac{0.0023_0}{0.00224} \times 15.68 = 16.10$ cm

$$\therefore \rho = \frac{RA}{L} = \frac{V}{I} \frac{A}{\ell} = \frac{V' \times 0.3583}{3.00 \times 16.10} \times 1000 = 7.41\ V'$$

where V' is the millivoltage across the potential leads.

4. Bridge equations:

L = 1.067 (A-73) microhenrys

R_e = 1030 - B ohms

5. Alternating field within solenoid:

Frequency = 50,000 cycles

Vacuum thermocouple galvanometer displacement with 1000 ohms external = 4.5 divisions

$I_{R.M.S.}$ = 12.5 milliamperes

$I_{max.}$ = 2 x 12.5 = 17.7 milliamperes

$h_{max.}$ = 0.8 oersteds

6. Temperature data:

(a) High frequency data

Time	Temperature mv	T	A	B	Bridge A-76	L	R_e
9:10	2.02	38	478	860	402	429	164
9:25	3.00	56	529	844	453	483	180
9:41	4.01	76	607	820	531	566	204
9:58	5.00	93	744	771	668	712	253
10:22	6.00	112	863	718	787	840	306
10:42	7.11	131	997	649	921	983	375
11:03	7.86	145	1015	616	939	1000	408
11:15	8.74	160	1168	607	1092	1157	417
11:50	10.00	184	1060	652	1004	1071	372
12:24	11.00	201	1006	659	930	993	365
12:46	12.03	220	908	656	832	898	365
12:59	12.81	237	897	649	821	876	375
1:15	14.11	256	868	631	793	845	393
1:28	14.93	270	860	615	784	836	409
1:47	16.20	292	845	583	769	820	441
2:02	17.05	307	822	566	746	796	458
2:19	18.00	324	740	575	664	708	449
2:36	19.00	342	524	645	448	477	379
2:55	20.00	356	367	740	291	311	284
3:10	21.05	377	275	790	199	212	234
3:34	22.10	396	241	796	165	176	228
3:50	23.10	413	226	797	150	160	227
4:02	24.15	431	219	794	143	153	230
4:16	25.10	448	217	790	141	150	234
4:26	26.10	467	216	786	140	149	238
4:47	27.46	490	216	780	140	149	244

6. Temperature data (continued):

(b) Resistivity Data

T	V_o	V	V_c	ρ
38	0	6.99	6.99	51.8
56	0	7.14	7.14	52.9
76	0	7.29	7.29	54.0
93	0	7.46	7.46	55.4
112	0	7.61	7.61	56.4
131	0	7.80	7.80	57.8
145	0	7.92	7.92	58.7
160	-0.01	8.04	8.05	59.6
184	-0.02	8.26	8.28	61.4
201	-0.02	8.41	8.43	62.4
220	-0.03	8.60	8.63	63.9
237	-0.03	8.73	8.76	65.0
256	-0.04	8.91	8.95	66.4
270	-0.04	9.03	9.07	67.2
292	-0.04	9.25	9.29	68.8
307	-0.05	9.39	9.44	69.9
324	-0.05	9.56	9.61	71.2
342	-0.05	9.76	9.81	72.8
359	-0.06	9.92	9.98	73.9
377	-0.05	10.10	10.15	75.2
396	-0.05	10.30	10.35	76.6
431	-0.04	10.64	10.68	79.0
448	-0.03	10.80	10.83	80.4
490	-0.04	11.01	11.05	82.0

B. Magnetization Curve.

1. Specimen: B31 (21.4% Mn, 78.6% Ni) cooled from 440° C to 380° C in 115 hours.

2. Windings:

Primary = 262.0 turns

Secondary = 100.0 turns

3. Equations:

$$H = \frac{1.257\ I_1 w_1}{\ell_m} = \frac{1.257\ I_1 \times 262.0}{20.14} = 16.35\ I_1$$

$$b = \frac{b\ R_2\ d_c}{2\ A w_2} \times 10^8 = \frac{b' \times 10^{-8} \times 25640 \times 10^8 d_c}{2 \times 0.657 \times 100.0} = 19.51\ b' d_c$$

4. Temperature = 31.5° C

5. Data:

H	I	d_o	d	d_c	b^1	B	μ
0.1	0.00612	118.4	135.2	16.8	1.115	365	3650
		117.6	134.3	16.7			
0.25	0.0153	118.4	180.0	61.6	1.098	1323	5300
		118.2	180.0	61.8			
0.5	0.036	118.0	215.7	97.7	1.086	2075	4050
		117.6	215.4	97.8			
0.75	0.0459	118.0	232.8	114.8	1.081	2443	3260
		117.3	232.2	114.9			
1	0.0612	117.5	244.4	126.9	1.078	2675	2675
		118.0	245.0	127.0			
2	0.1223	118.0	270.0	152.0	1.072	3185	1593
		117.6	269.7	152.1			
5	0.306	117.6	293.3	175.7	1.067	3560	712
		118.0	293.8	175.8			
10	0.612	117.9	301.1	183.2	1.066	3810	381
		117.3	300.8	183.5			
20	1.223	117.3	304.3	187.0	1.065	3880	194
		118.0	304.7	186.7			
30	1.836	118.0	306.0	188.0	1.065	3810	130
		117.7	304.7	-----			

C. Hysteresis Loop.

1. Specimen: As above

2. Windings: As above

3. Equations:

$$H = 16.35\ I$$

$$B = \frac{b\ R_2\ d}{A w_2} \times 10^8$$

$$= \frac{b' \times 10^{-9} \times 25640 \times 10^8 d}{0.657 \times 100.0} = 39.1\ b'd$$

4. Temperature = 28° C

5. Data:

H_1	H_2	d_o	d	d_c	D	H versus D
30	0	118.0	176.1	58.1	2500	30 : 3900
0	-30	118.0	245.0	127.0	5340	0 : 1420
					7840	
30	0.1	118.0	168.7	50.7	2200	
0.1	0	117.7	124.6	6.9	300	.1 : 1710
0	-0.1	117.7	132.2	14.5	630	
-0.1	-30	117.6	229.0	111.4	4710	-.1 : 800
					7840	
30	0.25	117.9	161.2	43.3	1870	
0.25	0	117.3	130.5	13.2	575	.25 : 2010
0	-0.25	117.4	174.2	56.8	2440	
-0.25	-30	117.3	184.5	67.2	2880	-.25 : -1020
					7765	
30	0.5	117.5	153.1	35.6	1540	
0.5	0	117.2	138.2	21.0	915	.5 : 2350
0	-0.5	117.1	198.0	80.9	3450	
-0.5	-30	117.0	160.5	43.5	1880	-.5 : -2020
					7785	
30	0.75	117.3	148.0	30.7	1330	
0.75	0	117.0	143.2	26.2	1140	.75 : 2560
0	-0.75	117.0	207.0	90.0	3840	
-0.75	-30	117.0	151.9	34.9	1515	-.75 : -2400
					7825	
30	1	117.3	143.7	26.4	1150	
1	0	117.0	147.5	30.5	1325	1 : 2750
0	-1	117.1	213.1	96.0	4080	
-1	-30	117.1	146.9	28.8	1255	-1 : 2550
					7810	
30	2	117.3	133.7	16.4	715	
2	0	117.0	157.6	40.6	1760	2 : 3180
0	-2	117.0	225.2	108.2	4580	
-2	-30	117.5	134.2	16.7	730	-2 : -3166
					7785	
30	5	117.0	123.4	6.4	280	
5	0	117.0	168.5	51.5	2230	5 : 3640
0	-5	117.0	236.5	119.5	5030	
-5	-30	117.0	123.4	6.4	280	-5 : -3620
					7820	
30	10	117.0	119.7	2.7	120	
10	0	117.0	172.0	55.0	2370	10 : 3795
0	-10	117.0	240.0	123.0	5160	
-10	-30	117.0	119.8	2.8	120	-10 : -3760
					7770	
30	20	117.0	117.9	0.9	40	
20	0	117.0	173.7	56.7	2440	20 : 3860
0	-20	117.0	242.0	125.0	5250	
-20	-30	117.0	117.8	0.8	35	-20 : -3850
					7765	

5. Data (continued):

$2B_{max.}$	$B_m - B_r$	$B_m + B_r$
7840	2500	5340
7840	2500	5340
7765	2445	5320
7785	2455	5330
7825	2470	5365
7810	2475	5335
7785	2475	5310
7820	2510	5310
7770	2490	5280
7765	2480	5295
7800 av.	2480 av.	5320 av.

$B_{max.} = 1/2\ (7800) = 3900$

$B_r = 1/2\ (5320 - 2480) = 1420$

5. Data (continued):

$2B_{max.}$	$B_m - B_r$	$B_m + B_r$
7840	2500	5340
7840	2500	5340
7765	2445	5320
7785	2455	5330
7825	2470	5355
7810	2475	5335
7785	2475	5310
7820	2510	5310
7770	2490	5280
7765	2480	5285
7800 av.	2480 av.	5320 av.

$B_{max.} = 1/2\ (7800) = 3900$

$B_r = 1/2\ (5320 - 2480) = 1420$

VIII. RESULTS

A. Temperature Runs on Nickel and Nickel-Manganese Alloys.

1. Nickel. Figure 13. These curves show the type of results obtained by the experimental procedure when a normal ferromagnetic metal, nickel, is heated through its Curie temperature. The frequency used was 61,000 cycles.

2. Nickel-Manganese Alloys. Figures 14 to 26. A chronological list of the heat treatments and data pertaining to the results shown by these figures is given in the following tables.

Table 5. Thermal History of the Ni-Mn Alloy Rods.

Designation	Specimen	Heat Treatment
Figure 14	Q63 21.5% Mn	Sealed in vacuum in fused silica tubing. Heated to 1000° C in 2 hours, kept at temperature for 40 minutes, furnace cooled to 600° C, kept at temperature for 1 hour, and air-quenched on a metal plate. Annealed in the temperature range of 415-420° for one week, and air-quenched to room temperature. The run was made on the alloy in this condition, heating in hyorogen to 535° C and furnace cooling.
Figure 15	Q61 24.4% Mn	Sealed in vacuum in fused silica tubing. Heated to 1000° C in 2 hours, kept at temperature 40 minutes, cooled to 600° C, kept there for 1 hour, and air-quenched on a metal plate. Resealed in pyrex and accidentally heated for several hours at 800° C, cooled to 600° C and air quenched. The pyrex tube collapsed around the rod, but the vacuum held, and no permanent damage seemed to have been suffered. Annealed for 96 hours in the temperature range 410-415° C, and air-quenched. Run made on alloy in this condition, data was taken during the heating of the alloy to 464° C only, the alloy was then furnace cooled.
Figure 16	Q61 24.4% Mn	Alloy in condition after the run above given in Figure 15, was slowly heated in hydrogen to 452° C, and cooled at the same rate.
Figure 17	Q63 21.5% Mn	Alloy after run of Figure 14 and accidentally heated for several hours at 800° C, cooled to 600° C, and air-quenched. (See remarks in section on Figure 15). Annealed for 96 hours in the temperature range 410-415° C, and air-quenched. Run made on alloy in this condition, heating in hydrogen to 422°, and furnace cooling.

Table 5. Thermal History of the Ni-Mn Alloy Rods (contd.).

Designation	Specimen	Heat Treatment
Figure 18	Q63 21.5% Mn	Alloy in condition after the run above, given in Figure 17, was heated to and cooled from 452° C in a hydrogen atmosphere during the run.
Figure 19	Q63 21.5% Mn	After run of Figure 18 the alloy was heated in vacuum at 600° C for 2-1/2 hours, cooled to 425° C in 1 hour, annealed in the temperature range 425-430° C for 87 hours, and air-quenched. The temperature run was heating to and cooling from 486° C in a hydrogen atmosphere.
Figure 20	Q62 23.2% Mn	The alloy was accidentally heated in vacuum at 800° C for several hours, (see remark in Section on Figure 15). The alloy was then given the same heat treatment as Q63 above. The alloy was heated to and cooled from 486° C in a hydrogen atmosphere during the temperature run.
Figure 21	Q61 24.4% Mn	After the run of Figure 16 the alloy was given the same heat treatment as that of Q63 and Q62 above. The alloy was heated to and cooled from 490° C in a hydrogen atmosphere during the temperature run.
Figure 22	Q63 21.5% Mn Q62 23.2% Mn	After runs of Figures 19 and 20, the alloys were sealed in vacuum and heated to 495° C in 8 hours and kept there for 6 hours. The temperature was lowered to 460° in 2 hours, and the alloys were annealed in the temperature range 460-470° C for 94 hours and air-quenched. Data were taken on heating Q63 to 161° C and on heating Q62 to 404° C in a hydrogen atmosphere.

Table 5. Thermal History of the Ni-Mn Alloy Rods (contd.).

Designation	Specimen	Heat Treatment
Figure 23	Q61 24.4% Mn	Same heat treatment as above. Data were taken on heating the alloy to 435° C in a hydrogen atmosphere.
Figure 24	Q63 21.5% Mn	The alloy was heated in vacuum at 600° C for 30 minutes. Then it was given 16 hours at 440-445° C, cooled to 420° C and kept there for 7 hours, cooled to 384° C and kept there for 96 hours, cooled to 366° C and kept there for 48 hours, cooled to 354° C, and kept there for 40 hours, and air-quenched. Data were taken on heating to 324° C in a hydrogen atmosphere.
Figure 25	Q62 23.2% Mn	Same heat treatment as above. Data were taken on heating to 393° C in a hydrogen atmosphere.
Figure 26	Q61 24.4% Mn	Same heat treatment as above. Data were taken on heating to 465° C.

Table 6. Data Pertaining to Individual Runs.

Run	Bridge		Average Thermal Rates		Time in Ordering Range (350°-500°C) Minutes	
	Type	Frequency cy. sec.	Heating °C/sec.	Cooling °C/sec.	Heating	Cooling
Nickel	Owen	61,000	---	---	---	---
Q63, 168 hrs. at 415-420° C.	"	46,500	ca. 2	---	---	---
Q61, 96 hrs. at 410-415° C	Max-well	46,500	1.0	---	98	---
Q61, as above heated to 464° C	Owen	46,500	1.6	1.5	62	81
Q63, 96 hrs. at 410-415° C	"	46,500	2.5	---	21	---
Q63, as above heated to 422° C	"	46,500	3.0	1.8	36	52
Q63, 87 hrs. at 425-430° C	"	50,000	1.3	1.4	85	88
Q62 (as above)	"	50,000	1.0	1.1	140	106
Q61 (as above)	"	50,000	1.0	1.4	122	140
Q63, 94 hrs. at 460-470° C	"	50,000	0.8	---	0	---
Q62 (as above)	"	50,000	1.1	---	65	---
Q61 (as above)	"	50,000	1.1	---	105	---
Q63 slow cool to 350° C	"	50,000	1.0	---	0	---
Q62 (as above)	"	50,000	0.7	---	39	---
Q61 (as above)	"	50,000	0.9	---	55	---

Table 7. Curie Points and Quantities Derived from Runs.

Alloy	Condition	Curie Point θ_c	Approach to θ_c	Maximum Inductance Magnitude	Maximum Inductance Temperature
Q63	168 hrs. at 415-420° C	320° C	sharp	1355 h	60° C
21.5% Mn	96 hrs. at 410-415° C	280	moderate	970	38
	As above, heated to 422° C	300	gradual	1020	30
	87 hrs. at 425-430° C	320	sharp	1040	47
	As above, heated to 486° C	180	gradual	855	28
	94 hrs. at 460-470° C	80	gradual	185	24
	Slow cooled to 350° C	325	sharp	1000	110
Q62	87 hrs. at 425-430° C	360	sharp	1200	174
23.2% Mn	As above, heated to 482° C	260	gradual	920	46
	94 hrs. at 460-470° C	400	gradual	260	30
	Slow cooled to 350° C	390	sharp	1170	190
Q61	96 hrs. at 410-415° C	460	moderate	1050	167
24.4% Mn	As above, heated to 464° C	430	moderate	1000	151
	87 hrs. at 425-430° C	440	moderate	1155	160
	As above, heated to 490° C	370	gradual	520	26
	94 hrs. at 460-470° C	410	sharp	670	160
	Slow cooled to 350° C	470	very gradual	490	170
Nickel		368	very sharp	300	357

FIGURE 13

ELECTROLYTIC NICKEL

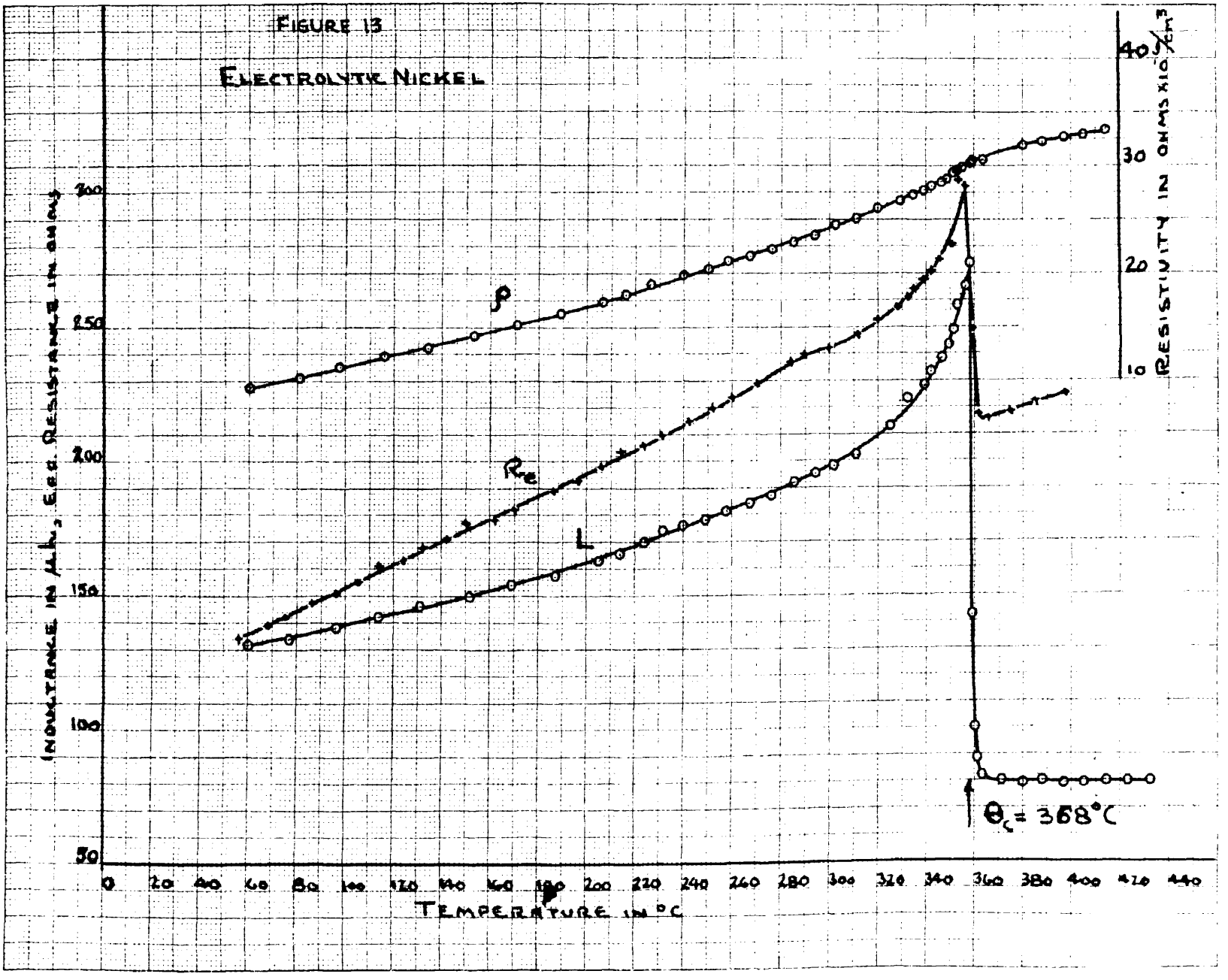

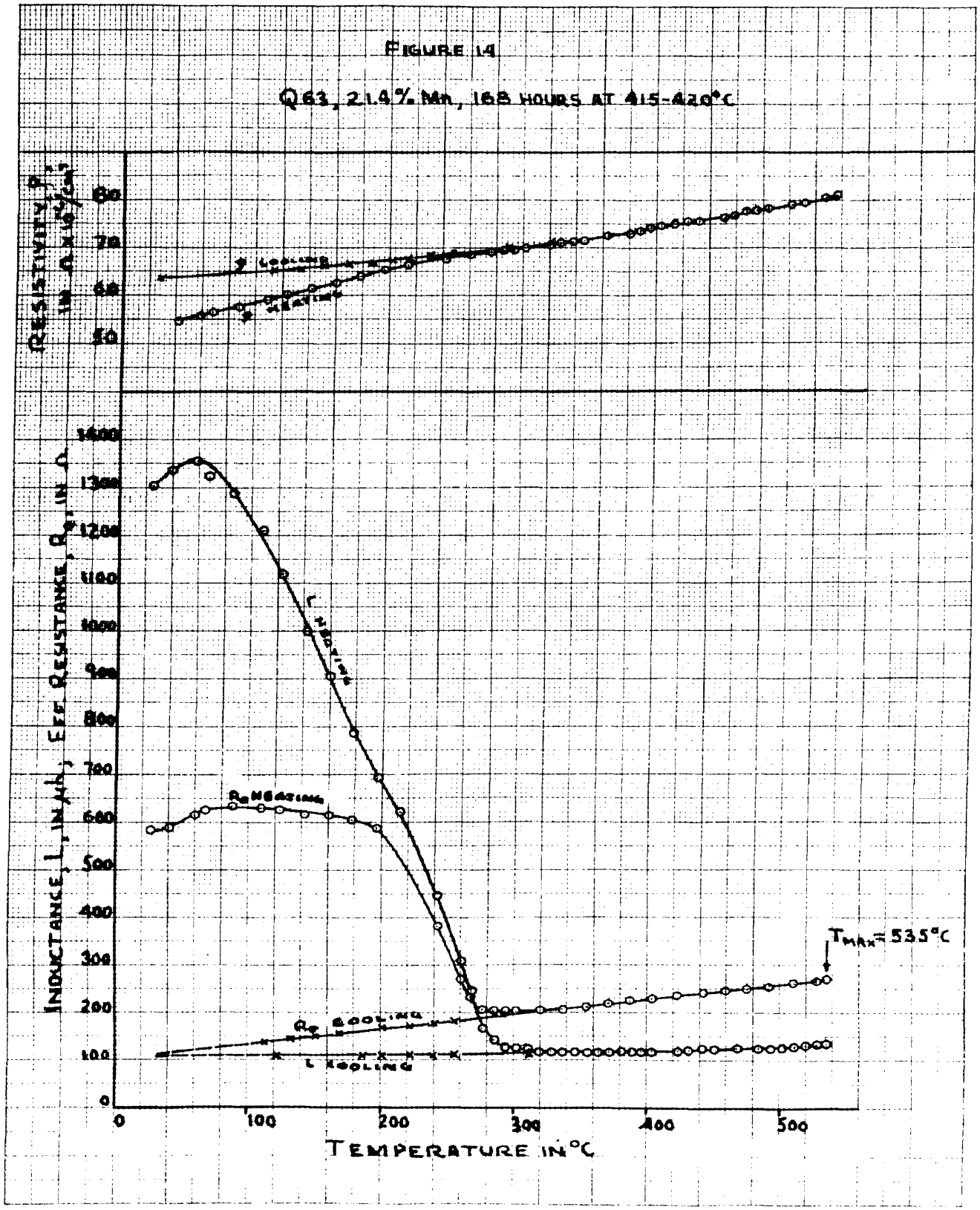
FIGURE 14
Q63, 2.14% Mn, 168 HOURS AT 415-420°C
RESISTIVITY, ρ, IN Ω x 10⁶ Ω/cm³
INDUCTANCE, L, IN μh; EFF. RESISTANCE, R_e, IN Ω
L HEATING
R_e HEATING
R_e COOLING
L COOLING
T_MAX = 535°C
TEMPERATURE IN °C
0
100
200
300
400
500

FIGURE 15

Q 61, 24.4% Mn, 96 HOURS AT 410-415°C

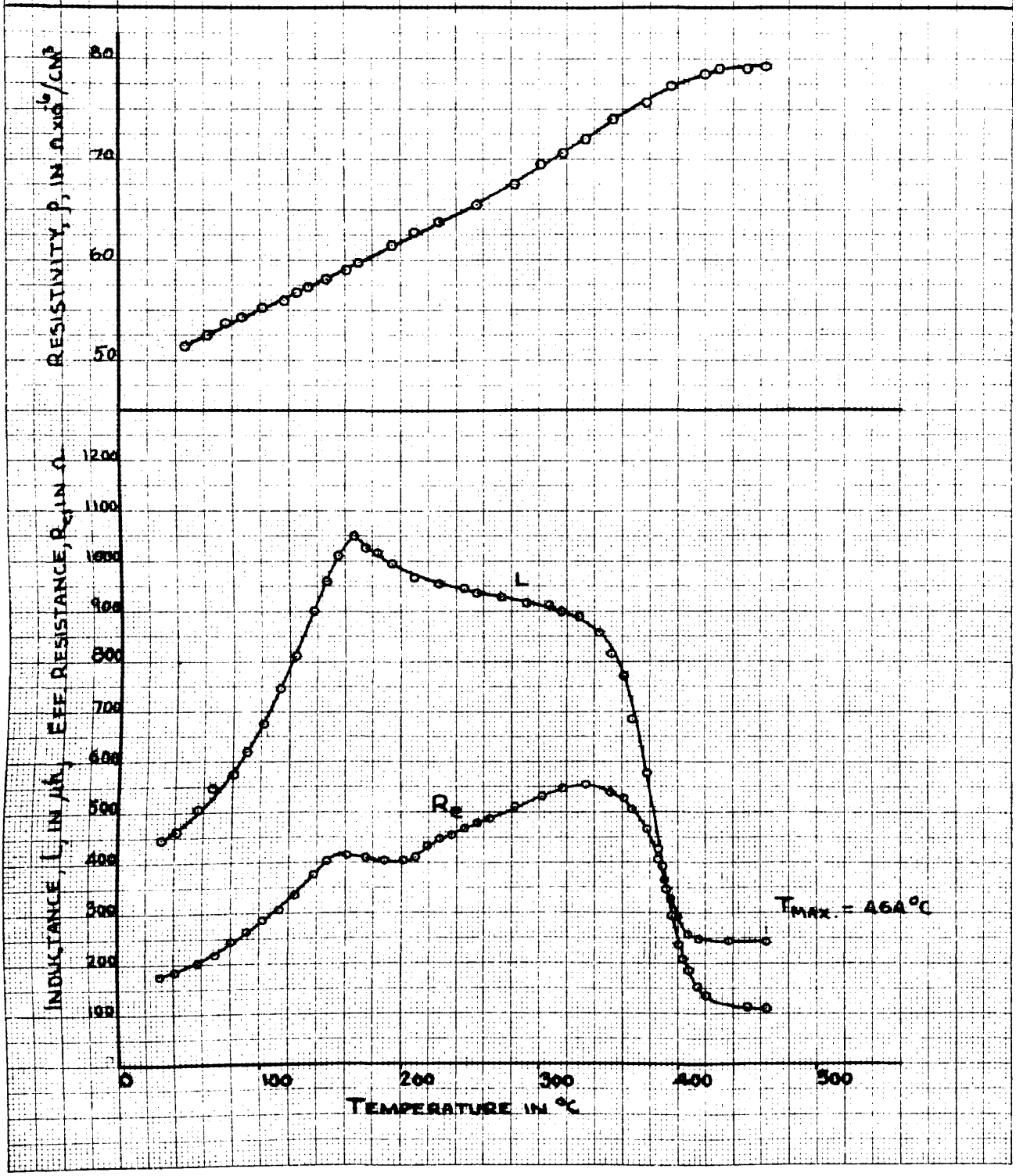

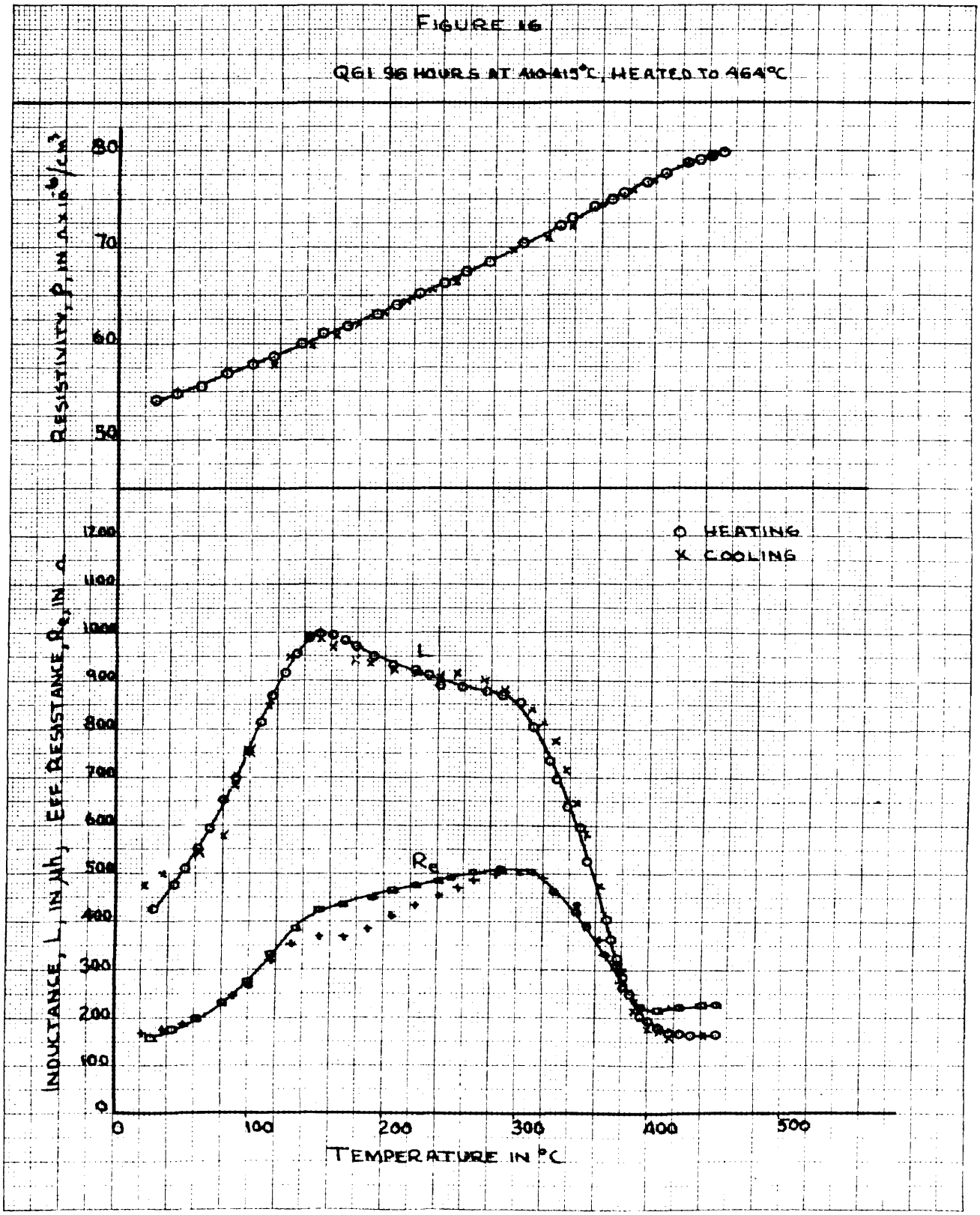
FIGURE 16
Q61 96 HOURS AT 410-415°C, HEATED TO 464°C
RESISTIVITY, ρ, IN Δ x 10⁻⁶ Ω/cm³
80
70
60
50
INDUCTANCE, L, IN μh; EFF. RESISTANCE, Rₑ, IN Ω
1200
1100
1000
900
800
700
600
500
400
300
200
100
0
HEATING
COOLING
L
Rₑ
0
100
200
300
400
500
TEMPERATURE IN °C

FIGURE 17

Q63, 2.14 % Mn, 96 HOURS AT 410-415°C

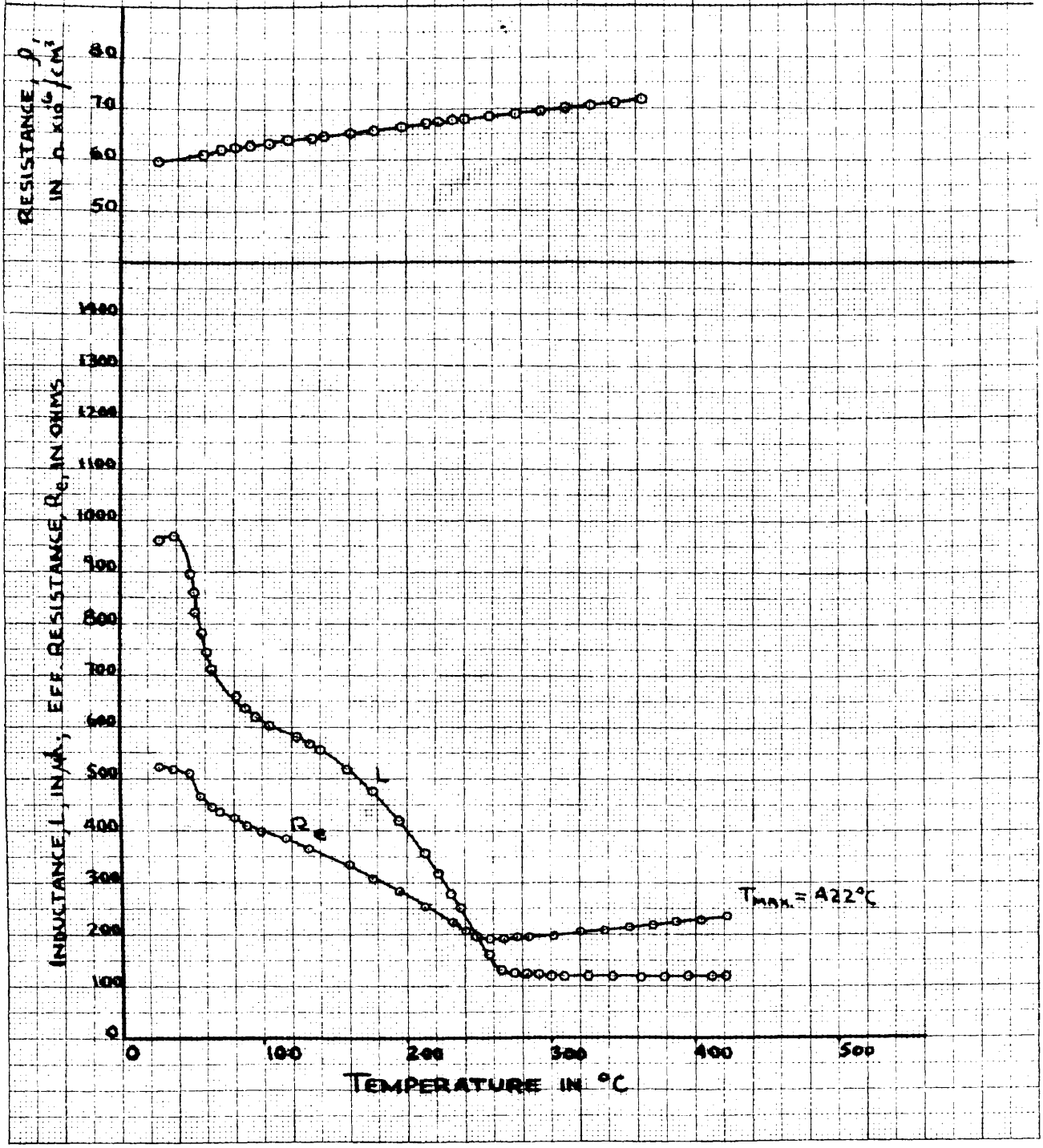

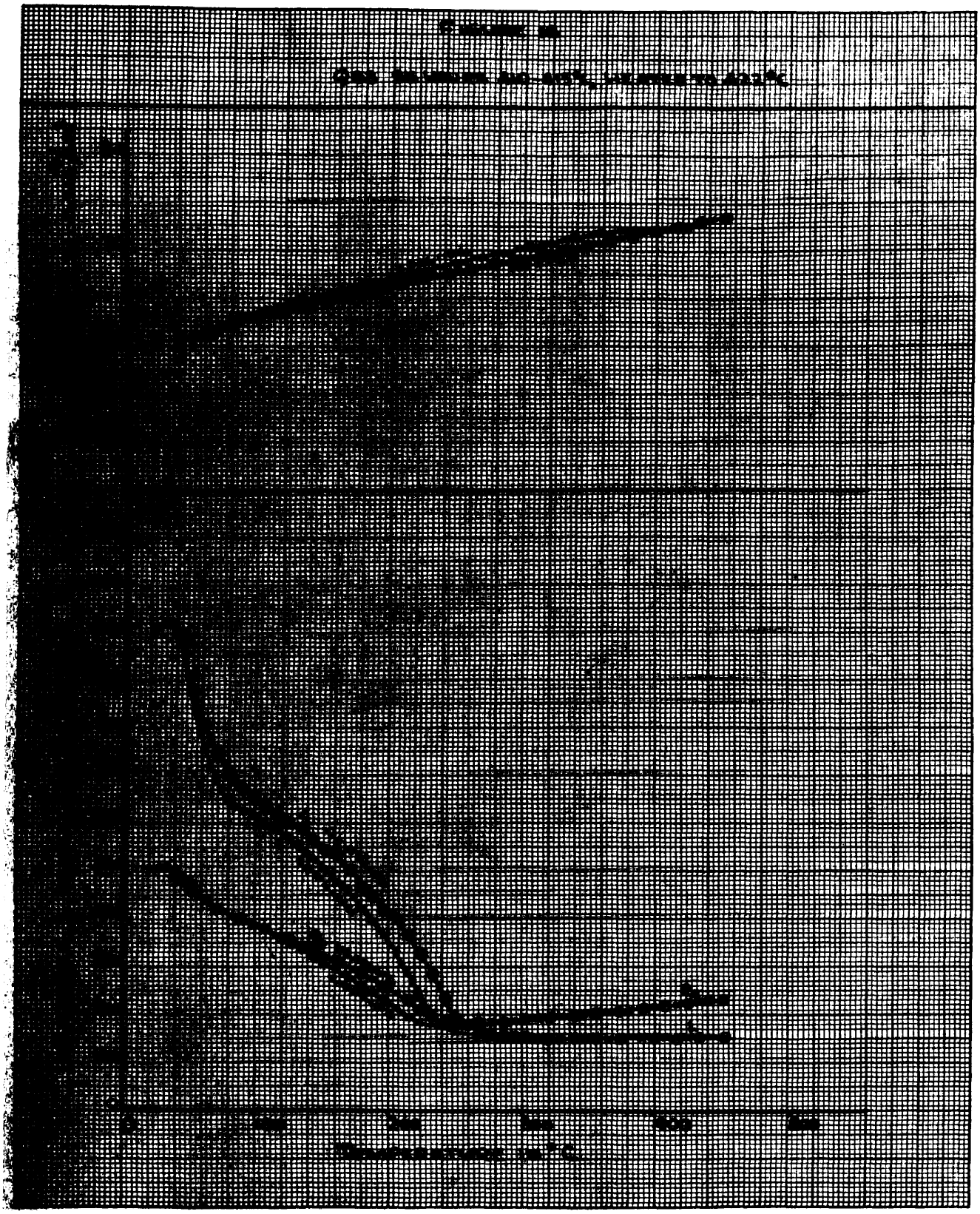

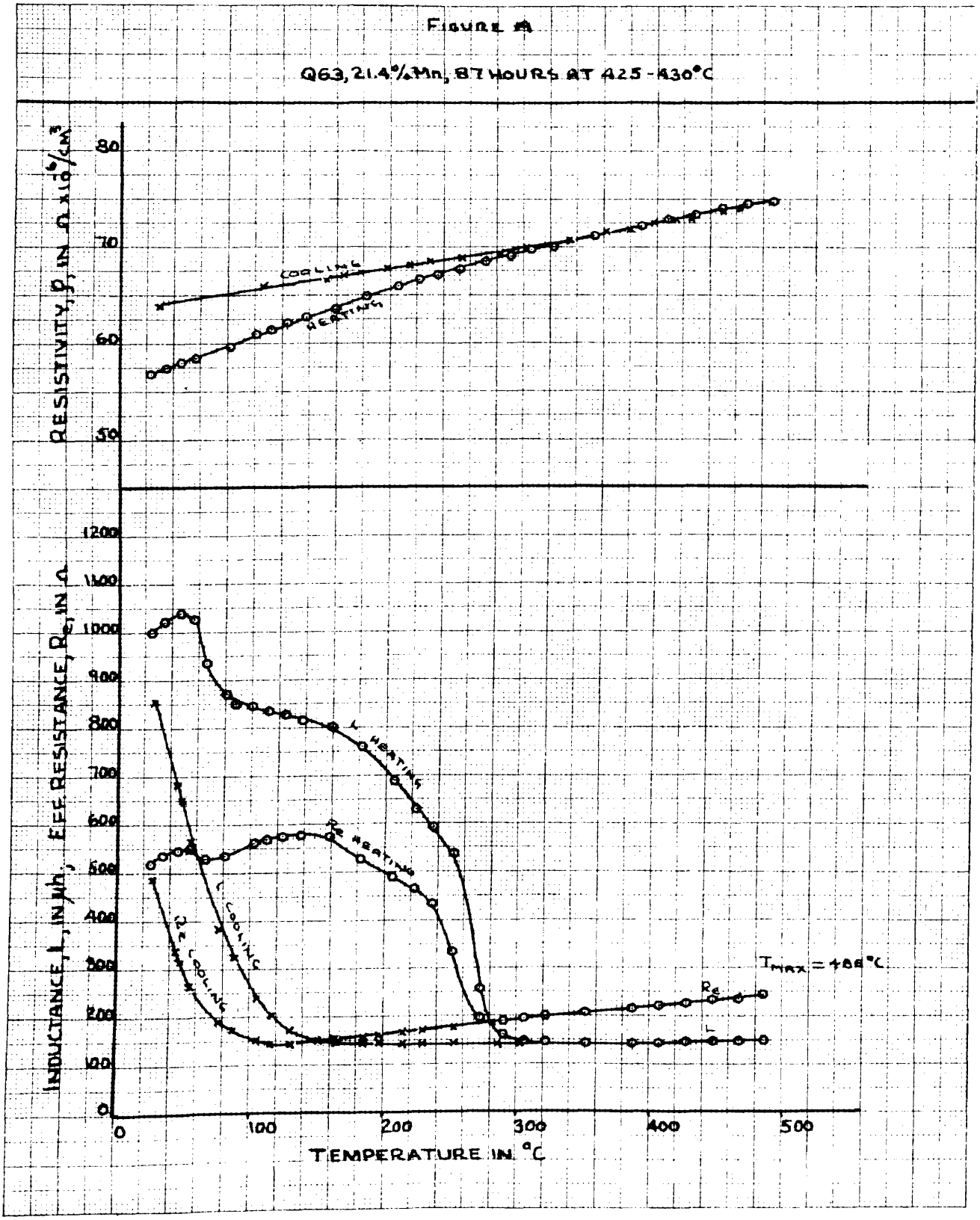
FIGURE 4
Q63, 21.4% Mn, 87 HOURS AT 425 - 430°C
RESISTIVITY, ρ, IN Ω x 10⁶/cm³
80
70
60
50
COOLING
HEATING
INDUCTANCE, L, IN μh, EFF. RESISTANCE, Rₑ, IN Ω
1200
1100
1000
900
800
700
600
500
400
300
200
100
0
L HEATING
Rₑ HEATING
L COOLING
Rₑ COOLING
T_MAX = 488°C
Rₑ
L
0
100
200
300
400
500
TEMPERATURE IN °C

FIGURE 20

Q62, 23.2% Mn, 87 HOURS AT 425-430°C

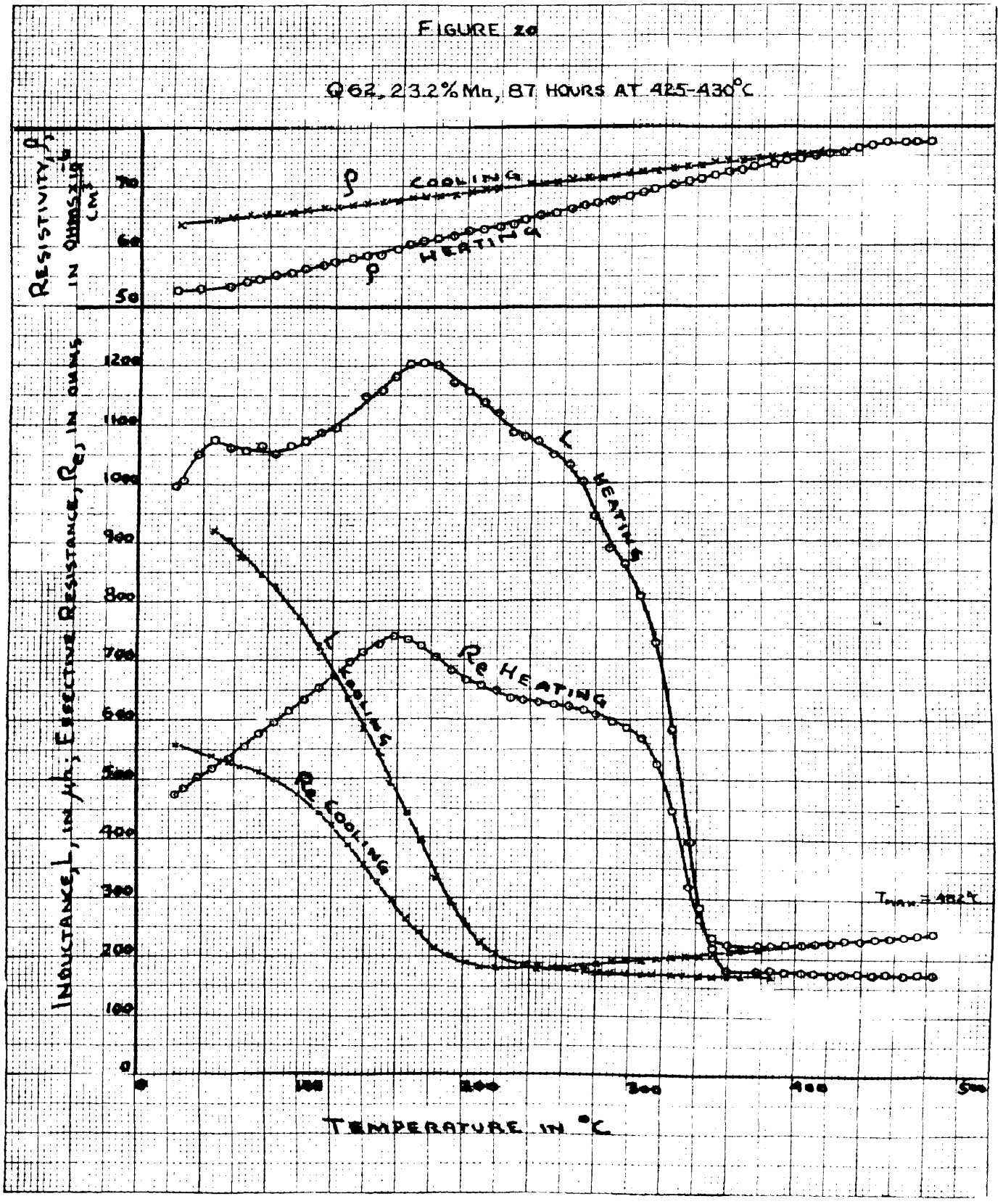

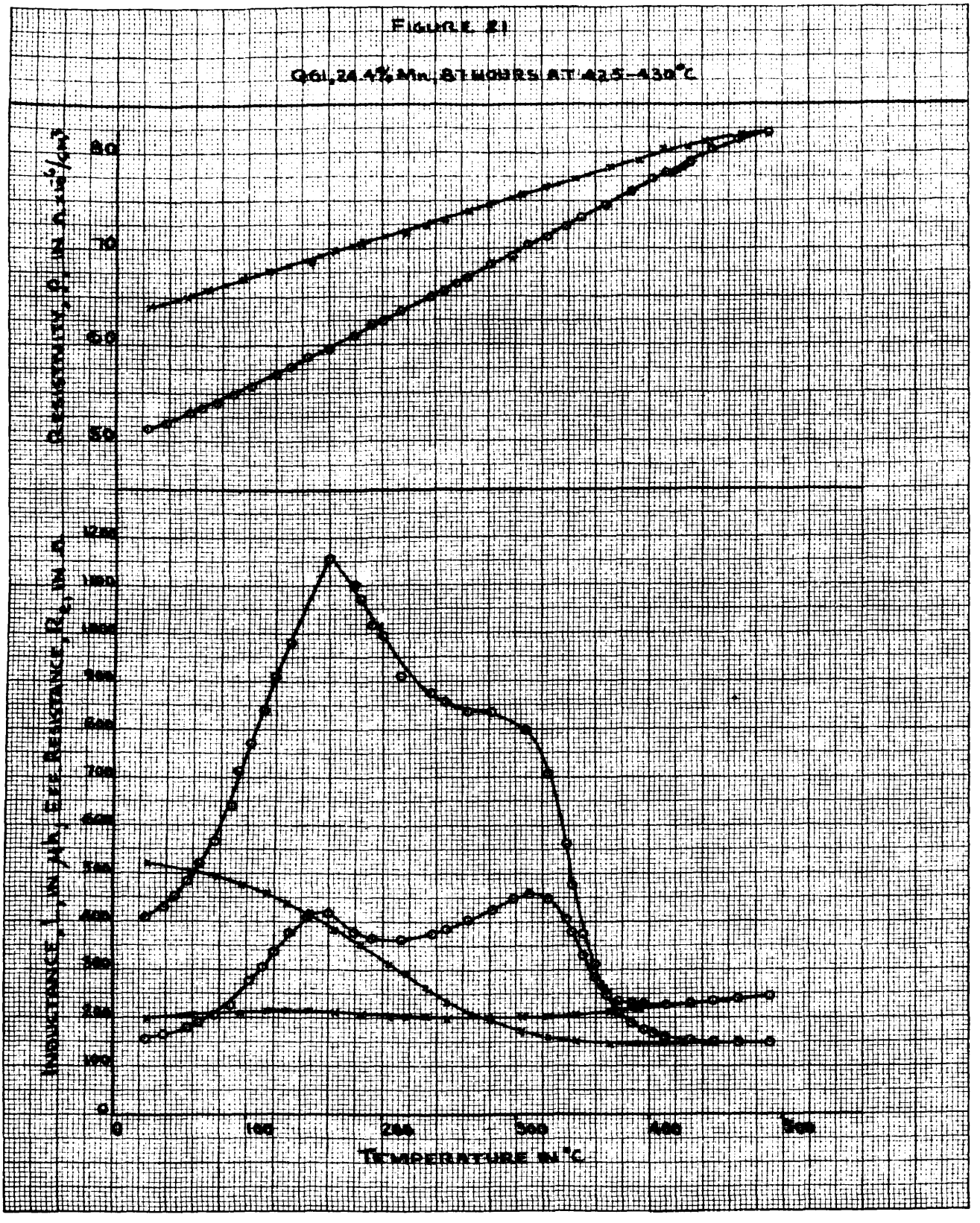
FIGURE 21
Q61, 24.4% Mn, 81 HOURS AT 425-430°C
CONDUCTANCE, σ^{-1}, IN MΩ, PER RESISTANCE, R_σ, IN Ω
CONDUCTIVITY, σ, IN Ω^{-1} cm^{-1} x 10^{-3}
TEMPERATURE IN °C
0
100
200
300
400
500
600
700
800
900
1000
1100
1200
50
60
70
80

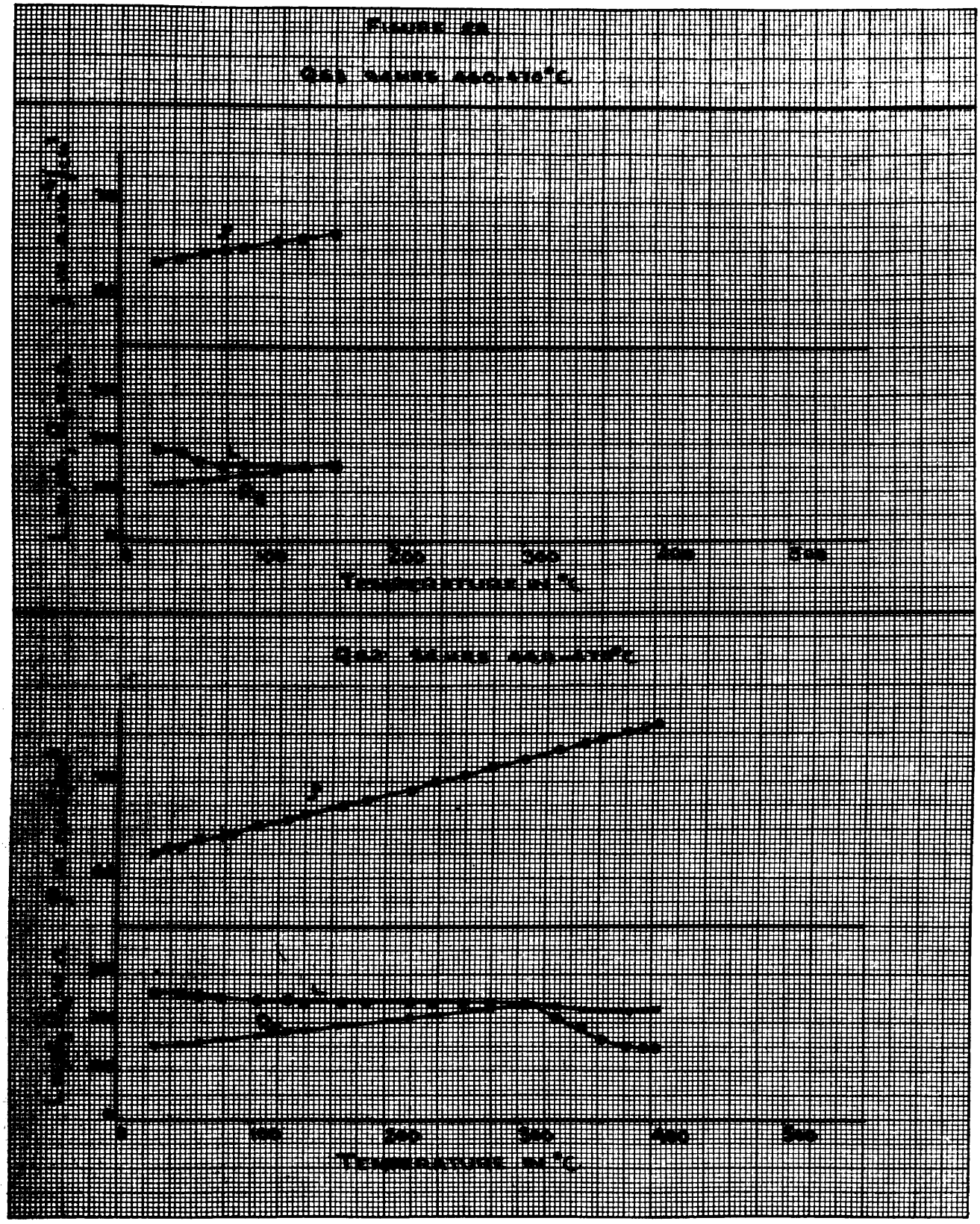

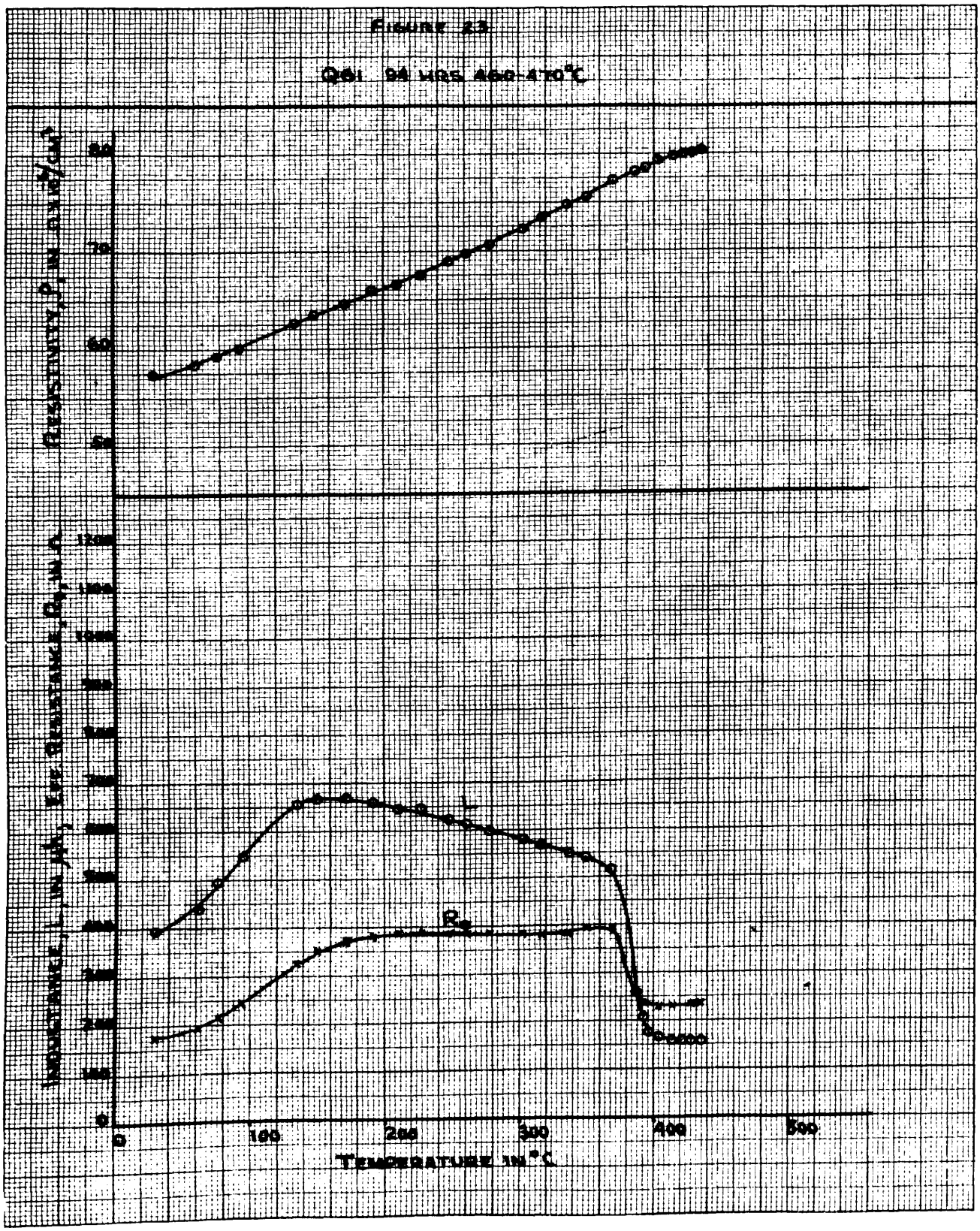
FIGURE 23
Q61 24 HRS 460-470°C
Capacitance, C, in μμf
Conductance, G, in μmho
Temperature in °C
0
100
200
300
400
500
R_s

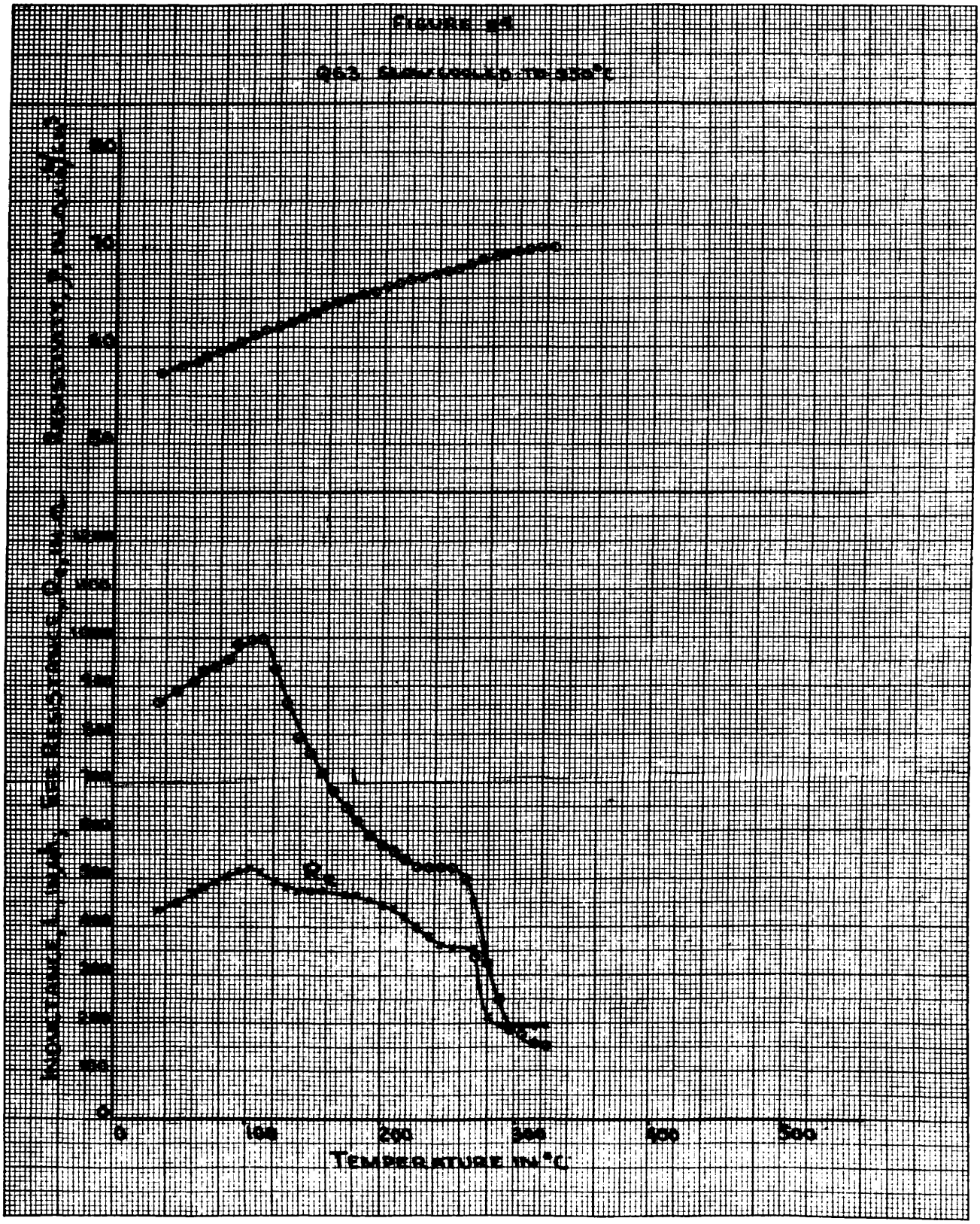
0
100
200
300
400
500
Temperature in °C

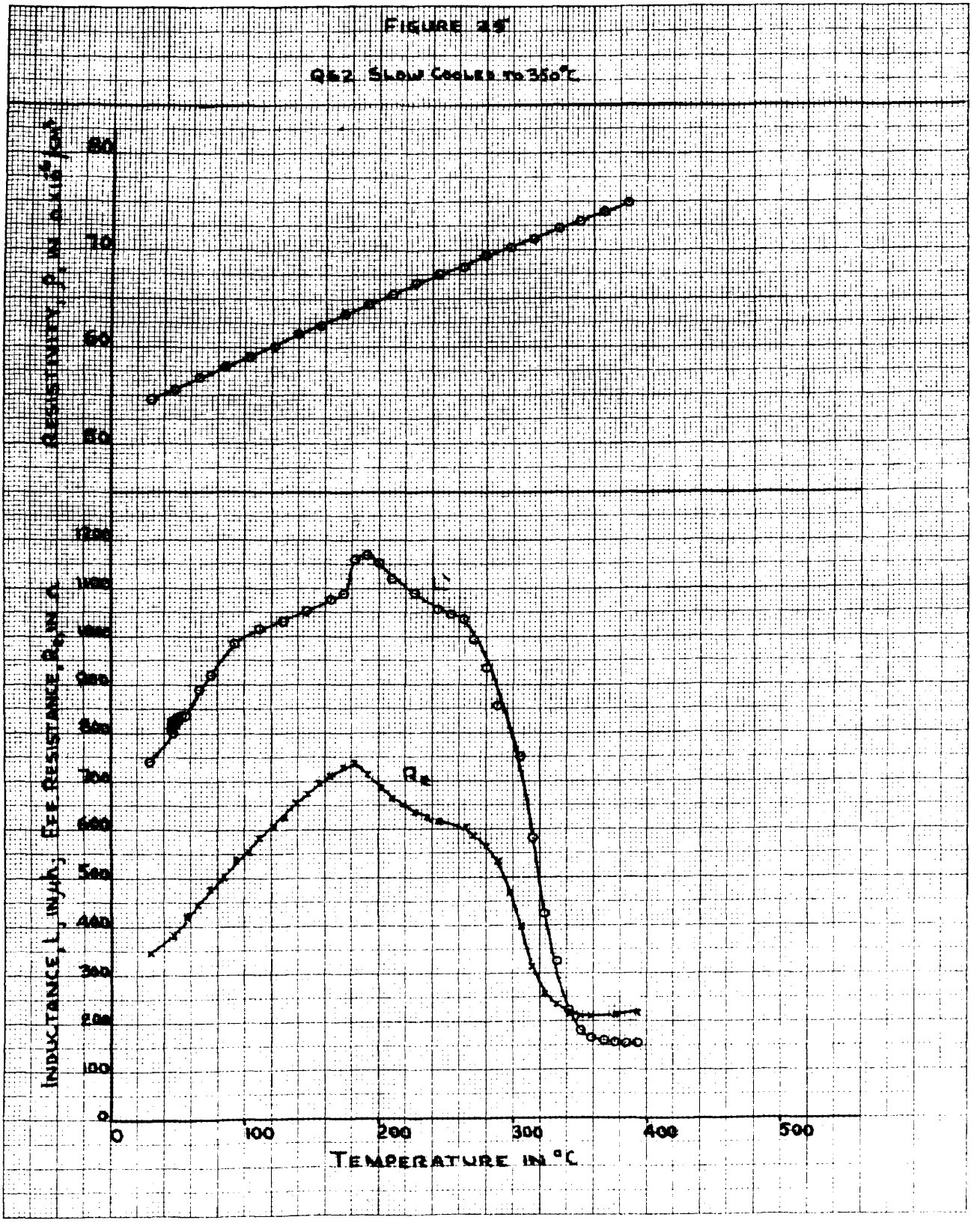
FIGURE 25
Q&2 SLOW COOLED TO 350°C
RESISTIVITY, ρ, IN Ω-KILO-CM
INDUCTANCE, L, IN μH; EFF. RESISTANCE, R_e, IN Ω
L
R_e
0
100
200
300
400
500
TEMPERATURE IN °C

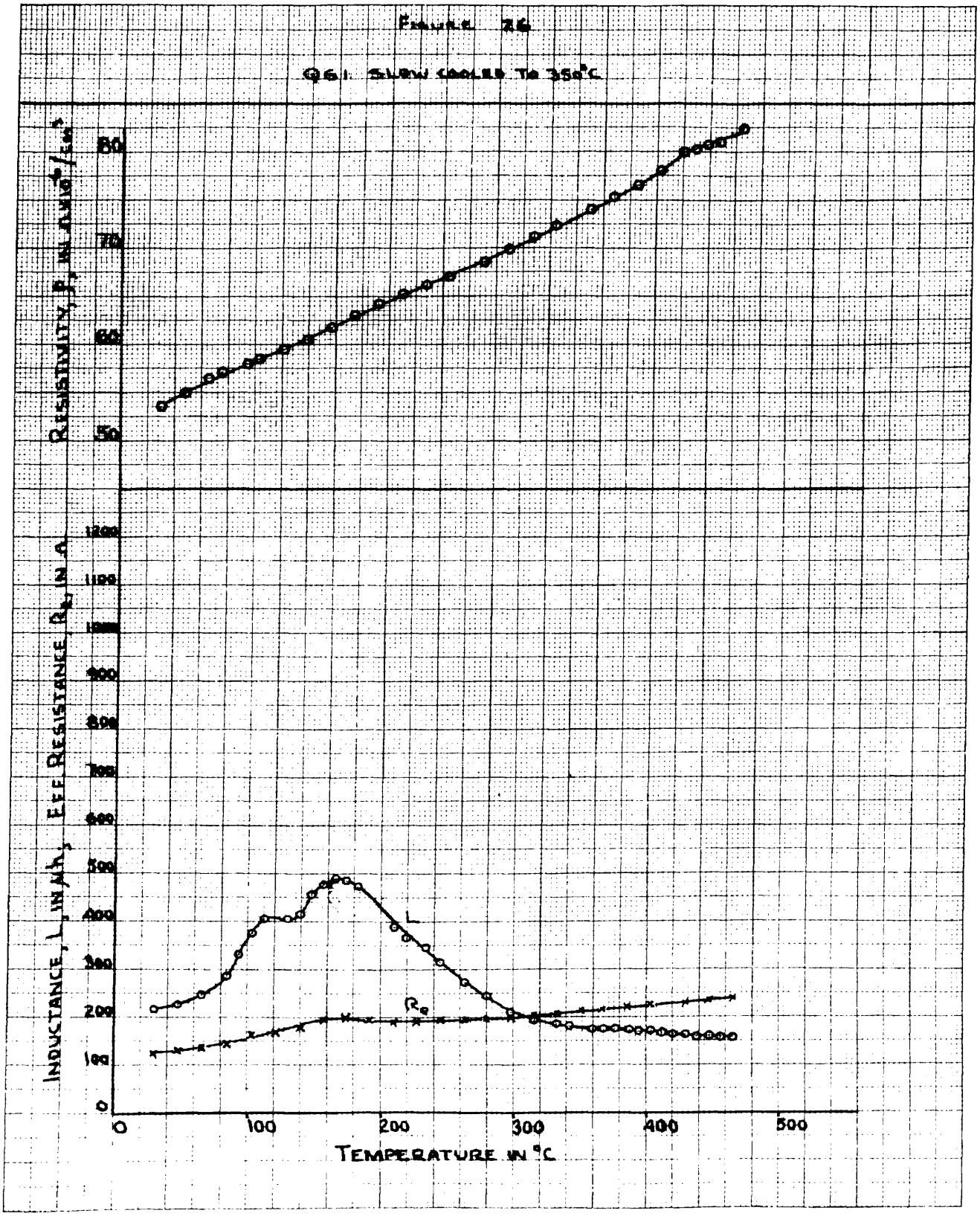
FIGURE 26
Q61. SLOW COOLED TO 350°C.
RESISTIVITY, ρ, IN Ω-MM²/M
INDUCTANCE, L, IN μH, EFF. RESISTANCE, Re, IN Ω
L
Re
TEMPERATURE IN °C
0
100
200
300
400
500
50
60
70
80
100
200
300
400
500
600
700
800
900
1000
1100
1200

6. Room Temperature Resistivities after Heat Treatment.

Table 6.

Alloy	Heat Treatment	Resistivity ohms x 10^{-6}/cm^3
Q63	As received	60.9
21.5%	Cooled rapidly from 800° C	63.8
Mn	168 hrs. at 415-420° C	55.06
	96 hrs. at 410-415° C	60.32
	As above, heated to 422° C	59.82
	87 hrs. at 425-430° C	56.82
	94 hrs. at 460-470° C	63.63
	Slow cool to 350° C	57.29
Q62	As received	63.9
23.2%	Cooled rapidly from 800° C	68.4
Mn	87 hrs. at 425-430° C	52.94
	94 hrs. at 460-470° C	62.84
	Slow cool to 350° C	54.67
Q61	As received	66.7
24.4%	Cooled rapidly from 800° C	72.3
Mn	96 hrs. at 410-415° C	51.02
	As above, heated to 464° C	54.09
	87 hrs. at 425-430° C	51.18
	94 hrs. at 460-470° C	57.06
	Slow cool to 350° C	53.46

C. Magnetization and Hysteresis of Nickel-Manganese Alloys.

1. Thermal History of Ni-Mn Alloy Ring Specimens.

a. B31, (21.4% Mn), 50 hours at 430° C plus 170 hours at 405° C. The alloy in a cold worked non-magnetic condition was heated in vacuum to 430° in about 6 hours. It was kept at that temperature for 50 hours, after which the temperature was lowered to 405° C in 7 hours, kept there for 170 hours, and furnace cooled to room temperature at almost 1° C per minute.

b. B31, (21.4% Mn), as above, rapidly cooled from 435° C. After measurements had been made upon B31 in the above condition, it was put in a muffle furnace at 435° C, heated at temperature for 15 minutes, and air-quenched on a heavy copper plate to room temperature. The cooling rate was about 10° C per second.

c. B31, (21.4% Mn), cooled through the ordering range at 2° C per minute. After the above treatment B31 was put in a muffle furnace at 660° C and cooled according to the following time-temperature data. It will be seen that the average rate of cooling in the ordering range, 510-380° C, was 1.5° C per minute.

Time (min.)	Temperature ° C
0	660
4	640
28	560
36	540
46	510
53	495
73	460
100	410
116	380

d. B21, (25.3% Mn), 116 hours at 440° C. B21 in the cold worked, non-magnetic condition was heated to 600° C in a muffle furnace, kept there 3/4 hours, and air-quenched. It was then heated in vacuum to 440° C in 5 hours, kept there for 116 hours, and furnace cooled at 2° C per minute.

c. B11, (20.1% Mn), air-quenched from 950° C. This specimen was magnetic in the cold-worked, as received, condition. It was put into a muffle at 950° C and air-quenched from that temperature. The scale forming from the high-temperature treatment was machined off.

f. B11, (20.1% Mn), B12, (20.1% Mn), B22 (25.3% Mn), and B31 (21.4% Mn), 72 hours at 450° C. Previous condition: B11, after air-quench from 950° C; B12, as received, machined into ring; B22, as received, machined into ring; B31, cooled from 660° C at 2° C per minute. The rings were heated in a muffle at 600° C for 1/2 hour and air-quenched. They were then heated in vacuum to 450° C in 8 hours, annealed at 450° C for 72 hours, and furnace cooled.

g. B12 (20.1% Mn), B22 (25.3% Mn), B31 (21.4% Mn): Slowly cooled to 380° C. Previous condition as of above. The alloys were heated at 600° C for 1/2 hour and air-quenched. They were then heated in vacuum to 560° C in 30 hours, cooled to 440° C in 13 hours, cooled to 400° C in 6 hours, kept at 400° C for 50 hours, cooled to 380° C in 6 hours, kept there for 60 hours, and furnace cooled.

2. Numerical Results.

a. B31, (21.4% Mn), 50 hours at 430° C and 170 hours at 405° C.

Table 9. Normal Magnetization from -13° C to 95° C.

Field: H	Induction B in Gausses and Permeability μ at Temperature -13° C		24° C		32° C		51° C		68° C		77° C		95° C	
Oe.	B	μ	B	μ	B	μ	B	μ	B	μ	B	μ	B	μ
0.1	76	760	140	1400	170	1700	220	2200	280	2800	295	2950	285	2850
0.25	550	2200	800	3200	865	3460	940	3760	1010	4040	980	3920	905	3620
0.5	1370	2740	1620	3240	1670	3340	1700	3400	1730	3460	1640	3280	1425	2850
0.75	1980	2505	2070	2760	2100	2800	2080	2790	2070	2760	1950	2600	1635	2200
1	2265	2265	2380	2380	2425	2425	2368	2368	2320	2320	2170	2170	1830	1830
2	--	--	--	--	--	--	2950	1475	2810	1405	2505	1302	2150	1075
2.5	3320	1330	3210	1320	3280	1310	--	--	--	--	--	--	--	--
5	4080	815	3940	790	3870	774	3600	720	3340	668	3040	608	2485	500
10	4675	468	4330	433	4215	422	3870	387	3570	357	3260	326	2705	270
20	5020	251	--	--	4420	221	4040	202	3720	187	3480	174	2915	146
25	--	--	4590	184	--	--	--	--	--	--	--	--	--	--
30	--	--	--	--	4480	149	4120	137	3840	128	3530	114	2980	102
35	5120	146	4600	131	--	--	--	--	--	--	--	--	--	--

Table 10. Additional Magnetization Data.

Induction B in Gausses and Permeability at Temperature								
-72° C			0° C			115° C		
H oe.	B	μ	H	B	μ	H	B	μ
0.101	50	490	0.01	7	700	0.1	280	2800
0.25	160	640	0.025	18	720	0.26	835	3210
0.51	984	1930	0.05	40	800	0.586	1255	2140
0.763	1595	2090	0.1	102	1020	0.92	1450	1580
1.02	1985	1985	0.2	442	2210	1.30	1580	1220
2.65	3240	1280	0.3	850	2830	2.74	1830	670
5.24	4120	790	0.4	1180	2950	6.9	2120	290
10.5	4900	470	0.5	1450	2900	12.9	2300	178
21.8	5440	250	0.6	1675	2790	20	2460	123
40.7	5695	140	0.7	1875	2680	30	2575	86
			0.8	2035	2550			
			1	2320	2320			
			2.5	3320	1330			
			5	4010	800			
			10	4550	455			
			20	4825	241			
			30	4905	164			
			40	4925	123			
			50	4940	97			

Table 11. Maximum Permeabilities.

Temperature	$\mu_{max.}$	$(H)\mu_{max.}$
-72° C	2040	0.75
-13	2750	0.48
0	2950	0.40
24	3320	0.35
32	3490	0.30
51	3760	0.25
66	4040	0.25*
77	3920	0.25*
95	3620	0.25*
115	3220	0.25*

* Approximate - data incomplete. See Figure 43 for better data on the variation of $\mu_{max.}$ with H.

FIGURE 29:
B 31, 21.4% Mn, 50 HOURS AT 430°C + 170 HRS AT 405°C

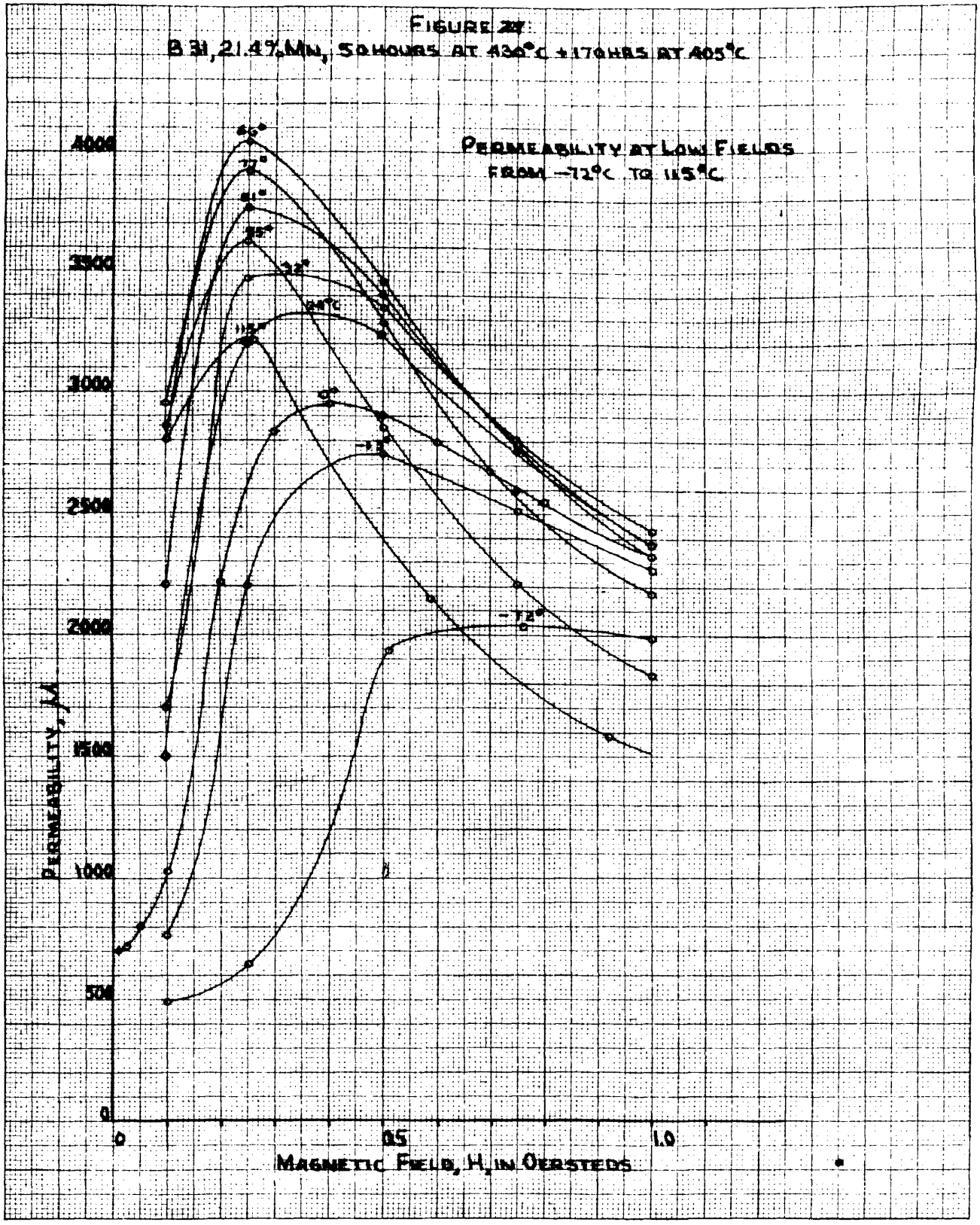

FIGURE 28
B31, 21.4% Mn, 50 HRS AT 430°C + 170 HRS 405°C

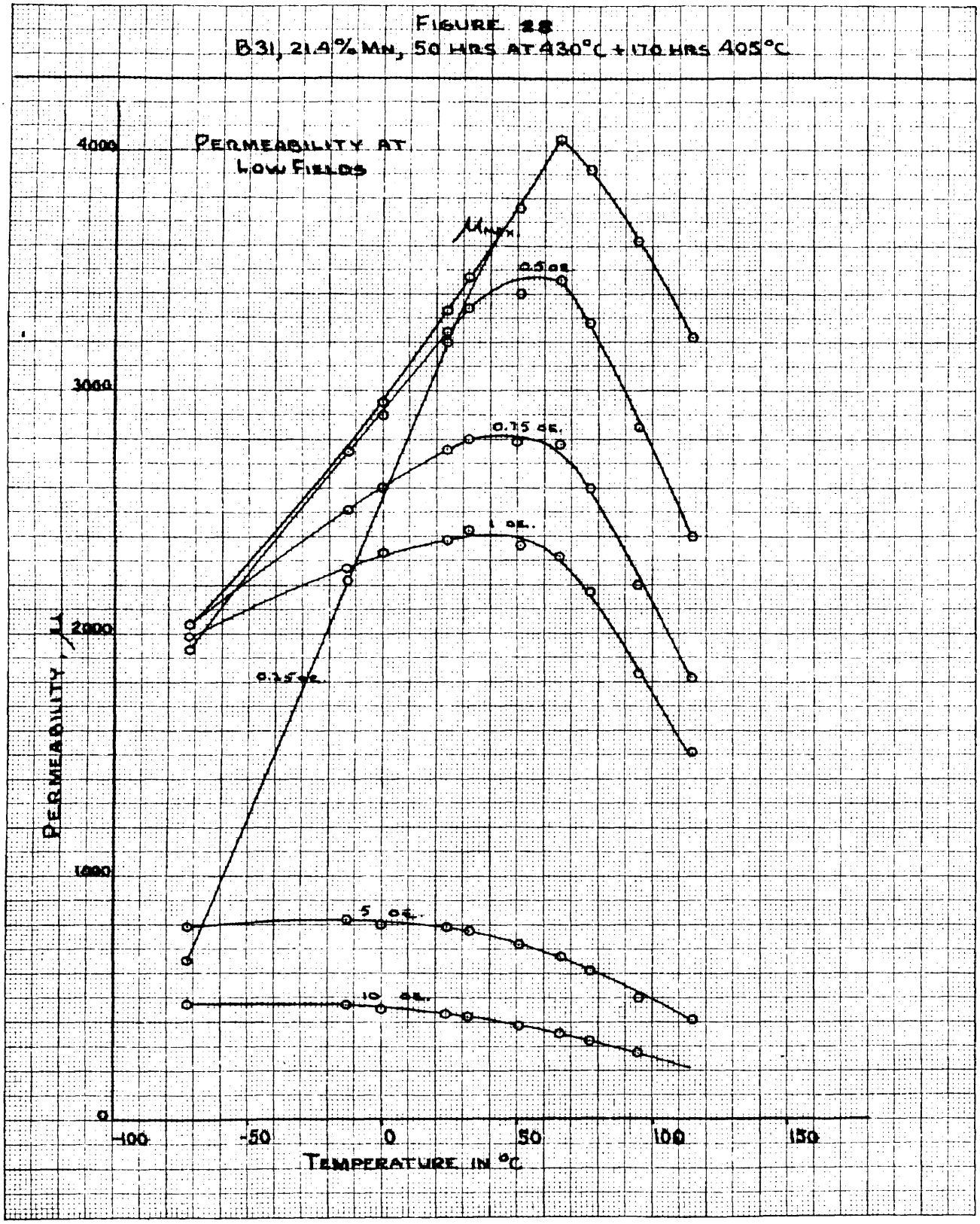

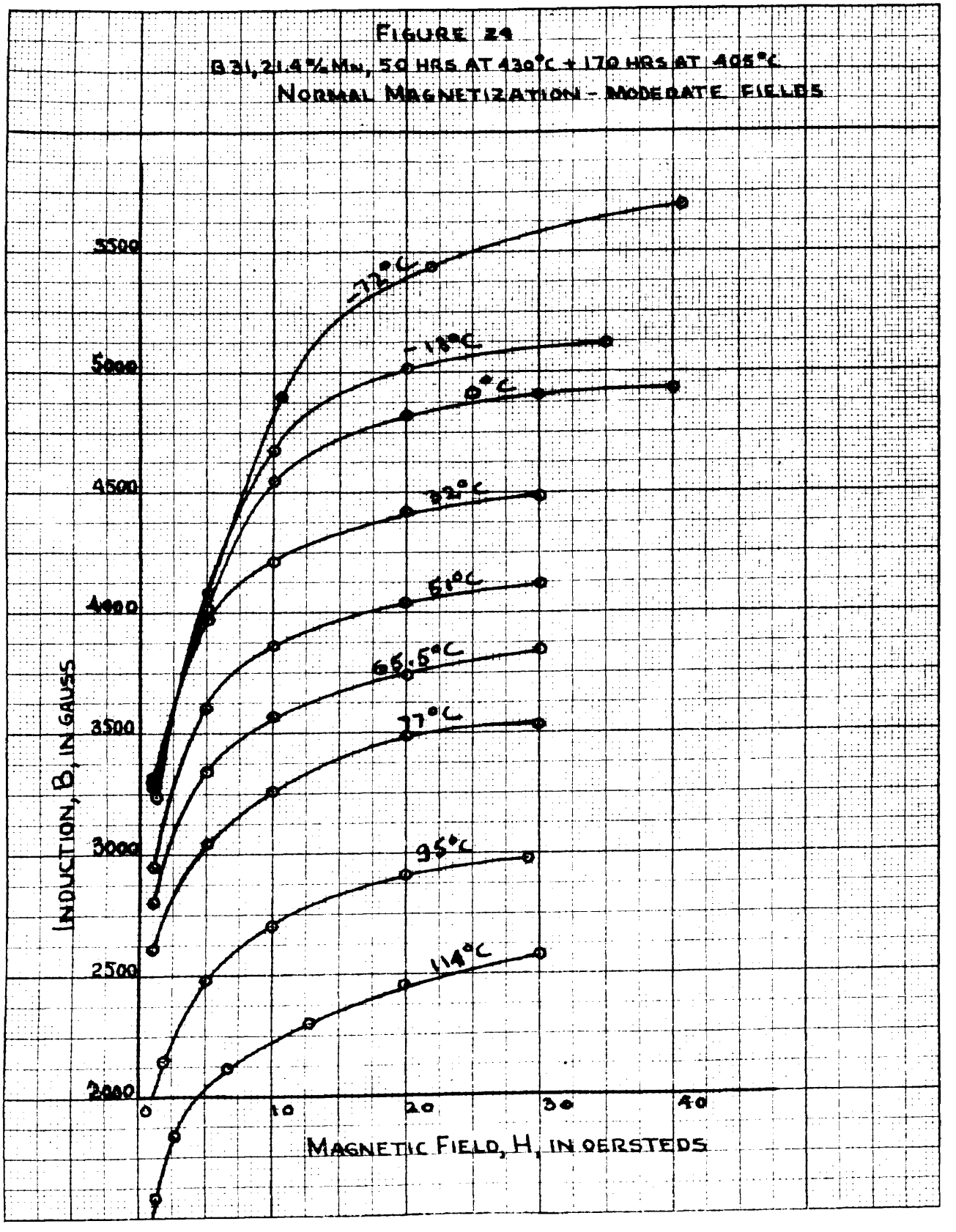
FIGURE 24
B31, 21.4% Mn, 50 HRS AT 430°C + 170 HRS AT 405°C
NORMAL MAGNETIZATION - MODERATE FIELDS
INDUCTION, B, IN GAUSS
5500
5000
4500
4000
3500
3000
2500
2000
-73°C
-18°C
0°C
32°C
61°C
65.6°C
77°C
95°C
114°C
0
10
20
30
40
MAGNETIC FIELD, H, IN OERSTEDS

Table 12. Demagnetization of S31, 50 hours at 430° C and 170 hours at 405° C.

Field H oe.	Magnetic Induction in Gausses							
	-130° C	0° C	24° C	32° C	51° C	66° C	77° C	95° C
35	5085	4930	4695	--	--	--	--	--
30	--	--	--	4510	4090	3800	3625	2980
25	--	4865	4625	--	--	--	--	--
20	4955	--	--	4415	4000	3715	3515	2850
10	4650	4560	4385	4235	3830	3515	3205	2635
5	4120	4100	--	3905	3575	3290	2980	2415
2.5	3475	3465	3445	3355	--	--	--	--
2	--	--	--	--	3010	2840	2600	2095
1	2770	2740	2740	2710	2560	2440	2255	1855
0.75	2585	2600	2550	2515	2390	2280	2110	1720
0.5	2385	2385	2355	2310	2190	2095	1920	1600
0.25	2130	2100	2055	2000	1885	1795	1655	1360
0.1	1930	1905	1850	1820	1660	1545	1430	1150
0	1785	1740	1655	1590	1430	1330	1190	930
-0.1	1580	1510	1360	1090	1010	820	660	435
-0.25	590	395	15	-85	-400	-570	-630	-690
-0.5	-885	-1035	-1285	-1390	-1540	-1630	-1550	-1355
-0.75	-1605	-1755	--	-1960	-2015	-2015	-1900	-1605
-1	-2130	-2215	-2310	-2340	-2340	-2295	-2130	-1785
-2	--	--	--	--	-2955	-2810	-2590	-2090
-2.5	-3310	-3320	-3295	-3270	--	--	--	--
-5	-4000	-4040	-3935	-3855	-3575	-3300	-2980	-2405
-10	-4620	-4535	-4345	-4210	-3830	-3515	-3205	-2625
-20	-4935	--	--	-4410	-4000	-3685	-3515	-2835
-25	--	-4865	-4610	--	--	--	--	--
-30	--	--	--	-4510	-4090	-3800	-3625	-2980
-35	-5085	-4930	-4695	--	--	--	--	--

Table 13. Additional Demagnetization of 831, 50 hours at 430° C plus 170 hours at 405° C.

-72° C		115° C	
H	B	H	B
40.7	5625	30	2530
21.8	5415	20	2375
10.5	4950	12.9	2230
5.24	4300	6.9	2030
2.53	3560	2.74	1770
1.02	2915	1.3	1545
0.763	2765	0.92	1460
0.51	2590	0.586	1330
0.25	2390	0.26	1135
0.101	2230	0.1	920
0	2110	0	730
-0.101	1975	-0.1	230
-0.25	1665	-0.26	-710
-0.51	20	-0.586	-1240
-0.703	-880	-0.92	-1415
-1.02	-1530	-1.3	-1540
-2.53	-3150	-2.74	-1775
-5.24	-4140	-6.9	-2015
-10.5	-4880	-12.9	-2200
-21.8	-5400	-20	-2345
-40.7	-5625	-30	-2530

Demagnetization Curves in Oersteds
3000
2000
1000
0
-1000
-2000
-3000
-2.0
-1.5
-1.0
-0.5
-0.0
-5
-10
-15
-20

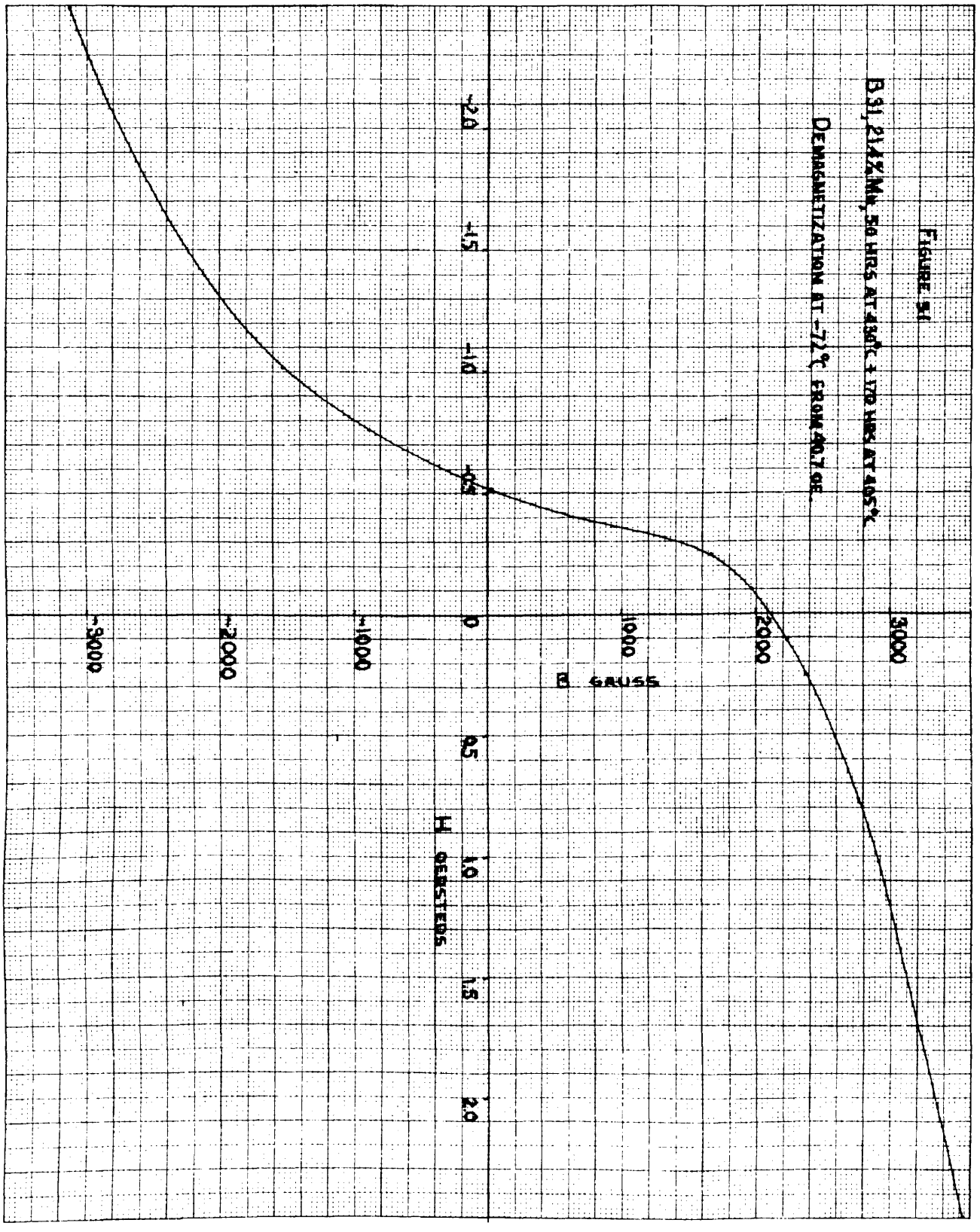
FIGURE 51
B 51, 21.4% Mn, 50 HRS AT 430°C + 170 HRS AT 405°C
DEMAGNETIZATION AT -72°C FROM 40.7 OE
B GAUSS
H OERSTEDS
3000
2000
1000
0
-1000
-2000
-3000
-2.0
-1.5
-1.0
-0.5
0.5
1.0
1.5
2.0

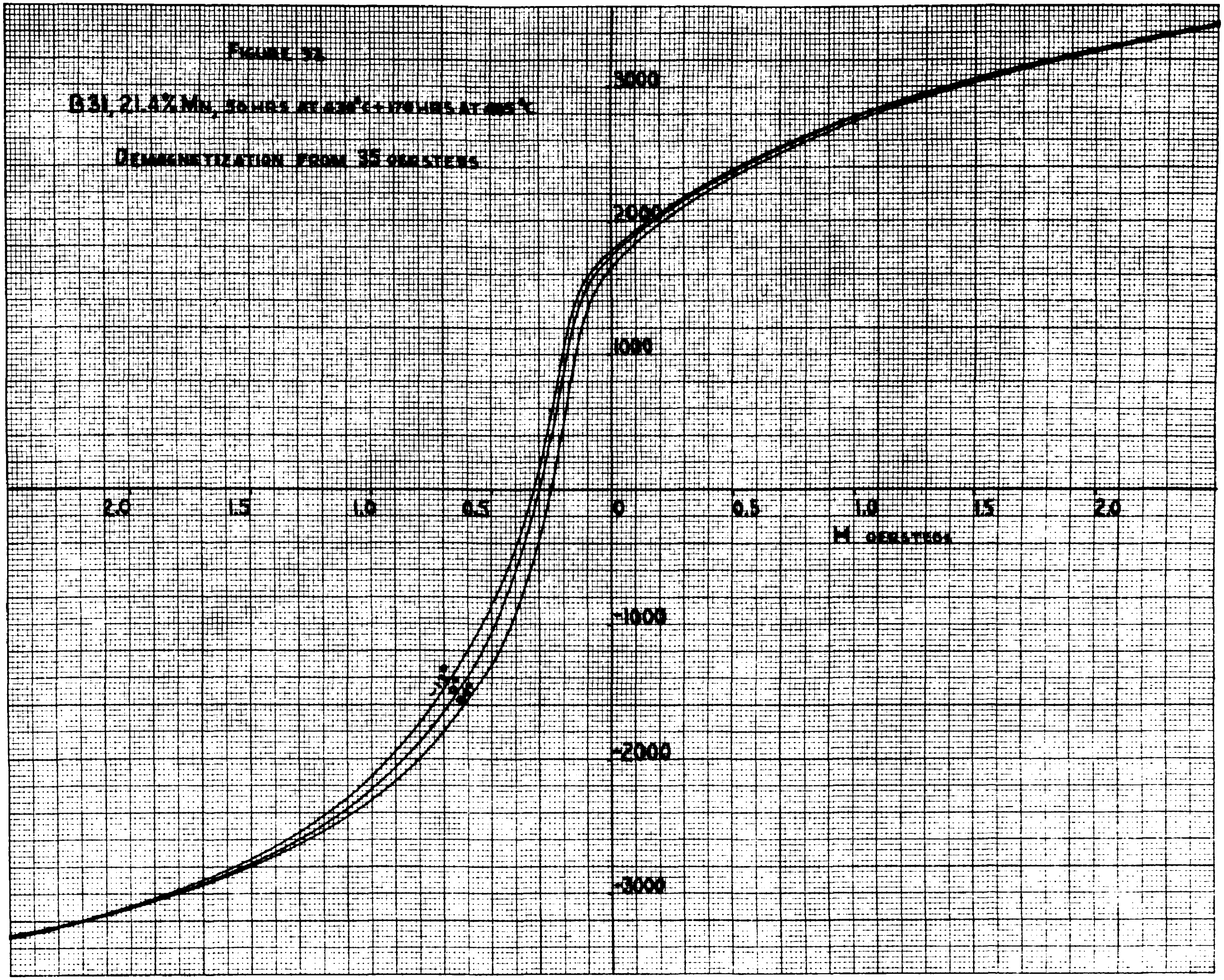
B31, 21.4% Mn,
Demagnetization from 35 oersteds
3000
2000
1000
-1000
-2000
-3000
2.0
1.5
1.0
0.5
0
0.5
1.0
1.5
2.0
H oersteds

Table 14. Hysteresis Constants of B31, 50 hours at 430° C plus 170 hours at 405° C.

Temperature °C	Maximum Field $H_{max.}$ oersteds	Maximum Induction $B_{max.}$ gausses	Remanence B_r gausses	Coercive Force H_c oersteds
-72	40.7	5625	2110	0.52
-13	35	5085	1785	0.32_5
0	35	4930	1740	0.30
24	35	4695	1655	0.25
32	30	4510	1590	0.24
51	30	4090	1430	0.20
66	30	3800	1330	0.18
77	30	3525	1190	0.17
95	30	2980	930	0.15
115	30	2530	730	0.12

FIGURE 13

B 31, 21.4% Mn, 50 HRS AT 430° + 170 HRS AT 405°

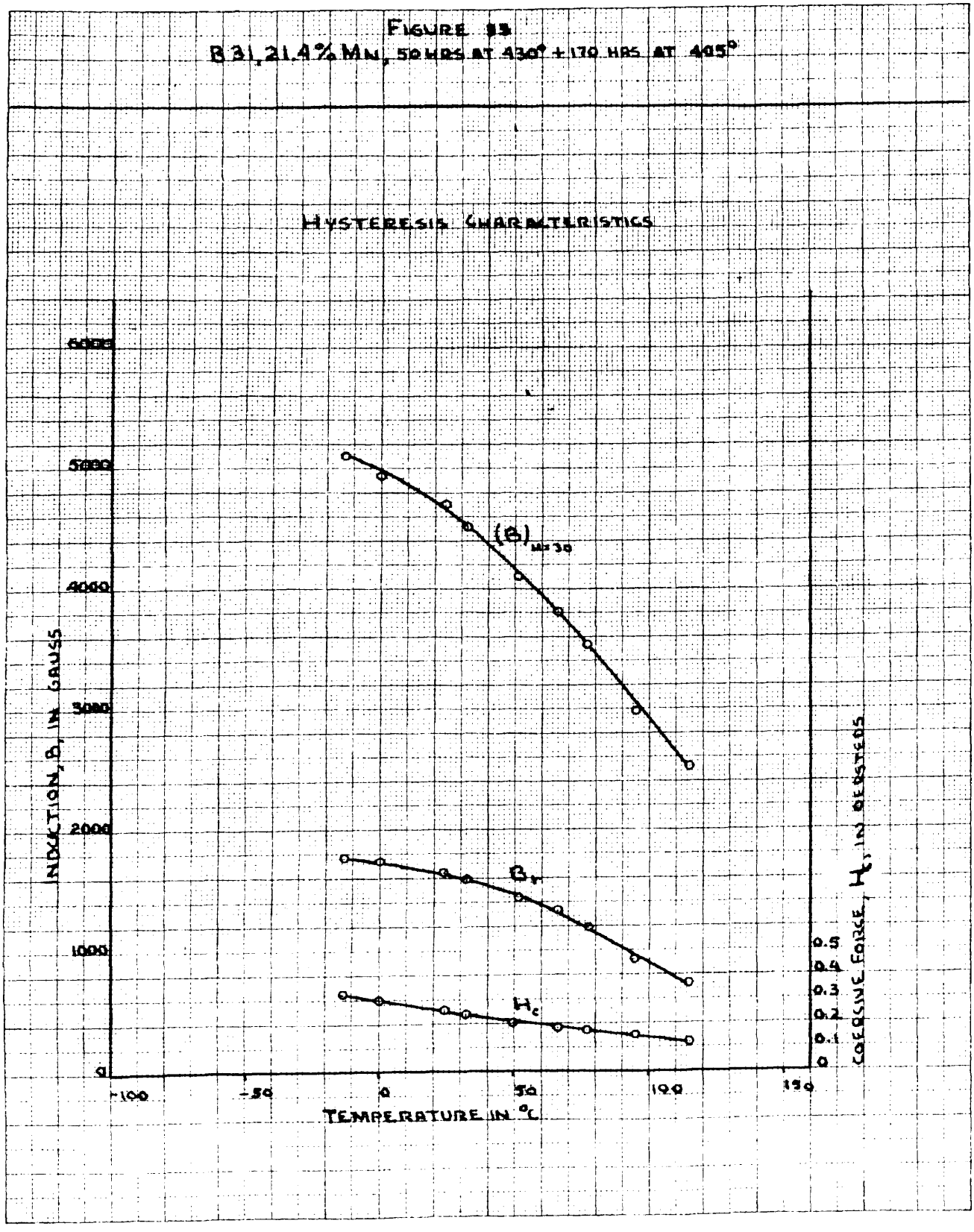

b. B31, 21.4% Mn, as before, rapidly cooled from 435° C.

Table 15. Normal Magnetization at 28° C.

H oersteds	B gausses	μ	H oersteds	B gausses	μ
0.1	155	1550	2	3045	1522
0.25	830	2320	5	3870	774
0.5	1565	3125	10	4275	428
0.75	2020	2940	20	4480	224
1	2345	2345	30	4540	151

Table 16. Hysteresis at 28° C.

H	B	H	B
30	4450	0	1565
20	4350	-.1	1270
10	4170	-.25	-100
5	3805	-.5	--
2	3120	-.75	-1905
1	2640	-1	-2295
.75	2470	-2	-3030
.5	2250	-5	-3810
.25	1980	-10	-4180
.1	1750	-20	-4360

c. B31, 21.4% Mn, cooled through the ordering range from 660° C at 2° per minute.

Table 17. Normal Magnetization at 30° C.

H oersteds	B gausses	μ	H oersteds	B gausses	μ
.1	--	--	2	5	2.5
.25	--	--	5	9	1.8
.5	--	--	10	16	1.6
.75	1	1.3	20	40	2.0
1	2	2.0	30	52	1.7

d. B21, 25.3% Mn, 116 hours at 440° C.

Table 18. Normal Magnetization at 30° C.

H oersteds	B gausses	μ	H oersteds	B gausses	μ
.1	10	100	2	372	186
.25	28	112	5	832	166
.5	56	112	10	1293	129
.75	111	146	20	1775	89
1	162	162	30	2050	68

Maximum permeability $\mu_{max.}$ = 186 at 2 oe.

Table 19. Hysteresis at 30° C.

H oersteds	B gausses	H oersteds	B gausses
30	1990	0	1036
20	1860	-1	838
10	1642	-2	563
5	1462	-5	-130
2	1268	-10	-938
1	1171	-20	-1711
		-30	-1990

Maximum induction $B_{max.}$ = 1990 gausses

Remanence B_r = 1035 gausses

Coercive force H_c = 4.3 oersteds

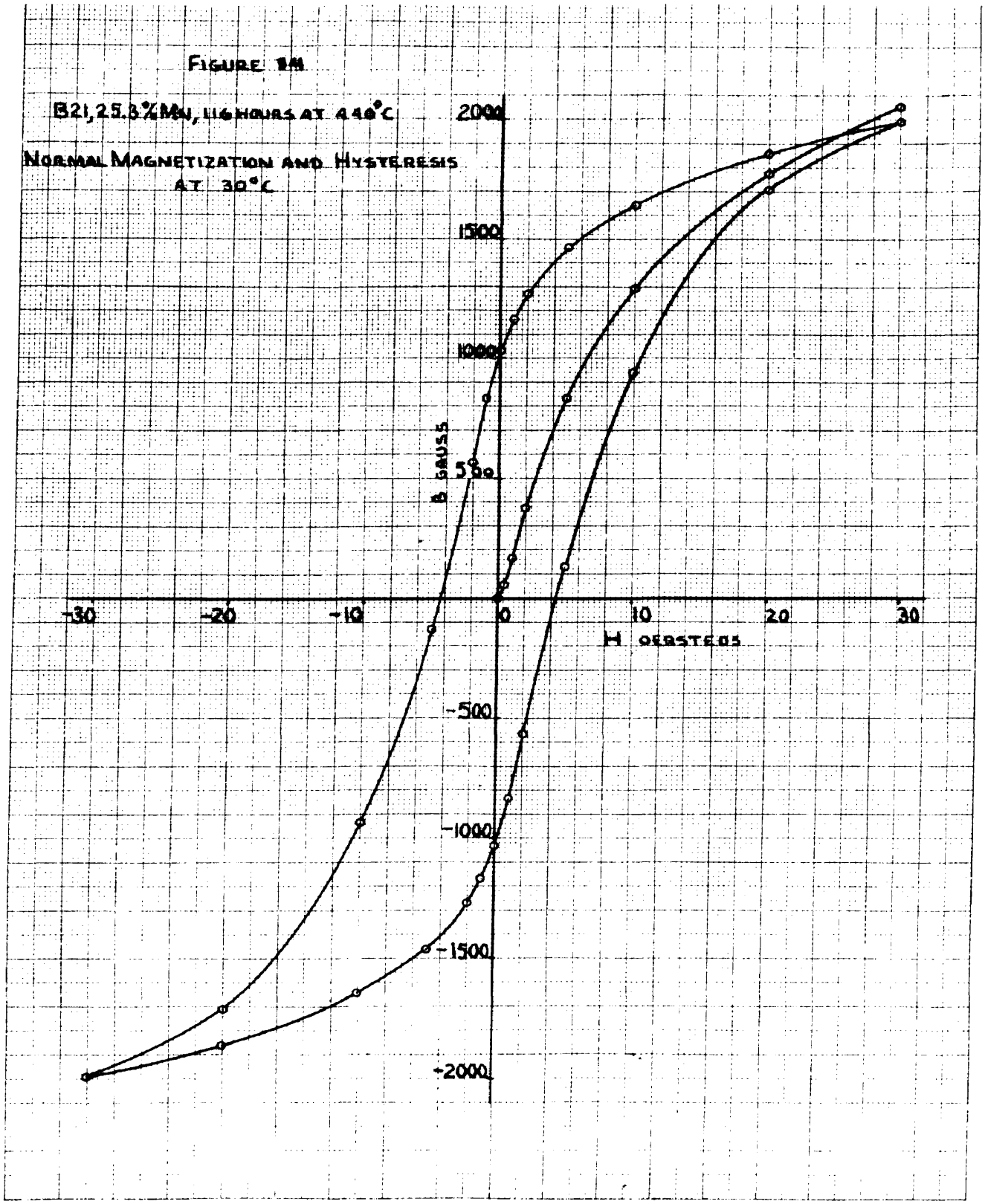
FIGURE 1M
B21, 25.3% Mn, 116 HOURS AT 440°C
NORMAL MAGNETIZATION AND HYSTERESIS AT 30°C
2000
1500
1000
500
B GAUSS
-30
-20
-10
0
10
20
30
H OERSTEDS
-500
-1000
-1500
-2000

e. B11, 20.1% Mn, air-quenched from 950° C.

Table 20. Normal Magnetization at 26° C.

H	B	μ	H	B	μ
.1	2	20	5	135	27
.25	13	50	10	195	20
.5	25	50	20	260	13
1	45	45	30	330	11
2	80	40			

f. B11, B12, B22, and B31: 72 hours at 450° C.

Table 21. Normal Magnetization at Room Temperatures.

H	B11		B12		B22		B31	
	B	μ	B	μ	B	μ	B	μ
.1	48	480	15	150	5	50	--	--
.25	169	679	53	212	14	56	--	--
.5	356	712	146	291	30	60	--	--
.75	438	574	232	310	57	76	0.7	1
1	490	490	282	282	92	92	1	1
2	607	307	419	210	221	110	3	1.5
5	780	136	596	119	523	105	9	1.8
10	904	90.4	724	72	841	84.1	15	1.5
20	1030	51.5	893	44.6	1204	60.2	39	1.9
30	1109	37	1000	33.3	1460	48.7	50	1.7

Maximum permeability, $\mu_{max.}$:

B11, 840 at 0.4 oersted.

B12, 325 at 0.7 oersted.

B22, 110 at 2.0 oersteds.

FIGURE 35

B11, B12, 20.1%, B22, 25.3% Mn, B31, 21.4% Mn: 72 HOURS 450°C
B11, AIR-QUENCHED FROM 950°C

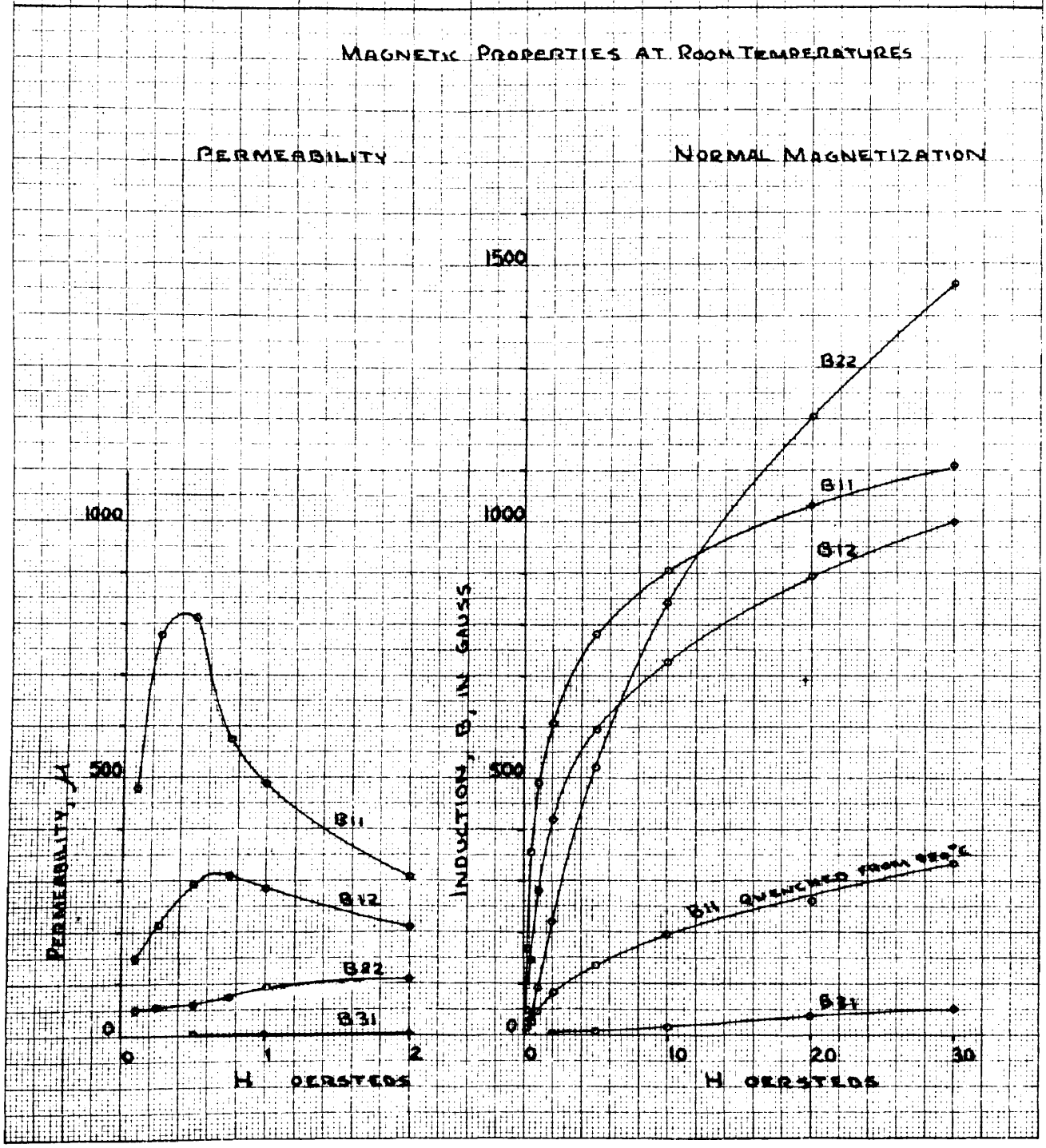

Table 22. Demagnetization Data on B11, B12 and B22 at Room Temperature of the 72 Hours at 450° C Anneal of B.

H	B in gausses B11	B12	B22	H	B in gausses B11	B12	B22
30	1135	976	1410	-.1	247	227	--
20	1000	868	1298	-.25	55	188	694
10	883	715	1125	-.5	-270	45	661
5	753	591	993	-.75	-363	-114	630
2	590	444	852	-1	-422	-202	587
1	508	371	792	-2	-560	-366	399
.75	478	350	768	-5	-726	-550	-33
.5	442	320	743	-10	-860	-688	-620
.25	388	284	730	-20	-1013	-868	-1187
.1	342	264	--	-30	-1135	-976	-1410
.0	302	250	713				

Coercive Force, H_c:

B11 = 0.46 oersted.

B12 = 0.57 oersted.

B22 = 4.7 oersteds.

Remanence, B_r:

B11 = 302 gausses.

B12 = 250 gausses.

B22 = 713 gausses.

FIGURE 56

Bll, 20.1% Mn, 72 HRS AT 450°C

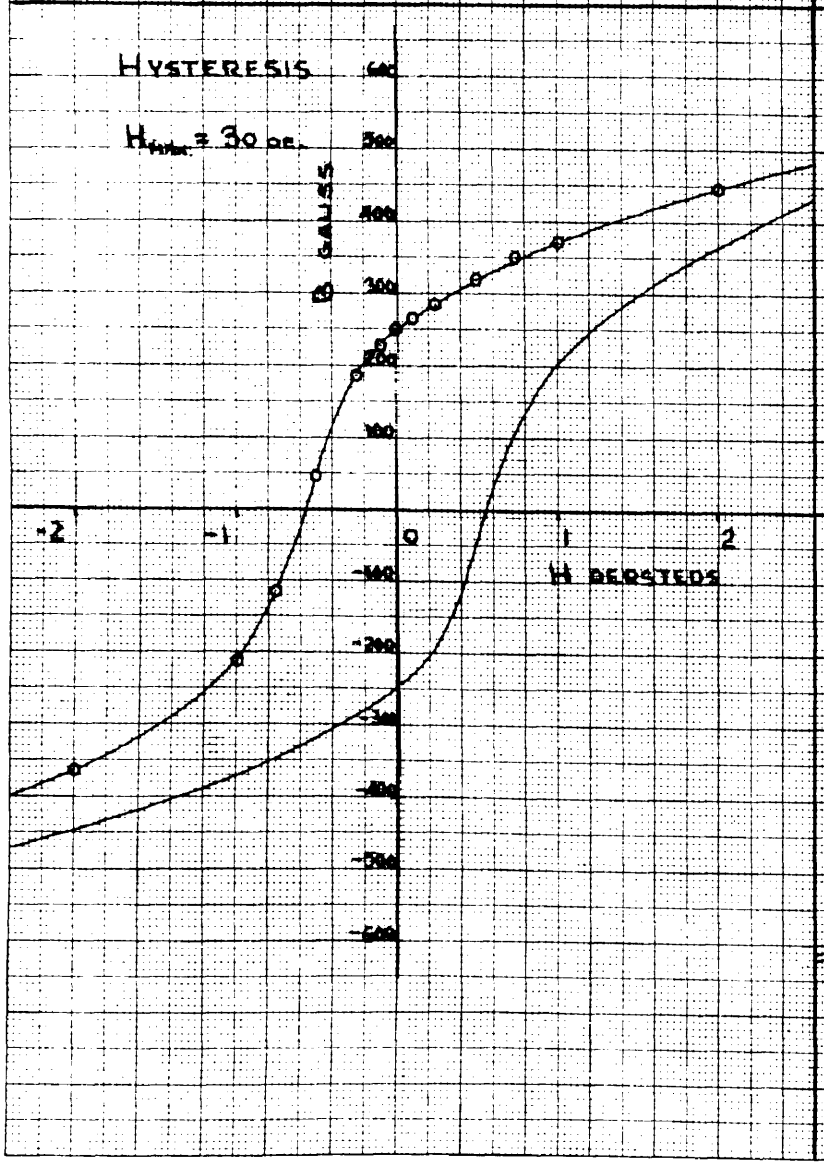

FIGURE 57

Bll, 20.1% Mn, 72 HRS AT 450°C

(PRE-TREATMENT INCLUDES QUENCH FROM 450°C)

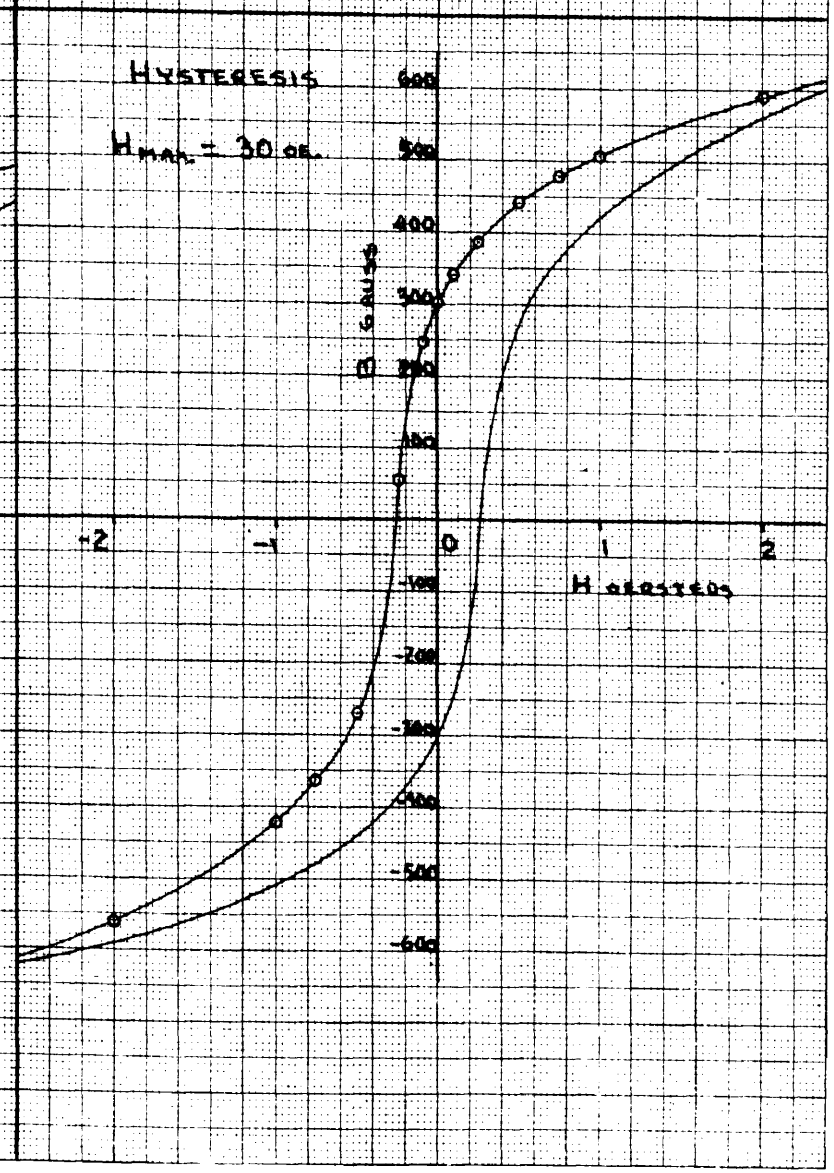

FIGURE 28

B22, 25.3% MN, 72 HRS AT 450°C

HYSTERESIS AT 28°C

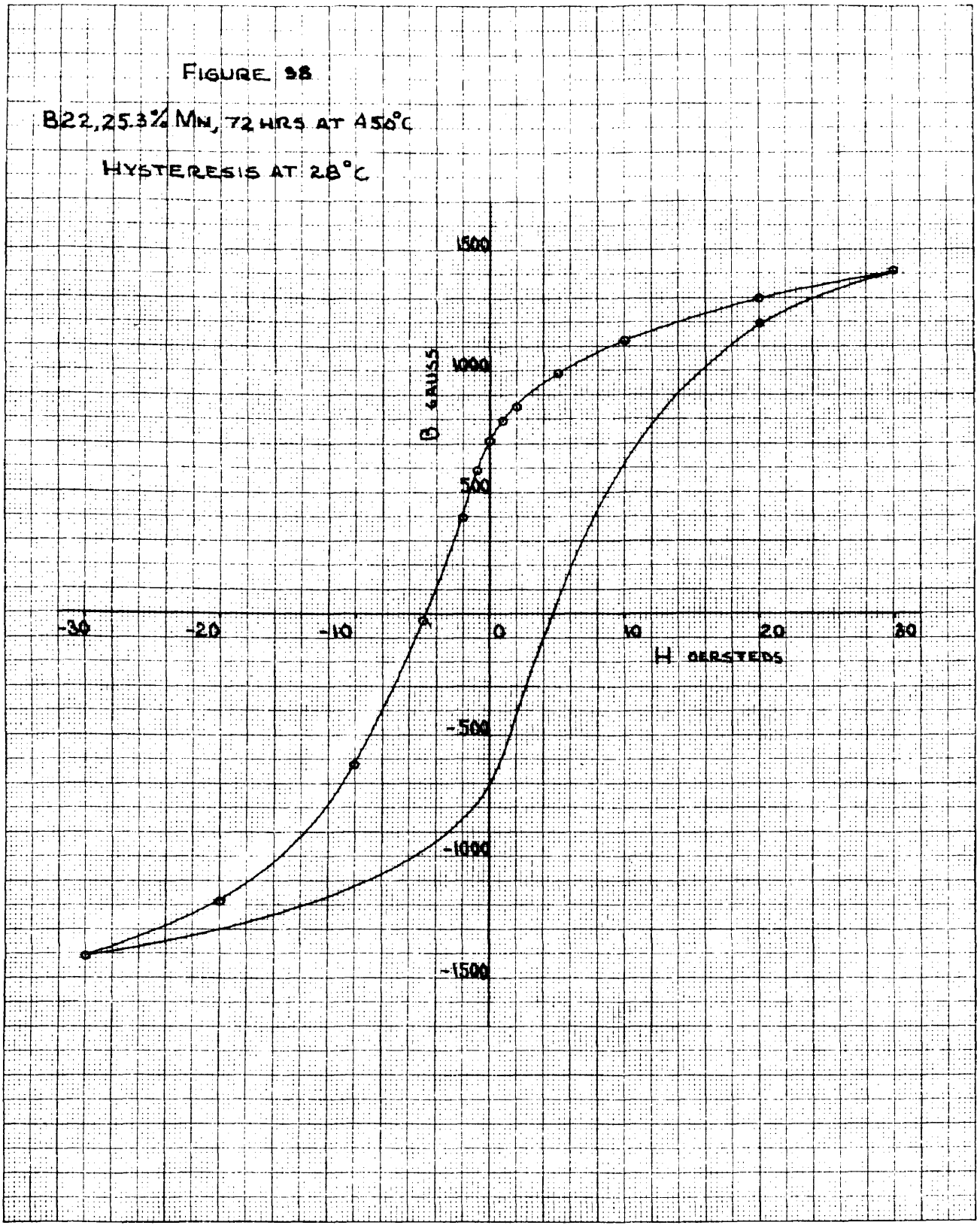

7. B12, B22, B31 slowly cooled to 380° C.

Table 23. Normal Magnetization at Room Temperature.

H	B12		B22		B31	
	B	μ	B	μ	B	μ
.1	54	540	4	40	365	3650
.25	175	700	10	40	1323	5300
.5	722	1444	27	54	2075	4050
.75	1346	1800	43	58	2443	3260
1	1756	1756	60	60	2675	2675
2	2550	1275	116	58	3185	1593
5	3360	675	269	54	3560	712
10	3820	382	440	44	3810	381
20	4080	204	706	35	3880	194
30	4130	138	885	29.5	3910	130

Maximum permeability, $\mu_{max.}$:

B12, 1800 at 0.8 oersted.
B22, 60 at 1 oersted.
B31, 5300 at 0.25 oersteds.

Table 24. Hysteresis at Room Temperature.

H	B in gausses			H	B in gausses		
	B12	B22	B31		B12	B22	B31
30	4115	865	3900	-0.1	1470	--	800
20	4006	707	3860	-0.25	1220	--	-1020
10	3820	588	3785	-0.5	140	258	-2020
5	3400	468	3640	-0.75	-1020	--	-2400
2	2740	364	3180	-1	-1580	209	-2650
1	2320	320	2750	-2	-2470	141	-3160
0.75	2180	--	2560	-5	-3300	-71	-3620
0.50	2020	299	2350	-10	-3750	-318	-3760
0.25	1820	--	2010	-20	-4010	-682	-3850
0.1	1690	--	1710	-30	-4115	-865	-3900
0	1590	260	1420				

Coercive Force, H_c:

B12 = 0.52 oersted.
B22 = 4.0 oersteds.
B31 = 0.15 oersted.

Remanence, B_r:

B12 = 1590 gausses
B22 = 260 gausses.
B31 = 1420 gausses

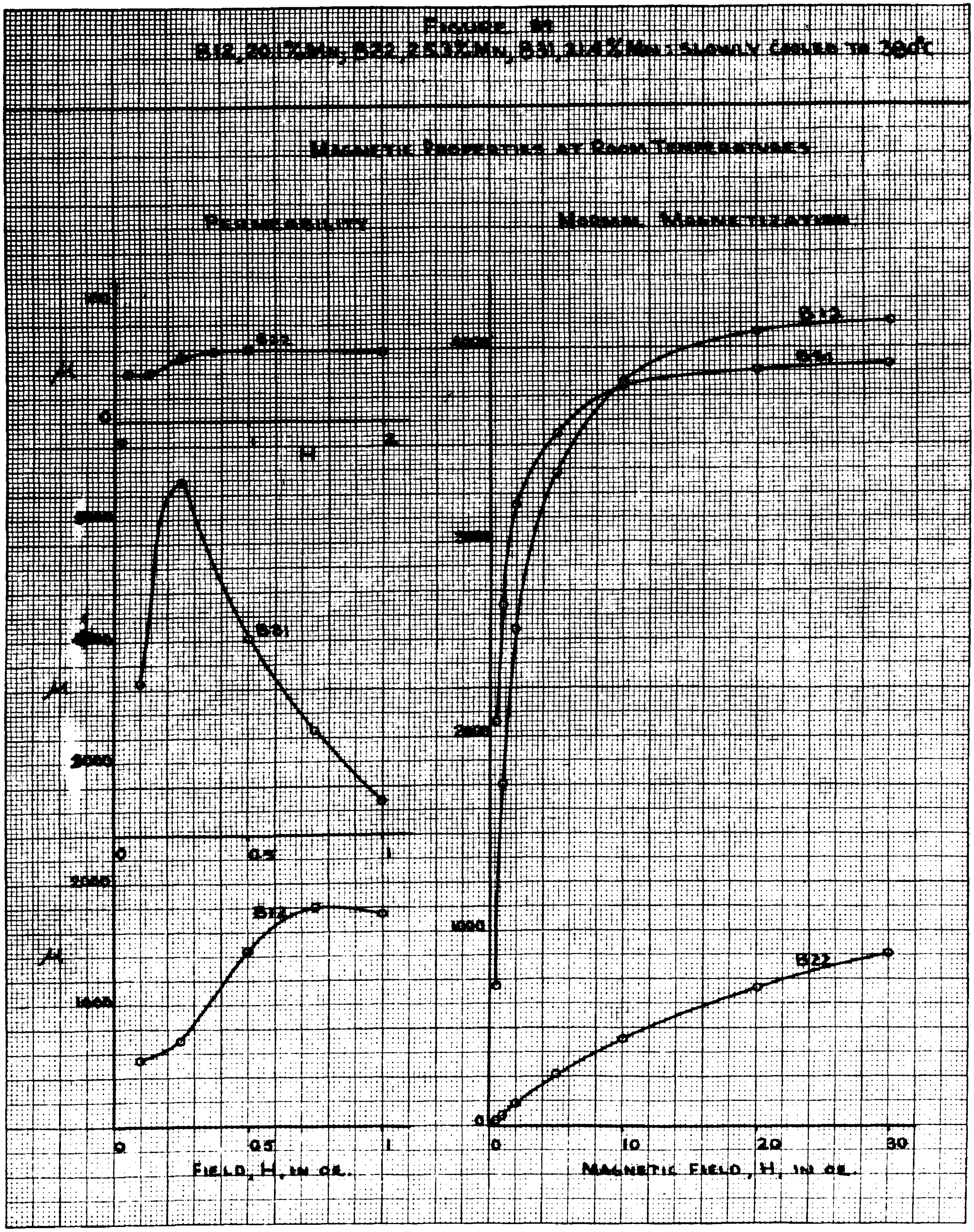
Magnetic Properties at Room Temperatures
Permeability
Normal Magnetization
B12
B31
B22
Field, H, in oe.
Magnetic Field, H, in oe.

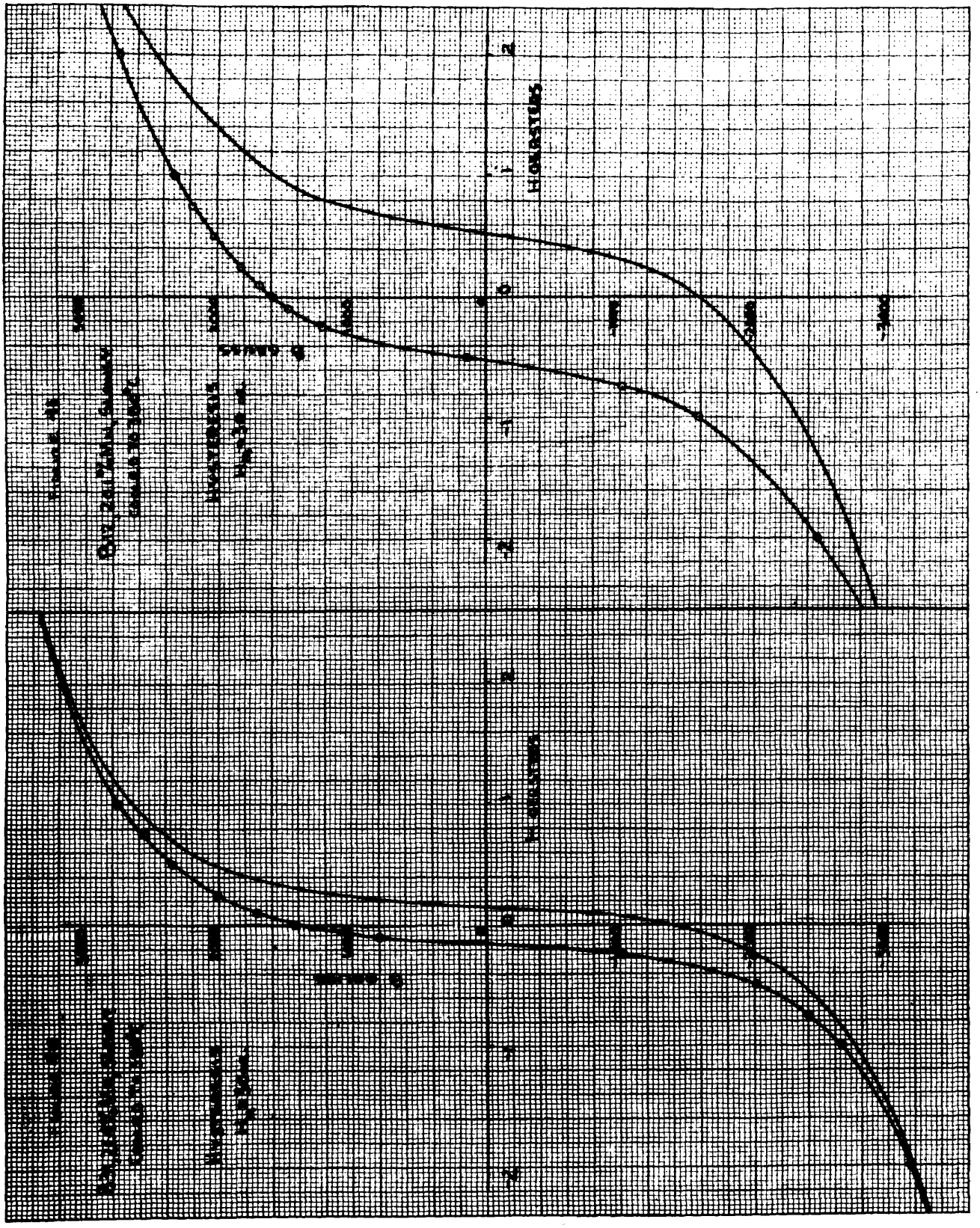

FIGURE 42

B22, 25.3% MN, SLOWLY COOLED FROM 380°C

HYSTERESIS

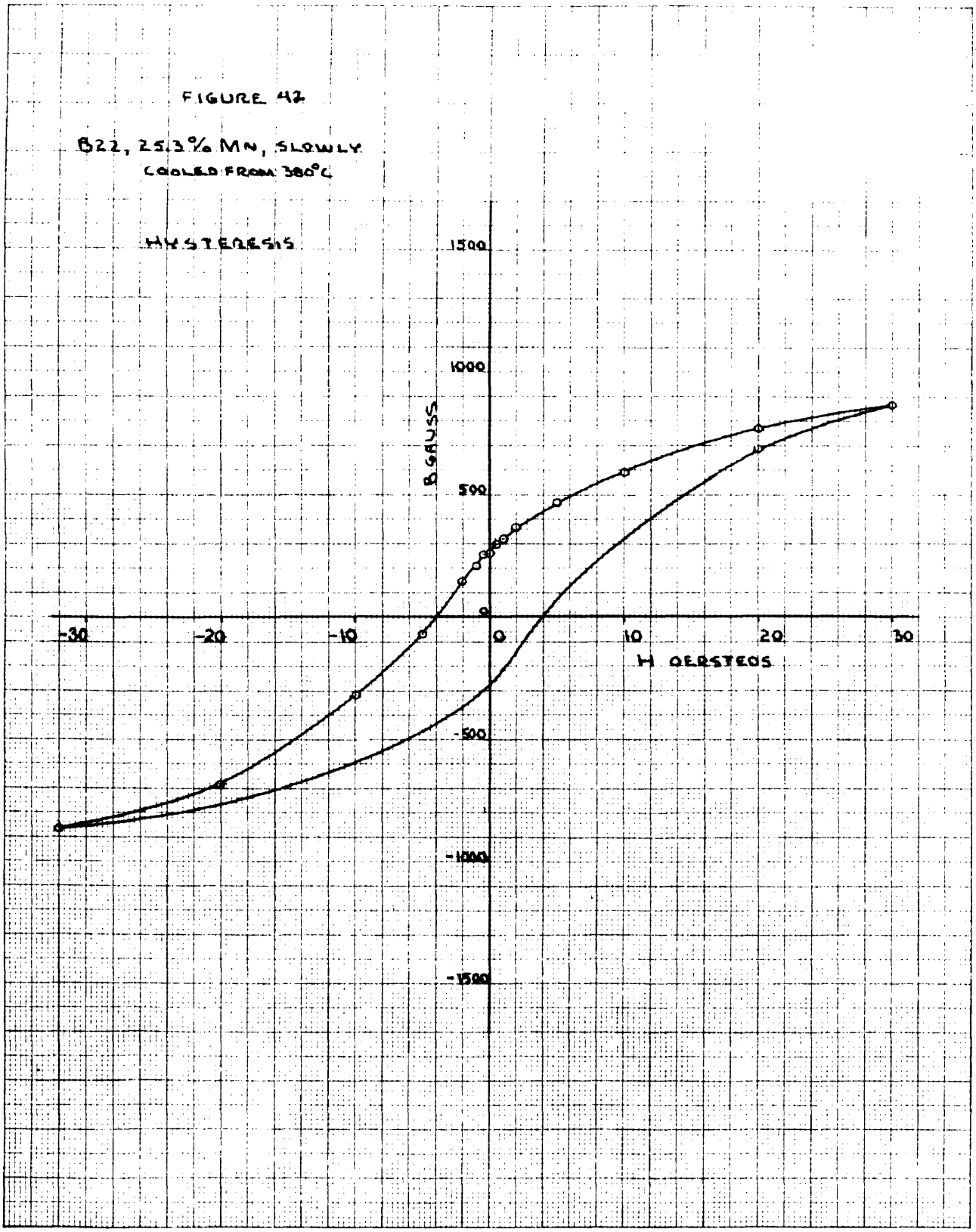

Table 25. Normal Magnetization of 031, 21.4% Mn, Slowly Cooled to 380° C, from 31° to 121° C.

Field H*	Induction B in Gausses and Permeability at Temperature											
	31° C		51° C		71° C		91° C		111° C		121° C	
oe.	B	μ	B	μ	B	μ	B	μ	B	μ	B	μ
--	44	1760	68	2260	100	3250	130	4170	108	3440	89	2830
	H = 0.025		H = 0.03		H = 0.0308		H = 0.0314		H = 0.0314		H = 0.0314	
0.05	102	2040	137	2740	216	4320	295	5900	228	4560	180	3600
0.075	185	2470	289	3850	463	6170	535	7140	393	5250	300	4000
0.1	352	3520	539	5390	715	7150	752	7520	543	5430	400	4000
0.15	744	4960	929	6190	1100	7330	1084	7220	717	4780	523	3480
0.2	1046	5230	1230	6150	1370	6850	1268	6340	825	4120	579	2900
0.25	1330	5320	1450	5800	1560	6250	1388	5550	900	3600	624	2490
0.3	1492	4980	1650	5500	1707	5690	1490	4970	950	3170	--	--
0.35	1700	4850	1830	5220	1824	5210	1560	4450	--	--	--	--
0.4	1858	4645	1920	4800	1915	4790	1630	4075	1028	2570	--	--
0.5	2060	4120	2110	4220	2050	4100	1720	3440	1076	2150	760	1520
0.6	2256	3760	2260	3770	2160	3430	1780	2970	--	--	--	--
0.7	2377	3396	2360	3370	2270	3240	1840	2630	1160	1545	810	1080
									H = 0.75		H = 0.75	
0.8	2490	3110	2480	3100	2350	2940	1880	2350	--	--	--	--
0.9	2577	2860	2540	2820	2410	2680	--	--	--	--	--	--
1	2685	2685	2630	2630	2470	2470	1940	1940	1217	1217	845	845
1.5	--	--	2880	1920	2650	1770	2060	1370	1295	863	--	--
2	3185	1593	3050	1525	2760	1380	2120	1060	--	--	--	--
2.5	--	--	--	--	2830	1130	2160	1370	1280	550	988	395
3	--	--	3240	1080	2870	957	--	--	--	--	--	--
4	--	--	3330	858	2930	732	--	--	--	--	--	--
5	3560	712	3390	685	2690	592	2280	456	1500	300	1080	240
7.5	--	--	3460	462	3010	402	--	--	--	--	--	--
10	3810	381	3490	349	3060	306	2400	240	1612	161	1250	125
20	3880	194	3520	176	3110	155	2490	125	1734	87	1400	70
30	3910	130	3550	118	3130	104	2490	83	1778	59	1450	48

* Where values of H do not correspond to those given in the first column, they are noted under the figures for B and μ.

Table 26. Maximum Permeabilities.

Temperature : T : °C	Maximum : Permeability : $\mu_{max.}$	Field for $\mu_{max.}$: (H) $\mu_{max.}$: oersteds
31	5320	0.24
51	6200	0.17
71	7320	0.14
91	7520	0.11
111	5400	0.10
121	4030	0.09

E. Thermoelectric.

1. The data of ordered and disordered Ni_3Mn vs. alumel was taken against a National Bureau of Standards Standard thermoelectric sample 118 alumel, whose calibration against National Bureau of Standards platinum standard Pt 27, is given in the following table. Cold junction at 0° C.

Table 27. Electromotive Force of Alumel - Pt 27 vs. Temperature.

Degrees Centigrade	International Millivolts
0	0.00
25	-.034
100	-.129
200	-2.16
300	-2.87
400	-3.61
500	-4.41
600	-5.26
700	-6.16
800	-7.07
900	-7.95
1000	-8.79
1100	-9.59
1200	-10.35
1300	-11.08

FIGURE 43
B31, 21.4% Mn, SLOWLY COOLED TO 380°C

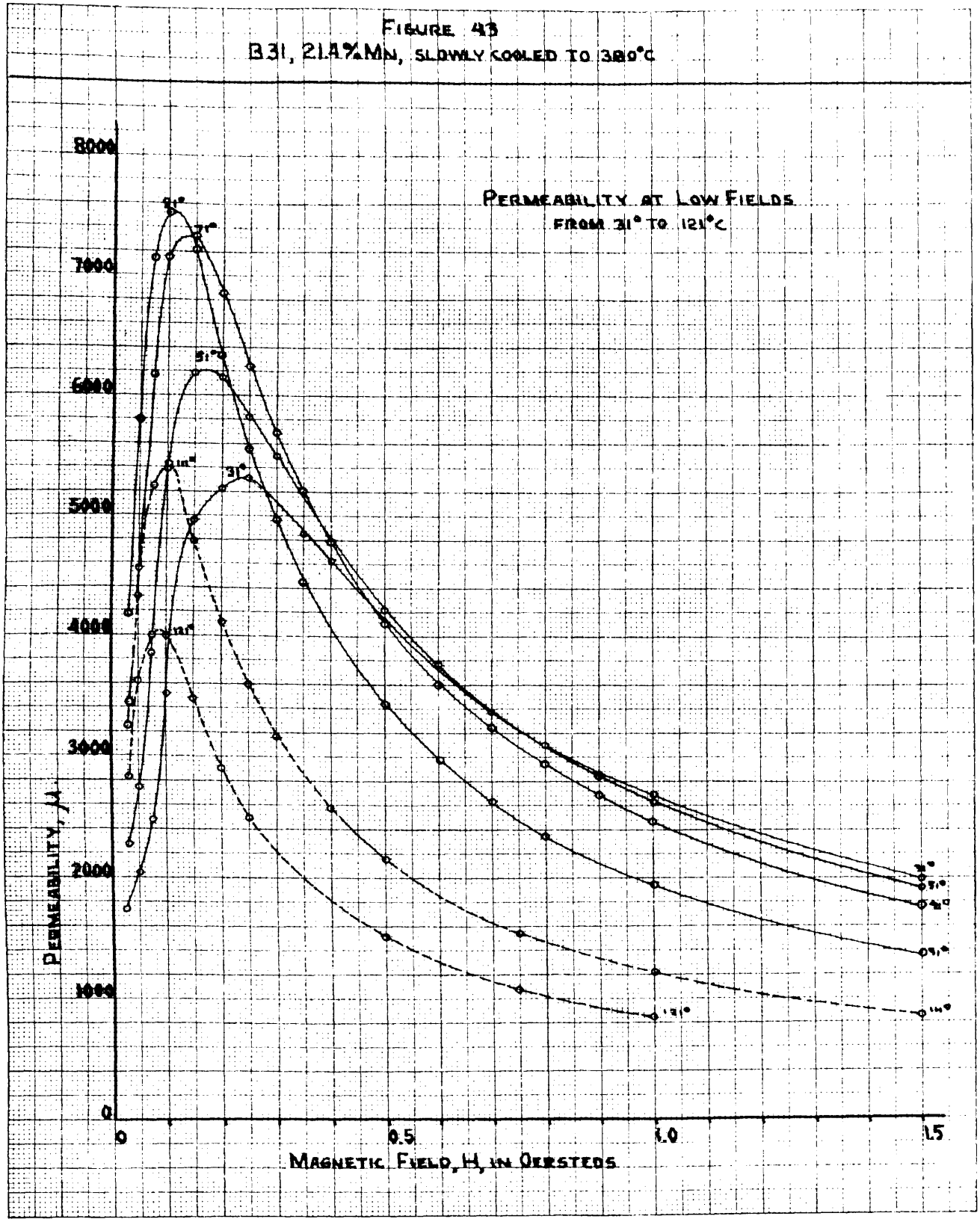

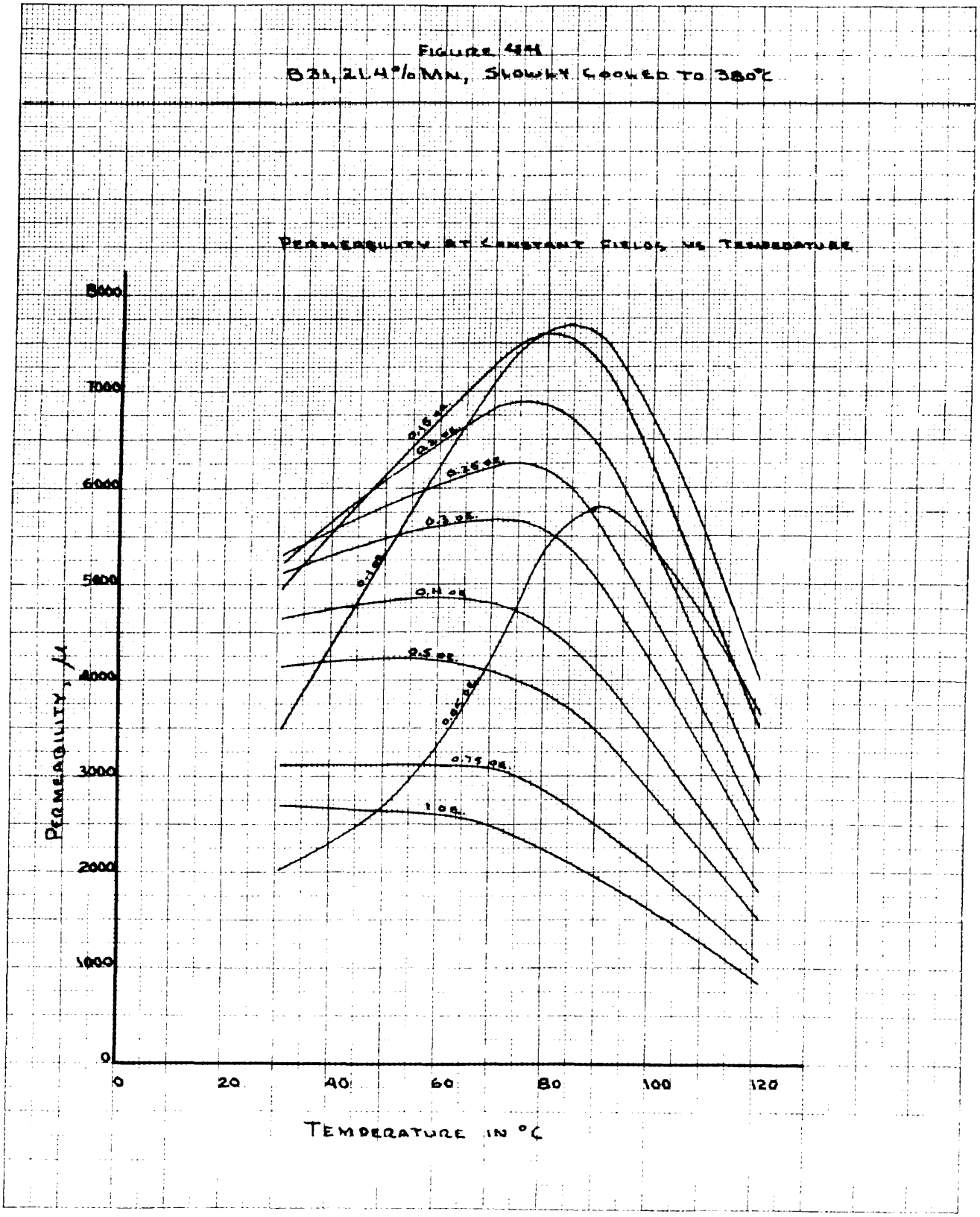
FIGURE 48A
B31, 21.4% MN, SLOWLY COOLED TO 380°C
PERMEABILITY AT CONSTANT FIELDS VS TEMPERATURE
PERMEABILITY, μ
TEMPERATURE IN °C
0
1000
2000
3000
4000
5000
6000
7000
8000
0
20
40
60
80
100
120
0.1 OE
0.2 OE
0.3 OE
0.4 OE
0.5 OE
0.6 OE
0.75 OE
1 OE

FIGURE 45
B31, 21.4% MN, SLOWLY COOLED TO 380°C

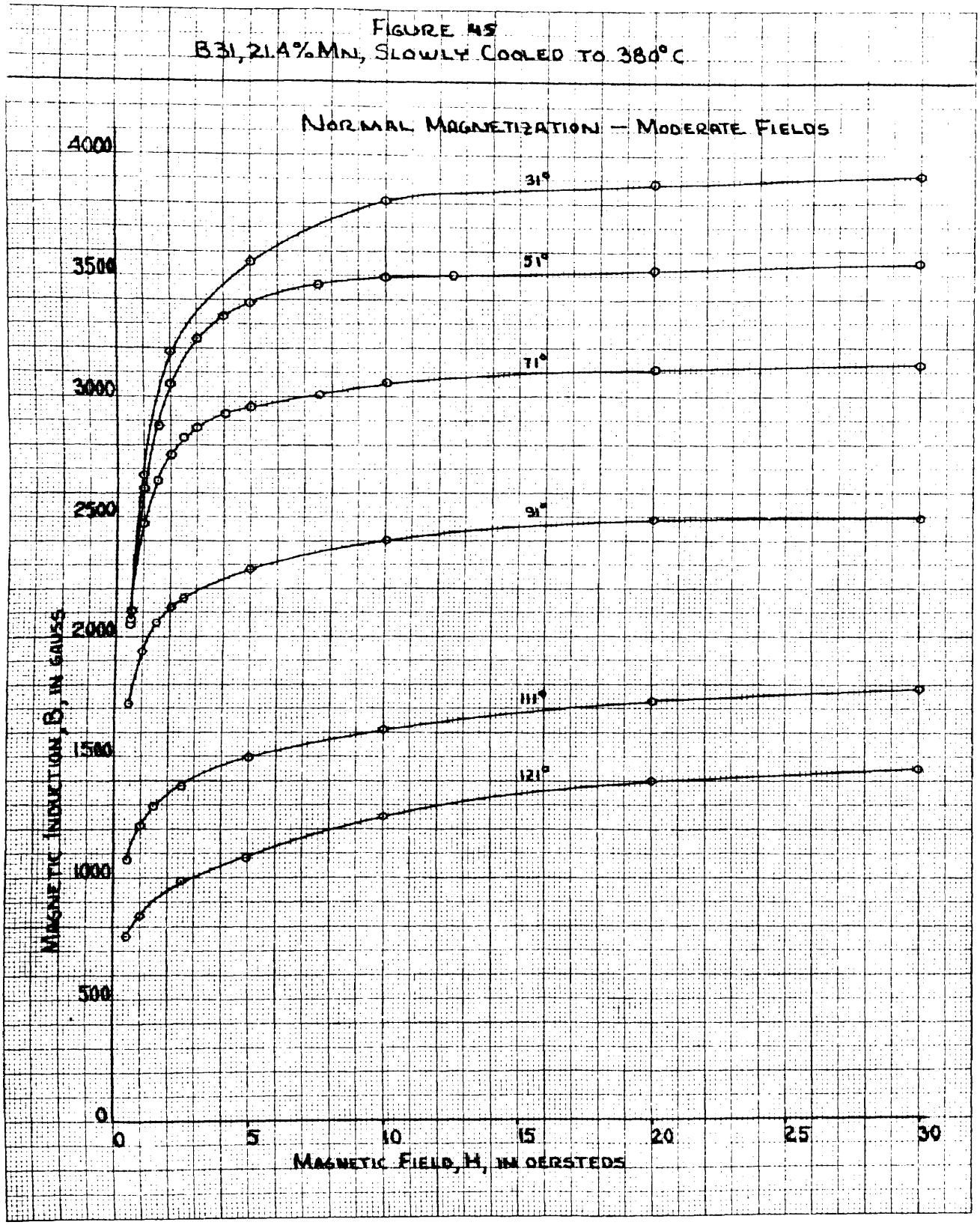

2. Disordered Ni_3Mn vs. Alumel. Q62 wire, 23.2% Mn, in the cold drawn non-magnetic condition. Average rate of heating to 530° C was 2.4° C per minute. Cold junction at 0° C.

Table 28. Disordered 23.2% Mn Alloy against Alumel. Thermoelectric Force vs. Temperature.*

Degrees Centigrade	International Millivolts
30.3	0.61
54.0	1.15
60.8	1.31
78.2	1.61
102.0	2.16
132.0	2.69
150.0	3.01
170.4	3.31
201.0	3.87
231.0	4.40
262.8	4.96
302.6	5.71
329.2	6.19
349.0	6.59
367.5	6.95
395.8	7.52
418.2	7.91
439.4	8.39
465.9	8.91
488.3	9.42
503.3	9.71
516.0	10.00
523.0	10.14
533.4	10.40

Thermoelectric force, disordered through ordering, at about 500° C = 0.0085 mv. per ° C.

* Temperatures considered precise to 0.5° C, and millivoltages to 0.07 mv.

3. 23.2% Mn Alloy Ordered by Very Slow Cooling Range vs. Alumel. The time taken to cool from 532° C to 300° C was 168 hours, or an average rate of cooling of 1.38° per hour. Cold junction at 0° C.

Table 29. Ordered 23.2% Mn Alloy against Alumel. Electromotive Force vs. Temperature.

Degrees Centigrade	International Millivolts	Degrees Centigrade	International Millivolts
532.0	10.35	308.6	5.09
526.2	10.24	300.0	4.94
521.2	10.13	291.3	4.79
515.3	10.00	281.6	4.63
511.6	9.90	271.6	4.45
505.9	9.78	262.7	4.31
497.1	9.59	251.7	4.12
487.9	9.35	242.1	3.97
481.5	9.19	232.5	3.85
475.3	9.04	222.4	3.69
469.5	8.89	212.1	3.52
465.2	8.74	202.2	3.38
461.2	8.62	192.2	3.23
455.0	8.47	181.8	3.06
448.9	8.30	169.4	2.90
443.0	8.16	159.2	2.76
430.9	7.84	148.3	2.60
423.9	7.66	137.2	2.45
418.2	7.49	125.0	2.25
410.8	7.30	112.6	2.04
402.8	7.10	99.6	1.85
395.8	6.94	87.0	1.66
388.9	6.78	74.1	1.40
381.5	6.60	67.4	1.27
374.4	6.45	62.5	1.18
361.1	6.15	54.9	1.05
352.7	5.98	46.6	0.92
344.8	5.81	43.9	0.86
336.8	5.65	38.8	0.76
328.5	5.50	31.9	0.65
320.1	5.33		

4. Difference Data between Disordered and Ordered 23.2% Mn Alloy.

Table 30. Emf. Difference vs. Temperature.

Degrees Centigrade	Disordered e_1	Ordered e_2	e
300	5.65	4.96	0.69
310	5.83	5.13	0.70
320	6.01	5.32	0.69
330	6.20	5.51	0.69
340	6.40	5.72	0.68
350	6.60	5.93	0.67
360	6.80	6.13	0.67
370	7.00	6.34	0.66
380	7.20	6.57	0.63
390	7.39	6.80	0.59
400	7.58	7.04	0.54
410	7.78	7.29	0.49
420	7.98	7.58	0.40
430	8.18	7.85	0.33
435	8.28	8.01	0.27
440	8.39	8.10	0.29
450	8.59	8.33	0.26
460	8.80	8.59	0.21
470	9.01	8.89	0.12
480	9.22	9.17	0.05
490	9.42	9.42	0.00
500	9.64	9.64	0.00
510	9.80	9.86	0.00
520	10.08	10.08	0.00

L. Calculations of Permeability from Inductance-Resistivity Data.

1. Equation.

$$\mu = \frac{K}{\rho}\left(\frac{L_m - L_c}{\pi r}\right)^2$$

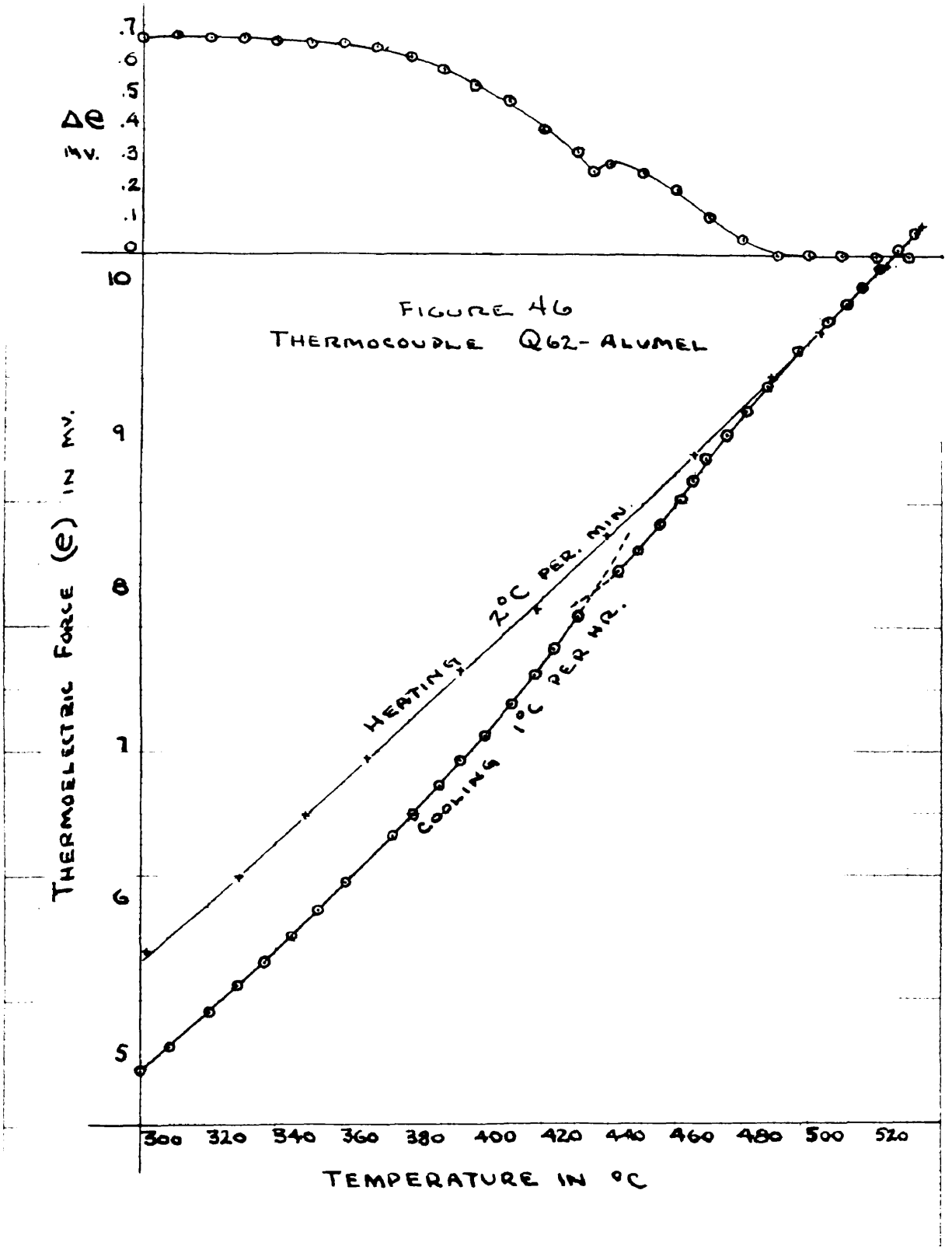

FIGURE 46
THERMOCOUPLE Q62- ALUMEL

2. Determination of Constant, K.

a. From experimental data on non-magnetic rods

$$K = \frac{\rho}{\left(\frac{L_m - L_c}{\pi r}\right)^2}$$

Frequency = 46,500 cycles

Area of solenoid = 0.757 cm.

Inductance of solenoid

(1) Measured, L = 112.8 μh

(2) Calculation from Nagaoka's formula, L = 115.8 μh

formula:

$$L_c = \frac{0.757 - A_b}{0.757}(112.8)$$

Note: L, measured, was used because the quantity $(L_m - L_c)$ is a difference, and any absolute error will be eliminated.

Table 31. Evaluation of Constant Using Non-Magnetic Rods.

Non-Magnetic Rods	Resistivity ρ $\mu\Omega/cm^3$	Radius r cm.	Inductances L_m μh	Inductances L_c μh	K
O-34: 63% Mn, 37% Cu	176.2	0.333	109.7	60.7	0.080
K-29: 72.5% Mn, 27.5% Cu	151.9	0.3225	108.0	64.0	0.080
R-64: 40% Mn, 40% Ni, 20% Cu	142.8	0.338	105.2	59.4	0.077
R-25: 90% Mn, 5% Sn, 5% Cu	146.6	0.335	109.0	60.2	0.068
M-20: 50% Mn, 5% Al, 45% Fe	121.9	0.333	103.7	60.6	0.072

Average K = 0.075 ± 0.002 (A. D.)

b. From theoretical equation

$$K = f\left(\frac{A_a}{5033\, L_a}\right)^2$$

$$= f\left(\frac{0.757}{5033 \times 115.8}\right)$$

$$= 1.69 \times 10^{-6} f$$

Note: The inductance used here is that calculated from the dimensions and winding of the solenoid by Nagaoka's formula.

at f = 46,500

$K = 1.69 \times 10^{-6} \times 46{,}500$

$= 0.0785$

3. Calculation of Permeabilities.

(1) Rod: Q63 (21.5% Mn) 168 hours at 415-420° C.

(2) Inductance measured at 46,500 cycles and a maximum field, $H_{max.}$, of about 0.75 oersted.

(3) Data and calculation:

$$L_c = \frac{0.757 - 0.358}{0.757} \times 112.8$$

$= 59.4\ \mu h, \quad r = 0.337$ cm.

Table 32. Calculation of Permeabilities from Inductance Data

Temperature: T	Inductance: L_m	Resistivity: ρ	$\left(\frac{L_m - L_q}{\pi r}\right)^2$	Permeability: exp. const.	Permeability: th. const.
°C	μh	$m\Omega / cm^3$	S	μ	μ
20	1290	53.0	25400	1910	2000
40	1340	54.5	27200	2040	2140
60	1360	56.0	26800	2010	2100
80	1310	57.3	24200	1820	1900
100	1230	58.5	21200	1590	1670
120	1130	60.0	17000	1270	1340

4. Comparison of Results with D. C. Results.

The ballistic data which comes closest to the conditions holding for Q63 in the above calculations are those of B31 (21.4% Mn), 50 hours at 430° C + 170 hours at 405° C. Figure 28 shows the permeability at 0.75 oersted found for the alloy at temperatures from 72° to 115° C.

Table 33. Permeabilities from Ballistic Data for Comparison

Temperature: T : ° C	Permeability at 0.75 oe. : μ
20	2740*
40	2810
60	2780
80	2520
100	2120
120	1700

*Errata: Figure 47 incorrectly shows this point as 2350.

F. Variation of Inductance and Effective Resistance with Magnetizing Field.

1. Specimen rod: Q63 (21.5% Mn) 64 hours at 425-430° C.

2. Frequency = 50,000 cycles.

3. Field equation:

$$H = 2\pi n I (\cos\theta_1 - \cos\theta_2)$$
$$= 2\pi \times \frac{92}{2.54} (0.995 + 0.995) I$$
$$= 44.6\ I \text{ oersteds at center}$$

FIGURE 47 COMPARISON OF PERMEABILITY CALCULATED FROM INDUCTANCE WITH D.C. RESULTS
NI-MN ALLOY, 21.5% MN
H = 0.75 OE.

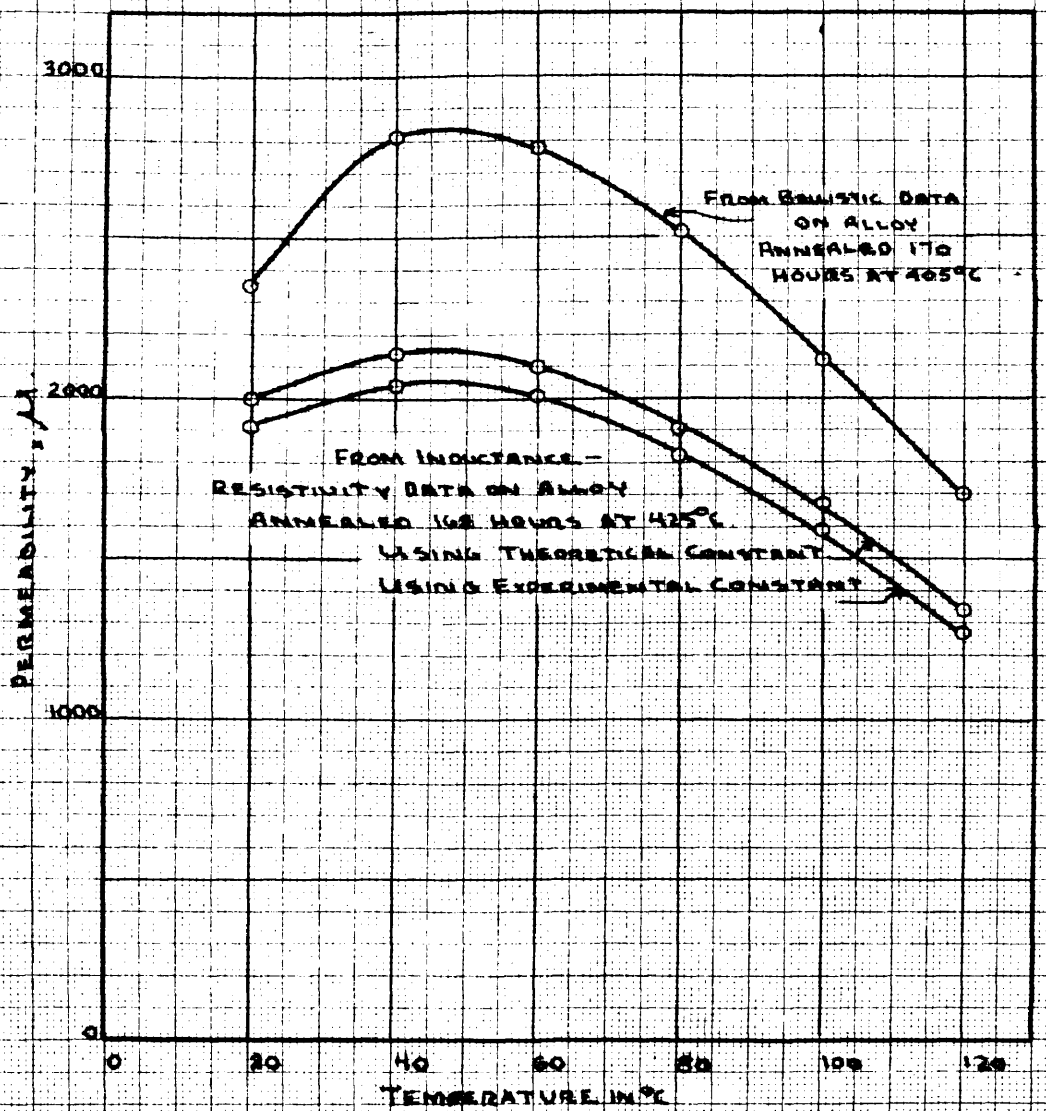

4. Data.

Table 34. Variation of L and R_e with H. F. Field.

Vacuum Thermocouple i (r.m.s.) ma.	Current $I_{max.}$ ma.	Field $H_{max.}$ oe.	Inductance L_m μh	Effective Resistance R_e ohms
4.5	6.4	0.30	924	403
5.7	8.1	0.37	939	412
6.1	11.0	0.40	958	429
8.0	14.1	0.50	979	456
10.0	14.1	0.63	994	484
11.0	16.7	0.75	995	510
12.5	17.7	0.80	1000	519
14.5	20.5	0.93	1007	536

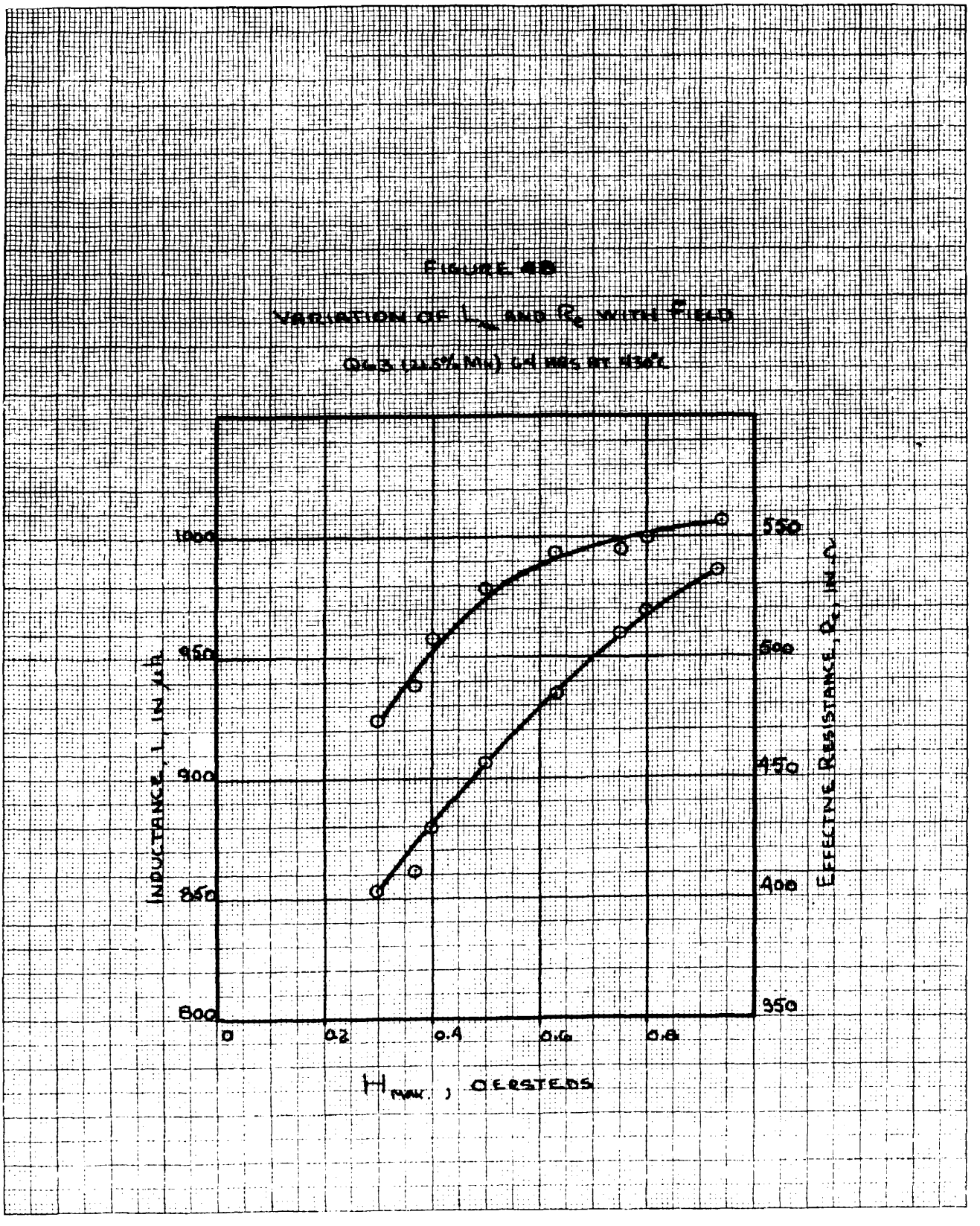

FIGURE 48

VARIATION OF L_{eq} AND R_e WITH FIELD

Q_{eq} (as 5% Mo) coil was at 45°C

IX. DISCUSSION

A. The Temperature Runs.

The magnetic properties shown by measurements of the inductance of a solenoid with a ferromagnetic core were in the present case limited by the fact that the maximum value of the alternating field was held constant. The complex nature of permeabilities at constant fields versus temperature is shown by the curves in Figures 28 and 44, which were derived from ballistic magnetic data. This complexity is particularly the case at the low fields of less than 1 oersted, which were the magnitude of fields generated by the solenoid. Hence, only a limited picture of the soft magnetic properties of the core material may be obtained from inductance-temperature measurements.

It was indicated in the theory of Section III A and experimentally demonstrated in the results of Section VIII B that permeabilities may be calculated from inductance-resistivity data. Hence, when the inductance is mentioned in the following, it can be taken as a measure of the permeability, being proportional to the square root of the permeability, and capable of being calculated by the equations of Section VIII E.

Pure ferromagnetic metals, as distinguished from ferromagnetic alloys, exhibit a normal behavior of permeability versus temperature, which is well illustrated

by the results for electrolytic nickel in Figure 13. Here, inductance is plotted versus temperature. The inductance increases gently with temperature until temperatures approaching the Curie point are reached. As the Curie point is approached the inductance increases sharply to a maximum, and falls practically vertically to a constant value corresponding to the non-magnetic inductance value.

Also plotted in Figure 13 are the resistivity-temperature data and the effective resistance-temperature data of the nickel rod specimen and the solenoid with nickel core on being heated. It has been stated in Section III A that the effective resistance was a measure of the hysteresis and eddy current losses in the core plus the losses in the solenoid winding itself. It is reasonable that the course of the effective resistance-temperature curve should follow the course of the inductance-temperature curve, as seen in Figure 13. This is because the area of the hysteresis loop traced out by the high frequency field will probably increase as the permeability increases, the coercive force will not change much, and $B_{max.}$ will increase since roughly $\mu = \frac{B_{max.}}{H_{max.}}$. Thus, it is seen in Figure 13 that the effective resistance follows fairly well the course of inductance, even showing the sharp increase just before the Curie point. The increase of R_e after the drop at the Curie point is due to the high temperature coefficient of resistance of the platinum winding of the solenoid. The resistivity of nickel as shown

in Figure 13 illustrates the well known experimental facts that the temperature coefficient is high and there is a slight discontinuity at the Curie point.

If the point of maximum slope of the permeability (or inductance) curve versus temperature were taken as the Curie point of nickel, the value of Θ_c from Figure 13 would be 358° C, but, as has been stated before, the more old-fashioned notion of taking the Curie point at complete non-magnetism has been used in this work, and the value taken was 368° C.

Temperature data on an ordered nickel-manganese alloy are shown in Figure 14. The alloy, 463 (21.5% Mn), has a composition on the nickel-rich side of the theoretical superlattice (23.78% Mn). Evidence that it has become ordered by the heat treatment of 165 hours at 415°-420° C is given by the low electrical resistivity at room temperature of 55.06 x 10^{-6} ohms per cm^3 over its pre-treatment resistivity of 60.0 x 10^{-6}, and by the fact that it was ferromagnetic after treatment and non-magnetic before. Both the inductance and the effective resistance curves show that it is possible to completely destroy the ordered state by heating to a sufficiently high temperature, 535° C in this case. The observation of the temperature difference between the Curie point and the critical ordering temperature, which was brought out by H. Thompson (2) and Kaya and Nakayama (3), was checked by the data in Figure 14: The ordered state was established by prolonged annealing at 415°-420° C,

and yet the Curie point for the alloy in this condition was at a lower temperature, 320° C. The course of the cooling curves of L and R_e, which are characteristic of the alloy heated to 535° C, follows the portion of the heating curve of the annealed alloy beyond the Curie point, establishing that the alloy has become non-magnetic. The approach of the alloy to the Curie point, as shown by the L and R_e curves of Figure 14, is gradual compared to the approach of nickel, as shown by the same curves in Figure 13. The resistivity curves in Figure 14 show that the resistivity of the ordered alloy is lower than that of the disordered alloy at temperatures below the Curie point, and that the disordered state (cooling curve) follows the course of the ordered state (heating curve) above the Curie point.

Figure 15 gives heating data for an ordered alloy of higher manganese content, Q61 (24.4% Mn), on the manganese-rich side of the theoretical superlattice. Annealing 96 hours at 410-415° C was sufficient to well order the alloy, as is shown by the low room temperature resistivity of 51.02 x 10^{-6} ohms per cm^3. The initial inductance was quite low, compared to the ordered 21.5% Mn alloy, but it picked up at higher temperatures, and extended over a larger temperature range to a Curie point of 460° C. This value of the Curie point is the one given by Thompson (2). The peak and dip in R_e at and after 130° C has no particular significance other than it is the

consequence of R_e following the $\perp$-curve which showed a rather sharp peak at 130° C; as has been mentioned, R_e, indicating magnetic losses, follows $\perp$, which is a measure of permeability. The electrical resistivity curve started leveling off at the Curie point, in agreement with Kaya and Nakayama's work (3). The heating of this alloy was taken just to the Curie point; no data were taken on cooling.

The fact that the ordered state of these alloys is little affected by heating to, but not beyond, the Curie point, is illustrated by Figure 16, which gives data on heating and cooling the C61 alloy after being cooled from the preceding run, Figure 15. The curves in Figure 16 are very similar in shape to those in Figure 15, indicating that the state of order was not affected much by the previous run to the Curie point, a result quite different from that shown in Figure 14, where the alloy was heated above the ordering range and was made non-magnetic as a consequence. Close examination of Figure 16 shows differences from Figure 15. The Curie point is lower, 430° C instead of 460° C, and the room temperature resistivity is higher, 54.09 x 10^{-6} instead of 51.02 x 10^{-6}. This indicates tentatively that the state of order which resulted from an annealing of 96 hours at 410-415° C, given numerical measure by a room temperature resistivity of $\int_o$ = 51.02 x 10^{-6}, was lowered by heating to 464° C, because now $\int_o$ = 54.09 x 10^{-6}. This observation that the state of order can be lowered by heating to higher temperature in the ordering range, resulting in lower Curie

points, is borne out by subsequent data. This idea is opposed to the conclusion of Thompson (2), who states "... the critical temperature for the ordering process is about 510° C. Quenching effected from above this temperature preserves the disorder and the paramagnetic state. Below it, the degree of order and, correspondingly the saturation magnetization at room temperature, increase as the annealing temperature is reduced, but for all states of order the Curie point is in the neighborhood of 460° C." However, Thompson's conclusion above had reference to alloys put into order-disorder equilibrium before being quenched to room temperature, while the conclusion arrived at from the present data applies to non-equilibrium, lower degrees of order brought about by momentary reheating to higher temperatures in the ordering range. Also in Figure 16, it will be seen that there is very little difference in the Curie points and in the resistivities on heating and cooling, principally because the alloy was heated to just past the Curie point, and not as high as in the previous run. The shapes of the L and R_e curves on heating and cooling are slightly different, but this could easily have been the result of small differences in the magnitude of the high frequency current, because of the sensitive response of inductance to magnetizing field in these alloys. Also the resistivities on heating and cooling were the same, and did not diverge at the Curie point, as they do when the alloys are heated higher.

The type of runs discussed for Q61 (24.4% Mn) in Figures 15 and 16 are given in Figures 17 and 18 for Q63 (21.5% Mn). Here it can be seen that the ordered structure is very little affected by heating to 422° C, since the curves are the same in the two figures. Heating the same alloy to 535° C made it non-magnetic, as was shown in Figure 14. Heating to 422° C, a temperature slightly greater than the annealing temperature 410-415° C, evidently did not lower the degree of order, and perhaps may have increased it slightly because $\int_o$ after heating to 422° C was 59.82 x 10^{-6} and before was 60.32 x 10^{-6}. The cooling curves in Figure 18 indicate that the degree of order of the alloy might have been lowered by heating to 462° C during the run, because L and R_e on cooling lagged behind the heating curves, the Curie point of the cooling curves being 270° C while that of the heating curves is 300° C.

More conclusive evidence on the above points are given in Figures 19, 20, and 21, which give data for three alloys Q63 (21.5% Mn), Q62 (23.2% Mn) and Q61 (24.4% Mn), annealed 87 hours at 425-430° C. This data was taken on being heated to and cooled from 480-490° C, a temperature quite close to the critical ordering temperature. The resistivity data shows that the degree of order was lowered by heating the ordered alloys to these temperatures. The L and R_e curves show that the Curie points have been lowered considerably by heating to these temperatures. The Curie point data taken from Figures 19, 20 and 21 (see Table 7) was:

Q63 (21.5% Mn)

Curie point after annealing	320° C
Curie point after heating to 486° C	180° C

Q62 (23.2% Mn)

Curie point after annealing	360° C
Curie point after heating to 482° C	260° C

Q61 (24.4% Mn)

Curie point after annealing	440° C
Curie point after heating to 490° C	430° C

The curves, marked L-cooling and R_e-cooling, were reversible characteristics of the alloys in their lower degree of order, and could be followed on heating and cooling without change in magnitude or shape; in fact, the lower temperature data, below 100° C, were determined by heating the alloys from room temperature on the day following the run because the furnace cooled so slowly at these low temperatures. The behavior was definitely not temperature hysteresis phenomenon such as is shown by iron-carbon alloys, Hopkinson's iron-nickel alloy (30% Fe), and some others mentioned by T. F. Wall (20) and other authors. A striking aspect of the results for the present alloys in the slightly disordered condition produced by the momentary heating to high temperature is the fact that the inductances rise to quite high values at low temperatures even though the Curie point was lowered so markedly; this is particularly true for Q63 (21.5% Mn) as shown in Figure 19. Also the inductance and effective resistance of the slightly disordered alloys show a smooth variation with temperature, while the annealed alloys show

a characteristic discontinuous variation. Also, the resistivity on cooling diverged from that on heating and the break in the curve on heating occurred at about the Curie point. The fact that the resistivity curves have deviated so markedly even though the alloys are still appreciably ordered indicates that such deviation is no proof of complete disordering.

It is evident that treatment at temperatures high in the ordering range has a potent effect on the magnetic properties. So far, data have been discussed on alloys which have been annealed at relatively low ordering temperatures or which, after such annealing, have been heated momentarily to high ordering temperatures. The effect of prolonged annealing at high ordering temperatures on L, H_c, and ρ is shown in Figures 22 and 23. The degree of order has been lowered undoubtedly by the high temperature treatment, but the striking feature of the data is the low values of inductance attained. Q63 (21.5% Mn) was scarcely ferromagnetic after prolonged annealing at 460-470° C. Q62 (23.2% Mn), also on the nickel-rich side of the superlattice, showed very low inductances over the entire heating range, but it is interesting to note that its Curie point was as high as it ever was in the low temperature annealing. Q61 (24.4% Mn), on the manganese-rich side, showed in Figure 23 lower inductance values than in the previous anneals at lower temperatures, but relatively higher values than that showed by the two alloys on the nickel-rich side; the Curie point, 410° C,

was lower than when annealed at lower temperatures (Figures 15 and 21) or lower than when after these anneals it was heated to 464° C, but it was higher than when it was heated to 490° C (see Figure 21).

Since apparently, higher inductance values are obtained by annealing at low ordering temperatures, about 400°-420° C, where according to theory and experiment higher degrees of order are attained, an attempt to put the alloys in as high a degree of order as possible by low temperature annealing was made. According to Kaya and Nakayama (3) the only way to attain equilibrium degrees of order at any particular temperature is by extremely slow rates of cooling through the ordering range from 600° C to the temperature, and that below 300° C no further alteration in the degree of order can be made by continued annealing. Their procedure was not followed exactly, as may be seen in Table 5 for Figures 24, 25, and 26; a discontinuous rate of cooling was employed, whereby the alloys were given 16 hours at 440°-445° C, cooled to 420° C and kept there 96 hours, cooled to 366° C and kept there 48 hours, cooled to 354° C and kept there 40 hours. The results of this anneal are shown in Figures 24, 25 and 26. It can be seen that Q63 (21.4% Mn) and Q62 (23.2% Mn) attained fairly high inductance values, but that Q61 (24.4% Mn) had quite low inductances. This indicates that the temperatures at which the longer annealing took place was too low for Q61, but sufficiently high for Q63 and Q62 in order for the order-disorder transformation to take place to a reasonable extent. Evidently the temperature range in which the rate of transformation

is sufficiently high to promote a degree of order appreciably close to the equilibrium value is highest for Q61 (24.4% Mn), lower for Q62 (23.2% Mn), and lowest for Q63 (21.5% Mn). This observation is not checked by Kaya and Nakayama's results as shown in Figure 36, the curve of T_o vs. %Mn, where the higher manganese alloys are seen to have lower critical ordering temperatures.

The shapes of the inductance and effective resistance curves are quite characteristic for each alloy. Thus for Q63, in a well ordered condition, there is a maximum in inductance at about room temperature, which is followed by a fall with rising temperatures, a leveling off, and a second fall to the Curie point. The inductance of Q61 in the well ordered state has quite low values at room temperatures, rises rapidly to a peak, falls slightly, levels off, and then falls sharply to the Curie point. The inductance curves on heating the well ordered alloys momenterily at temperatures high in the ordering range are quite characteristic, too, showing a smooth and continuous variation with temperature; these curves are steepest for the higher nickel content alloys. Attention is also drawn to the type of curves found for the alloys annealed at high ordering temperatures, as shown in Figures 22 and 23.

It is believed that the exposure of the rods to oxidation and silica contamination mentioned in Table 5 for Figures 15, 17 and 20 had a deleterious effect on the inductances found, because Q63 (21.5% Mn) never again showed quite as high inductance values as it did in the run shown

in Figure 14, which was made before the annealing mishap occurred.

On comparing the Curie points of the well ordered alloys, as shown in Table 7, with those found by previous investigators, Kaya and Kussmann (1) and N. Thompson (2) (see Figure 2c), and Kaya and Nakayama (3) (see Figure 3b), it will be seen that the Curie points in the present investigation checked best with those of Kaya and Nakayama, as shown in their curve marked T_{λ}.C.

B. Magnetization and Hysteresis of Nickel-Manganese Alloys.

Extensive data was taken on B31 (21.4% Mn) in a fairly well ordered condition, because the temperature runs had indicated that the alloy of this composition, C63 (21.5% Mn), had its maximum in soft magnetic properties at about room temperature. Tables 9 to 11 are magnetization results and Tables 12 to 14 are hysteresis results for the alloy when put into the ordered state by annealing 50 hours at 430° C followed by 170 hours at 405° C. Figure 27 was plotted from values in Tables 9 and 10, and shows the strong dependence of permeability at low fields (less than 1 oe.) on temperature. It will be seen that these permeability curves were shifted up and to the left and then down and to the left with increasing temperature from -72° C. to 115° C. Another way of plotting the data in Tables 9 and 10 is shown in Figure 28, in which the permeability at constant field is plotted versus temperature. These curves are the direct current equivalent of the high frequency

inductance curves already discussed. The data for the higher fields are shown in Figure 29 in the form of B-H curves for the various temperatures. Here again the strong dependence of magnetic induction on temperature is apparent. The rapid decrease of induction with temperature is indicative that the Curie point is being approached, although the temperature-inductance data show that it will not be reached until 280°-300° C. Comparison of these results for this particular anneal with the properties of common soft magnetic materials (26) shows that unusually high inductions at low fields have been attained. These inductions are higher than those of common electric sheet, silicon transformer sheet, Armco iron, etc., but lower than the special alloys, permalloy and hipernik, and vacuum fused, hydrogen purified iron. The inductions at higher fields are comparatively low, however.

Hysteresis data on the ordered B31 alloy, for which the magnetization results were discussed above, are shown in Figures 30 to 33. The soft magnetic properties are further illustrated by the low coercive forces shown. Hysteresis data were taken at temperature from -72° to 115° C in order to make a more complete picture of the magnetic properties of at least one of these ordered alloys. The summary of the data, in Figure 33, shows that the remanence, B_r, falls with increasing temperature, as does the normal induction at 30 oersteds, B_{30}, but at a less rapid rate. Also the coercive force falls with increasing temperature, being the low value

of 0.25 oersted at room temperature and the still lower value of 0.12 at 115° C. Unfortunately, all of the data was not taken for a maximum field of 30 oersteds. Thus some of the data listed in Table 14 is not shown in Figure 33.

A second ring of the same composition as that of B31 was annealed along with it. Data taken on this specimen closely checked that of B31, and were not included in the results.

It was thought that rapid cooling from the ordering range would improve the magnetic softness of the ordered alloy. The ordering heat treatment of the alloy discussed above was concluded by slow furnace cooling in vacuum. After the measurements were made on it in this condition, it was reheated to 435° C and rapidly cooled on a heavy copper plate. The normal magnetization and hysteresis results at room temperature for this alloy are shown in Tables 16 and 17. The fact that the magnetic properties have not been appreciably changed may be verified by comparing the results with those of Tables 9 and 12.

It was thought from the high frequency data on B33 in Figure 19 that a cooling through the ordering range of 2° C per minute would result in the type of permeability versus temperature curve indicated in that Figure. Later considerations brought out that the important factor in bringing about this result was the temperature to which the ordered alloy is heated, since the desired properties

depend on a slight disordering of a well ordered structure, instead of a complete building up of an ordered structure by cooling through the range. The very feeble magnetic state of the specimen after being reheated to 660° C and cooled at 2° C per minute is given in Table 17. The induction was only 52 gauss at 30 oersteds, or a magnetization, $4\pi I$, of 22.

Data on an ordered alloy of higher manganese content than has yet been discussed is shown by Tables 18 and 19 and in Figure 34. The alloy, B21 (25.3% Mn), on the manganese-rich side of the superlattice (23.8% Mn), was annealed 116 hours at 440° C. The normal magnetization results shown are quite different from those of B31 (21.4% Mn), being much harder magnetically. The permeabilities are low and reach a maximum of 186 at 2 oersteds; the induction at 30 oersteds is 2050; and the coercive force is 4.3 oersteds. This observation that 1.5% Mn above Ni_3Mn the well ordered alloy is quite hard magnetically and 2.4% Mn below Ni_3Mn the well ordered alloy is very soft magnetically is worth stressing.

B11 (20.1% Mn) had more nickel in it than any other of the alloys investigated, except B12, which, of course, had the same composition since they were machined from the same plate. These alloys had enough nickel in them to be ferromagnetic without heat treatment. In order to be sure that the perfectly random state was ferromagnetic, B11 (20.1% Mn) was heated to 950° C and air-quenched to room temperature; Table 20 shows the ferromagnetism to be weak. However, the

other specimen of this composition, B12, did not receive this high temperature treatment, and its consistently poorer magnetic properties, as shown by data to be discussed, is believed to be due to this difference in heat treatment.

The anneal of 72 hours at 450° C on B11, B12 (20.1% Mn), B22 (25.3% Mn) and B31 (21.4% Mn) is at a temperature fairly high in the ordering range, at least as far as the nickel-rich alloys are concerned. The normal magnetization data on B31 shows that only a feeble ferromagnetism has been attained, very similar in magnitude to that in Table 17 for the same alloy cooled from 660° C at 2° C per minute. Yet the alloys on the two sides of B31 developed appreciable ferromagnetism. This was expected for the high manganese alloy, B22, from previous high frequency data, but the appreciable ferromagnetism of the 20.1% Mn alloys, B11 and B12, must principally be due to its normal slight ferromagnetism becoming greatly enhanced by the slight superlattice formation. The magnetization and hysteresis data are plotted in Figures 35, 36, 37 and 38. It is seen that B11, the alloy which had the high temperature pre-treatment, had much better soft magnetic properties than B12, not pre-treated. Thus, as is recorded in the results:

Maximum permeability:

B11, pre-treated at 950° C	840 at 0.4 oe.
B12, no pre-treatment	325 at 0.7 oe.

Coercive force:

B11, pre-treated at 950°	0.46 oe.
B12, no pre-treatment	0.57 oe.

These properties are not particularly high, as far as soft magnetic properties go, but they show the relative effect of a high temperature pre-treatment. The fact that their soft magnetic properties are relatively poor is further evidence for the contention that alloys ordered at high temperatures in the ordering range have poorer soft magnetic properties than those ordered at low temperatures. B22, a high manganese alloy of 25.3% Mn, developed hard magnetic properties from the anneal; the data are shown in Tables 21 and 22 and in Figures 35 and 38. The ordering temperature was not relatively as high for the 25.3% Mn alloy as it was for the alloys lower in manganese, because the ordering range of the 25.3% Mn alloy is probably higher. The high frequency results also indicate this. From this it appears that the critical ordering temperatures increase with Mn content. Kaya and Nakayama concur with this but N. Thompson doesn't.

A slow cooling made up of intermittent anneals to 350° C on Q63, Q62, and Q61 rods resulted in high inductances for the nickel-rich alloys and low inductances in the manganese rich alloy, as was previously discussed. An equivalent anneal on the ring specimens B12, B22, and B31 was carried out (see Results, C 1, for details). The results of the room temperature

measurements are given in Tables 23 and 24 and in Figures 39, 40, 41 and 42. The most striking feature of the data are the unusually high permeabilities of 831 (21.4% Mn) after this low temperature ordering treatment. The maximum permeabilities attained by this alloy after three types of heat treatment are shown below for comparison:

Heat Treatment	Permeability	Induction at 30 oe.
1. 72 hours at 450° C	Ca. 2	50
2. 50 hours at 430 + 170 hours at 405° C	3220 at 0.35 oe.	4600
3. Slowly cooled, mainly 50 hours at 400° C + 60 hours at 380° C	5300 at 0.25 oe.	3910

The main difference between the second and third anneal is that the third is at a temperature 25° below the second, and yet the difference in maximum permeability is almost twice. It is interesting to compare the inductances at 30 oersteds of the 405° C anneal and the slow cool anneal. Low inductions at high fields occurring in conjunction with high permeabilities at low fields is the condition here, and this may be compared with magnetic results on the same alloy as a function of temperatures. It will be seen that the low temperature annealing treatment seemed to bring the magnetic state which occurs somewhat below the Curie point - very high μ's and low B's - to room temperature. This result is exactly the opposite of the case for permalloy as reported by Kaya (28).

The coercive force of slowly cooled 851 was 0.16, considerably lower than the 0.25 found for the 405° C anneal. 812 (20.1% Mn) showed a great improvement of soft magnetic properties by the low temperature ordering in this slow cool treatment. The maximum permeability was 1800 at 0.8 oersted, considerably greater than its previous 510 at 0.70 oersted, in the 450° anneal. The coercive force at room temperature was 0.58, not much less than the 0.57 found for the 450° C anneal. It is interesting to note that the induction of this 20.1% Mn alloy was greater than the 21.4% alloy, although its permeabilities at low fields were much less.

High frequency results had shown that heat treatment at and below 400° C was too low to appreciably order the 24.4% Mn alloy. Similarly the slow cool treatment did not produce high inductions in the 25.3% Mn ring specimen. The coercive force for this alloy was 4.0 oersteds.

The effect of temperature on the magnetization of 851 (21.4% Mn) after the slow cooling to 330° C treatment is given in Tables 25 and 26 and in Figures 43, 44, and 45. The data were quite complete for low fields, and show the μ vs. H and the $(\mu)_H$ vs. T curves in much greater detail than similar curves for the 405° C anneal. From the curves the highest permeability possible is 7700 at 0.1 oersted at 85° C. The maximum of the μ vs. T curves shifts to lower fields and has a maximum value itself as temperature rises. The $(\mu)_H$ vs. T curves in Figure 44,

which are the d.c. equivalents of the μ vs. T high frequency curves, are seen to vary greatly with temperature and field; the top envelope of these curves is seen to be a plot of $\mu_{max.}$ vs. T. The B-H curves at different temperatures for this alloy are shown in Figure 45. In comparison with similar curves after the 405° C anneal, it is seen that the inductions at higher fields are considerably lower, the bend sharper, and top flatter. The inductions at 30 oersteds are seen to be falling rapidly with temperature.

C. The Magnetic Results in General.

There is an interesting analogy to be drawn between the results found for the nickel-manganese alloys around Ni_3Mn and the nickel-iron alloys around Ni_3Fe. The nickel percentage in Ni_3Mn is 76.2%, and in Ni_3Fe 75.9%, practically the same amount. Elmen (27) has shown that the permeabilities at very low fields, or initial permeability, of the air-quenched nickel iron alloys reached a maximum at 78.5% Ni. In the present investigation on nickel-manganese alloys there has also been found a maximum in permeability at low fields at 78.6% Ni (the three closest compositions to this value being 79.9% Ni, 78.5% Ni, and 76.6% Ni).

There are differences between Ni_3Mn and Ni_3Fe, too. Elmen found that the highest permeabilities were obtained when the alloy was air-quenched from about 600° C, which is the ferromagnetic Curie point. S. Kaya (28) found the critical ordering temperature of Ni_3Fe to be 490° C, a

temperature below the Curie point. The exact heat treatment used by Elmen was to heat the alloy to 900°-1000° C and hold at temperature for one hour, furnace cool at about 1.5° C per minute to room temperature, reheat to 600° C and hold for fifteen minutes, and air-quench on a heavy copper plate. The cooling rate of the air-quench was about 20° C per second; Elmen has presented data showing that the optimum cooling rate was about 60° C per second for maximum $\mu_{max.}$, and 20° C per second for maximum μ_o. Long annealing at 425° C, or "baking" as Elmen called it, produced much lower permeabilities.

The opposite situation to the above prevails with the nickel-manganese alloys. The Curie point is below the critical ordering temperature, and not above. Permalloy is quenched through the ordering range, and the nickel-manganese alloys must be "baked" at a low temperature in order to bring about the highest permeabilities.

S. Kaya (28) has published some interesting data on the variation of the coercive force of iron-nickel alloys with composition and heat treatment. The data in the following table was taken from his paper.

Table 35. Dependence of Coercive Force of Permalloys with Heat Treatment (after Kaya).

Composition % Fe	H_c in oe. Completely Annealed	H_c in oe. Slowly Cooled	H_c in oe. Water Quenched	H_c in oe. Air Quenched
18.5	0.436	0.185	0.196	0.320
20	0.380	0.184	0.033	0.164
21.5	0.269	0.184	0.045	0.081
24.1	0.205	--	0.053	0.035
25	0.238	0.215	0.042	0.030
30	0.400	0.260	0.259	--

It is seen from this data that there is a fairly sharp minimum in H_c at 21.4% Fe for the completely annealed alloys, and a somewhat flatter minima in H_c at 21.5 Fe for the other heat treatments. Similar, but much more incomplete data were taken on the annealed nickel-manganese alloys in this investigation. The values of H_c, taken from the results are in the following table.

Table 36. Dependence of Coercive Force of Ni_3Mn Alloys with Heat Treatment.

Composition % Mn	H_c in oe. Completely Annealed
20.1	0.52
21.4	0.15
25.3	4.70

Inductive reasoning from the high frequency data leads one to believe that the 23.2% Mn alloy (462) would have a low coercive force, since it was almost as magnetically soft as the 21.5% alloy, and that the 24.4% Mn alloy would have a quite high coercive force, of the order of several oersteds. These data indicate that there is an even more marked anomaly in coercive force in the nickel-manganese system than in the nickel-iron system. Although the data is incomplete, it is reasonable to believe that all the compositions on the nickel-rich side of Ni_3Mn, which undergo the order-disorder transformation, will have fairly low coercive forces, while the compositions on the manganese-rich side of Ni_3Mn will have much higher coercive forces. This means that an ordered structure of Ni_3Mn with excess nickel atoms is magnetically soft, with 21.5% Mn as the softest composition, and an ordered structure of Ni_3Mn with excess manganese atoms will be magnetically hard.

There are two possible reasons why Valentiner and Becker (4) did not observe the very soft nature of the nickel-rich Ni_3Mn alloys in their magnetic investigation: (1) impurities in the alloys, and (2) insufficient alloys. The manganese they used was "Mangan nach Goldschmidt", a rather impure product. In view of the sensitive response of magnetic softness to impurities, this factor was probably effective. Also, they only investigated the 20% Mn and 25% Mn alloys in the vicinity of Ni_3Mn, which means that only

one nickel-rich Ni_3Mn alloy was investigated. The results in the present investigation have shown that the 20.1% Mn alloy is not outstandingly soft.

Compared to the iron-nickel alloys like permalloy or hypernik, or to extremely pure iron, freed from oxygen and sulfur by vacuum melting or hydrogen annealing, the soft magnetic properties of the well ordered 21.5% Mn alloy are not particularly outstanding. But the production of so high a degree of magnetic softness in a non-ferrous alloy, which is normally non-magnetic, is indeed remarkable.

D. Thermoelectric Evidence of the Order-Disorder and the Magnetic Transformation.

The existence of two critical temperatures in ordered Ni_3Mn, the Curie point and the critical ordering temperature, have already been brought out by previous investigators. The point was also to be unmistakably inferred from the results of the temperature runs. The data of Kaya and Nakayama (3) did not show any effect at the Curie point. It is probably true that in their method, measuring the thermoelectric force of the alloy quenched from temperature, Kaya and Nakayama desired only to determine the temperature of the onset of order. Measurements made on quenched alloys would not be expected to show the Curie point, because all of the alloys quenched in the ordered condition would be ferromagnetic at room temperature.

The thermoelectric force of the 23.2 Mn alloy vs. alumel, whose emf. against standard Pt 27 was known (Table 27), is given for the disordered, cold drawn condition in Table 28, and for the condition resulting from very slow cooling at an average rate of 1.4° C per hour in Table 29. The data at temperatures from 300° to 525° C are shown in Figure 46. Inspection of the curves shows that as the alloy became ordered, its emf. against alumel became lower than in the disordered state. The emf. deviation of the ordered from the disordered curve is very gradual at the start; this is a further indication that the ordered and disordered states must be electrically quite similar (the lack of a sharp break in electrical resistivity in going from the ordered state to the disordered state is illustrative of the same idea).

Further inspection of the ordered curve shows that there is a slight, but definite anomaly at 435° C, which is about the Curie point for the 23.2% alloy in a very well ordered state. This anomaly is an upward break in the curve, and is clearly brought out by the upper curve of Figure 46, which is the difference between the ordered and disordered emf. curves against temperature.

It was necessary to extrapolate the data above and below the break in order to identify its exact position, but it is believed that the course of the data from 30° C below the break to 30° C above the break justifies this extrapolation.

E. The High Frequency Measurements.

Sections E and F of the Results present data and equations for the calculation and interpretation of the high frequency inductance measurements in terms of more fundamental units.

The constant in the equation for calculating permeability from inductance and resistivity (see Section III A for derivation and further discussion) was obtained both experimentally with nonmagnetic rods and theoretically. The agreement found for the experimental and theoretical constants (experimentally K = 0.075 and theoretically K = 0.0785) was much better than expected.

Calculations of permeability at different temperatures from inductance-resistivity data on an ordered nickel-manganese alloy were made, and are compared with ballistically determined permeabilities in Figure 47. A great deal of accuracy cannot be expected from this comparison for several reasons: (1) the determination of the r.m.s. value of the high frequency current was not precise; (2) the calculation of the peak value of the h. f. current (or the h. f. field) assumed a sinusoidal wave, an approximation at best; (3) the h.f. current, or field, was not very constant; and (4) the ballistic data was on a different specimen, although of the same composition, which was in a somewhat higher degree of order, and hence may be expected to have higher permeabilities. The comparison showed the calculated permeabilities to be of the correct order of magnitude, and was therefore a successful demonstration of the validity of the equations.

It is apparent that the high frequency data does afford a means for obtaining soft magnetic properties rapidly, although somewhat incompletely and inaccurately, and is an excellent method for permeability vs. temperature measurements. Knowledge of the h. f. field and the d. c. resistivity is imperative for calculating permeability and interpreting the data, and, after this has been done, approximate values of permeability at a given field are the results. In the data presented in section, Results A, permeabilities were not calculated, but only the inductance-resistivity data presented, because it was felt that their values, coupled with the knowledge that permeability was proportional to the square of inductance, were sufficient for the purposes at hand.

Results showing how the inductance and effective resistance varied with the high frequency field are given in Part F, and shown graphically in Figure 48. The marked variation of these properties with field illustrates the importance of operating at a constant field. The L vs. $H_{max.}$ curve, the high frequency equivalent of the ballistic μ vs. H curve, is seen to be somewhat different from that curve in that the maximum in L takes place at a higher field, H, than the maximum in μ.

The maxima in the μ vs. T curves in Figure 47 occurred at the same temperature for both the calculated h. f. permeability and the d. c. permeability.

X. CONCLUSIONS

1. Alloys of the composition Ni_3Mn or in its vicinity undergo an order-disorder transformation on annealing in the temperature range 300-500° C.

(a) Below 300° C the rate of transformation probably is too low for any appreciable amount of the transformation to take place.*

(b) Above about 500° C the ordered state is not stable. Thus, about 500° C is the critical ordering temperature.*

(c) The critical ordering temperature is not truly critical in that there are no very marked anomalies of properties in passing through it.*

(d) The critical ordering temperature of the 23.2% Mn alloy is 490° C, according to the results of thermoelectric measurements on the alloy cooled very slowly through the ordering range.

(e) The critical ordering temperatures reported by Kaya and Nakayama are higher than the one found directly or others whose approximate values were indicated indirectly. The value reported by N. Thompson, 510° C, was only slightly higher.

---

* Findings of previous investigators which have been verified.

(f) Indirect evidence in the present investigation indicates that the critical ordering temperature increases with manganese content in agreement with Kaya and Nakayama, but not in agreement with N. Thompson's interpretation of Kaya and Kussmann's data.

2. The ordered Ni_3Mn alloys are ferromagnetic; their magnetic properties are very dependent on composition.

(a) The 21.5% Mn alloy is the most magnetically soft of the compositions investigated. The softest properties found for this alloy at room temperature were a permeability of 5300 at 0.24 oersted and a coercive force of 0.15 oersted after demagnetization from 30 oersteds.

(b) The softest properties of the 20.1% Mn after heat treatment were a permeability of 1800 at 0.8 oersted and a coercive force of 0.52 oersted after demagnetization from 30 oersteds.

(c) High frequency permeabilities of the 23.2% Mn alloy are high, but not as high as the 21.5% alloy.

(d) The magnetic properties of the 25.3% Mn alloy are extremely hard compared to the alloys of higher nickel content, the highest permeability found after heat treatment was 186 at 2 oersteds and a coercive force of 4.3 oersteds after demagnetization from 30 oersteds.

(e) High frequency results on the magnetic properties of the 24.4% Mn alloy show that its permeability at room temperature is very low.

(f) The composition dividing soft and hard magnetic Ni_3Mn alloys is probably close to the theoretical composition Ni_3Mn, 23.78% Mn, the nickel-rich alloys being quite soft, and the manganese alloys quite hard.

3. The magnetic properties of the Ni_3Mn alloys are very sensitive to heat treatment.

(a) The Curie points found for the alloys, when they were in a well ordered condition, were in better agreement with the results of Kaya and Nakayama than with N. Thompson or Kaya and Kussmann, particularly in the case of the nickel-rich alloys.

(b) The Curie points of the well ordered alloys were drastically lowered by momentarily heating them to temperatures high in the ordering range.

(c) It was not possible to tell with certainty from the data whether the Curie points of the alloys annealed for long periods of time at temperatures high in the ordering range were lower than the Curie points after low temperature annealing.

(d) The best soft magnetic properties of the nickel-rich alloys are obtained by annealing for as long a time and at as low a temperature as possible. Thus, high degrees of order in these alloys promote magnetic softness. When the alloys were annealed at temperatures high in the ordering range the magnetism was feeble, or poor at best.

(e) The permeabilities at room temperature after the momentary heating of the well ordered alloys to temperatures high in the ordering range were of the same order of magnitude or even a little higher than in the annealed state.

(f) Three types of permeability-temperature curves were observed: (1) after annealing at a low ordering temperature, the permeabilities were quite high in a definite temperature range, the curve was somewhat irregular with temperature, and the position of the highest permeabilities shifted to higher temperatures as the manganese content of the alloys increased; (2) after annealing at a low ordering temperatures, the permeabilities were low for the whole temperature range up to the Curie point, and (3) after heating a well ordered alloy momentarily to a high ordering temperature, the curve was smooth, moving from high values at room temperature to a lower Curie point than it formerly possessed.

4. Normal magnetization data at temperatures up to about 120° C were taken on the 21.5% Mn alloy in two states of high order, and hysteresis data in the same temperature range were taken on the 21.5% Mn alloy in one state of high order.

5. Thermoelectric evidence on an ordered 23.2% Mn alloy show that there is an anomaly at the Curie point as well as at the critical ordering temperature, when the measurements are made at temperature.

6. A high frequency inductance method for measuring magnetic properties at low fields was investigated and found to yield

satisfactory, although approximate, results in temperature runs. The constants of a formula for calculating permeability from inductance-resistivity data were evaluated experimentally and theoretically, both evaluations yielding about the same value.

XI. BIBLIOGRAPHY

1. S. Kaya and A. Kussmann. Ferromagnetismus und Phasengestaltung im Zweistoffsystem Nickel-Mangan. Zeit. f. Phys., 72 (1931) pp. 253-309.

2. E. Thompson. The Order-Disorder Transformation in the Alloy Ni_3Mn. Proc. Phys. Soc. (London), 52 (1940) pp. 217-228.

3. S. Kaya and K. Nakayama. Die Nachbarschaftsordnung in den Nickel-Mangan Legierungen. Proc. Phys. Math. Soc. Japan, 22 (1940) pp. 126-141.

4. E. Valentiner and G. Becker. Ueber das System Nickel-Mangan. Zeit. f. Phys., 93 (1935) pp. 795-803.

5. T. F. Wall. The Mechanism of Magnetization I. The Engineer. (1940) pp. 273-276.

6. Prof. Tait. Trans. Roy. Soc. Edin. (1875) p. 125.

7. L. W. McKeehan. The Measurement of Magnetic Quantities. J.O.S.A. and R.S.I., 19 (1929) p. 242.

8. D. E. Hughes, Proc. Roy. Soc., 29, pp. 56-65.

9. Report of Investigations 3477, Manganese and Its Alloys. Progress Reports, Metallurgical Division, Bureau of Mines, No. 33 (1939) pp. 43-46.

10. V. E. Legg. Magnetic Measurements at Low Flux Densities Using the A. C. Bridge. Bell Syst. Techn. Journ., XV (1936) pp. 39-62.

11. J. E. Bryant and J. S. Welch. Determination of Curie Point by H. F. Resistance Method. R.S.I., 10 (1939) pp. 47-48.

12. Van Lanckner. Soc. Franc. Elec. Bull., 9 (1939) pp. 969-980.

13. G. Iotapenko and K. Senger. Zeit. f. Phys. 104 11-12 (1937) pp. 779-803.

14. R. Becker. Ann. d. Phys., 27 (1936) pp. 123-128.

15. K. Kreielsheimer. Zeit. f. Phys., 55 (1929) pp. 753-770.

16. C. R. Wait. Phys. Rev., 29 (1927) pp. 566-578.

17. W. B. Kouwenhoven and G. F. Laiger. The Measurement of Specific Resistance by Eddy Current Shielding. R. S. I., 5 (1934) pp. 94-101.

18. R. Becker. Ferromagnetism in High Frequency Alternating Fields. Zeit. f. Techn. Phys., 19 12 (1938) pp. 542-546.

19. J. G. Ferguson. Measurement of Inductance by the Shielded Owen Bridge. Bell Syst. Tech. Journ., 6 (1927) pp. 375-386.

20. T. F. Wall. Applied Magnetism, London, E. Benn, Ltd. (1927).

21. R. L. Sanford. Magnetic Testing. Bureau of Standards Circular C415 (1937) p. 33.

22. J. F. Koehler. The 685 Alternating Current Bridge Detector. R.S.I., 8 (1937) p. 450.

23. General Radio Company, Catalog K (1939) p. 84.

24. M. Benedict. Use of an Alternating Current Bridge in Laboratory Temperature Control. R.S.I., 8 (1937) pp. 252-254.

25. R. S. Dean. Electrolytic Manganese and Its Alloys. Progress Reports, Metallurgical Division, Bureau of Mines Report of Investigations 3580 (1941) p. 21.

26. T. S. Spooner. Properties and Testing of Magnetic Materials. McGraw-Hill, 1926.

27. G. W. Elmen. Magnetic Alloys of Iron, Nickel and Cobalt. J. of Franklin Inst., 207 (1929) pp. 583-617.

28. S. Kaya. J. of Faculty of Science, Hokkaido Imp. Univ., 2 (1933) pp. 26-53.